University of Zurich[UZH]

# Variability in Streamflow and Electrical Conductivity in Temporary Headwater Streams on Zürichberg

GEO 511 Master's Thesis

**Author**
Anja Fischer
18-717-454

**Supervised by**
Dr. Ilja van Meerveld

**Faculty representative**
Prof. Dr. Jan Seibert

30.09.2023
Department of Geography, University of Zurich

**Abstract**

The understanding of streamflow generation in temporary headwater streams is greatly restricted. Our limited knowledge can be partly attributed to insufficient data on streamflow in these types of streams, as well as complexities arising from a variety of influencing factors and variations among headwater catchments. Their impact on the water quantity and quality of the downstream river network reinforces the urgent need for further research in this field, especially in light of expected developments under climate and land use changes. To achieve sustainable management of these ecosystems, a more in-depth understanding of their functioning is essential. This thesis presents the results of manual surveys conducted on discharge and streamwater electric conductivity (EC) in the headwater catchment on Zürichberg. The study analyzed the spatiotemporal patterns of absolute values and variability in streamflow and water chemistry of temporal streams. It also examined the correlation between these measurements and various catchment characteristics such as elevation, slope, and geology. Additionally, the study investigated the potential to predict flow cessation or the duration of dry streambed conditions based on the coefficient of variation in discharge and EC values. The measured data exhibited complex spatiotemporal patterns for both discharge and EC. Different sites and streams display patterns influenced by varying factors such as topography, springs, and geology. The entire study area displays intensified influence of deeper groundwater at lower elevations and in steeper catchments. The presence of Molasse only moderately correlates with the variability in EC, indicating a weak trend of more stable water sources in Molasse areas. The negative correlation between the mean EC, a proxy for water age, and discharge variability renders a balancing effect of deeper groundwater on streamflow. In contrast, younger streamflow displays a trend towards greater discharge variability. However, the data on variability cannot predict the probability of a stream segment drying up during low-flow conditions towards the end of summer. Further research is needed to fully understand how the complex features of headwater catchments affect the generation of streamflow in temporary headwater streams and to be able to implement sustainable management practices and predict the impact of global change.

# Acknowledgments

I would like to express my gratitude to several people who contributed to the completion of this thesis. First and foremost, I would like to thank my supervisor, Ilja van Meerveld. Thank you for your guidance through this thesis from the decisions on methodology, many tips on the analyses, and detailed feedback on the graphics, maps, and texts. Thank you also for always taking time for me! I would also like to thank Mirjam Scheller for sharing valuable tips and insights with me. Special thanks also go to Marc Vis, who patiently helped me solve program installation problems. Finally, I am grateful to all those who have supported and motivated me in various ways throughout this thesis.

A few more acknowledgments that might not typically be mentioned, but they did help me a lot or just made my day when out on Zürichberg doing fieldwork. The many encounters with forest wildlife (ticks excluded!) and some more exotic individuals from the zoo always put a smile on my face. I also gained a new appreciation for canned ravioli from a thermos, which are much more delicious when eaten while squatting in a streambed with frozen fingers. And finally, the bike that allowed me to collect so many data points and carried all the equipment. We had our rough moments from sliding down icy roads to broken breaks while riding downhill and in the end, holding it together with zip ties but it kept going until the end of fieldwork.

# Contents

# List of Figures

# List of Tables

# 1 Introduction

## 1.1 Headwater streams

The uppermost segments of streams i.e., first- or second-order streams, are known as headwater streams (Wohl 2017b). Goodrich et al. (2018) refers to them more broadly as "low order, small streams at the top of a watershed [. . . ]". Because of their smaller catchment areas, these streams are smaller than their downstream counterparts (Wohl 2017b). Headwater streams comprise a substantial fraction of the stream network, though the exact percentage varies depending on how they are defined (Godsey and Kirchner 2014; Kaule and Frei 2022). Various estimates suggest that headwater streams comprise between 70 and 89% of the total stream length (Allen et al. 2018; Hatley et al. 2023; MacDonald and Coe 2007; Ward et al. 2020; Wohl 2017b). Headwater streams often start above the highest point of a stream where there is year-round flow and emerge in areas where enough surface runoff is collected to create a geomorphic stream channel. They may also be initiated by springs (Wohl 2017b). Despite their small size and relatively low absolute discharge, headwater streams play an integral role in connecting uphill areas with lower stream reaches because of their abundance (Godsey and Kirchner 2014; Goodrich et al. 2018). They function as the initial point of interaction between the upland area and the large downstream rivers (Kampf et al. 2021) and serve as a vital source of water, solutes, mineral sediments, and organic material for the downstream network (Wohl 2017b).

The exchange of matter and organisms between the stream segments and the adjacent landscapes mainly depends on the spatial and temporal variation of stream characteristics (Wohl 2017a). Alterations made at the local level in headwater catchments can propagate through the stream network and have far-reaching consequences for the perennial streams (Swenson et al. 2023). Headwater streams are crucial water resources for providing drinking water and supporting agriculture, as well as offering a range of vital ecosystem services on a global scale (Kaule and Frei 2022; Messager et al. 2021; Swenson et al. 2023). However, the demand for water is rising, and its availability is changing due to the impact of climate change, thus heightening the pressure on these invaluable streams (Nabih et al. 2021). In addition, headwater streams are critical for recharging alluvial aquifers and regional groundwater reservoirs that provide critical base flows to higher-order streams (Goodrich et al. 2018). Thus, headwater streams play a vital role in maintaining the health of the entire river ecosystem and the services it provides.

Headwater streams typically drain areas that are much smaller and therefore have less diverse climate characteristics and lower surface and subsurface storage capacities. Headwater streams respond more rapidly to precipitation inputs because of their shorter and steeper flow paths from uplands to the stream channel (Messager et al. 2021; Wohl 2017b), which reduces their capacity to mitigate variations in precipitation (Messager et al. 2021). Further downstream in the river network, the catchment size increases along with internal diversity, temporary

storage, and groundwater contributions to baseflow. As a result, there is a more balanced discharge, and perennial flow (Kaule and Frei 2022; Messager et al. 2021). In contrast, headwater streams depend heavily on local precipitation (Kaule and Frei 2022). The closer connection between precipitation and runoff leads to substantial spatial and temporal variation in the extent of surface streamflow in headwater stream channels (Botter et al. 2021). Thus, numerous headwater stream segments do not have perennial flow, but the surface flow ceases during certain periods of the year, particularly during the dry season (Goodrich et al. 2018; Kaule and Frei 2022; van Meerveld et al. 2020; Wohl 2017b).

## 1.2 Temporary streams

### 1.2.1 What are temporary streams

Non-perennial streams is a broad term and encompasses a variety of hydrologically diverse flow patterns (Busch et al. 2020). More specific terms include intermittent and ephemeral streams. Intermittent streams flow seasonally and are sustained by groundwater (gaining system) and transition to a losing system when the groundwater table falls below the streambed. Ephemeral streams, on the other hand, are losing systems throughout the year and flow only in direct response to intense precipitation or melt events (Goodrich et al. 2018). Hereafter, streams with recurring no-flow phases of varying durations will be referred to as temporary streams, which include intermittent and ephemeral streams (Busch et al. 2020). Conversely, large rivers that are able to sustain flowing water throughout the year are referred to as perennial streams (Goodrich et al. 2018).

Temporary streams are common in arid and semi-arid regions, but they exist in all climatic regions (Shanafield et al. 2021). In temperate climates, temporary streams are predominantly located in the headwater regions (Kaplan et al. 2020). Headwater streams transport water from high elevation regions to downstream perennial rivers. The flow patterns in temporary headwater streams significantly impact the quantity and quality of water supply in downstream reaches (Djodjic et al. 2021; Godsey and Kirchner 2014; Kaule and Frei 2022; van Meerveld et al. 2020; Whiting and Godsey 2016). Recent advancements in recognizing temporary streams have shown that these streams account for more than 50% of the world's stream length and up to 50% of the global discharge (Hammond et al. 2021; Hatley et al. 2023; Messager et al. 2021). They have, therefore, recently been called the 'world's dominant type of river ecosystem' (Truchy et al. 2023). In the past five decades, there has been a rise in the number of streams that have shifted from previously perennial flow to a temporary flow regime (Messager et al. 2021). Given that climatic factors account for most of the large-scale variability in intermittency, it is predicted that their extent will expand further due to the impact of global change, in particular, due to the projected rise in temperature by future climate scenarios (Hammond et al. 2021; Tramblay et al. 2021; Truchy et al. 2023; Ward et al. 2020).

### 1.2.2 Underrepresented in maps and data

For a significant time in history, streams were perceived as static features in landscapes. However, in recent years, there has been a substantial growth in scientific discourse and awareness concerning the flow dynamics and existence of temporary streams (Botter and Durighetto 2020). Regardless of this recent recognition, the extent of their presence is inadequately represented in many of the official maps (van Meerveld et al. 2019). This is in part due to the limited tools for identifying the variable extent of stream networks over time (Botter and Durighetto 2020). In many cases, the locations of the streambeds are acquired from geospatial datasets. Thus, a better resolution allows for the identification of more headwater streambeds (Kampf et al. 2021). This, however, does not enable precise categorization of the temporary headwater streams, as their flow regime depends on multiple factors, with topography being a crucial but not singular influence. Further methodological limitations include the challenge that small first-order streams are generally not detectable in aerial imagery and field campaigns to manually map them are highly labor-intensive, and limited in accessibility due to the topography (Wohl 2017b). The variability in flow patterns cannot accurately be determined only with topographical maps and Kampf et al. (2021) therefore suggests that field visits are necessary to map the dynamic flow paths. However, Hafen et al. (2020) have shown that stream classification based on field surveys is in many cases also not reliable, because of differences in annual climate conditions.

Besides the fact that temporary headwater streams are underrepresented in maps, they are also regularly missing from hydrological datasets. Gauging stations are generally installed in stream reaches with sustained perennial flow, leaving many temporary headwater streams unmonitored (Krabbenhoft et al. 2022; van Meerveld et al. 2020; Truchy et al. 2023). Such an absence is also observed in the official dataset of Switzerland. The monitoring network for surface water by the Federal Office for the Environment (FOEN) includes all 260 gauging stations for surface waters in Switzerland and data about water levels and discharge dates as far back as the mid-nineteenth century. Nevertheless, a brief analysis of the complete gauging station dataset reveals that stations with larger catchment areas and at lower elevations are significantly more prevalent (FOEN 2023). When applying the definition of MacDonald and Coe (2007) that headwater streams have a catchment area no larger than 10 $km^2$ to the current monitoring network in Switzerland, only 4.35% of the stations take measurements in headwater catchments. This is a significant underrepresentation, as it is reasonable to assume that headwater streams constitute a larger proportion of the total stream length when considering a range of estimates, ranging from 70 up to 89% (Allen et al. 2018; MacDonald and Coe 2007; Ward et al. 2020; Wohl 2017b). The precise proportion of headwater streams is challenging to determine since official maps frequently exclude them or considerably underestimate their extent (Kampf et al. 2021; van Meerveld et al. 2020). Due to the inadequate number of gauging stations in headwater streams, especially those with temporary flow regimes, hydrological datasets are not representative of them (Acuña et al.

2014). This has led to a gap in knowledge regarding the spatial extent, magnitude, frequency, and duration of surface flow in temporary headwater streams as well as the variability of these factors (Borg Galea et al. 2019; Wohl 2017b). Reasons for this bias towards perennial streams are diverse. Access to headwater streams may be limited due to their geographical location, and taking measurements in these areas can be challenging due to various geomorphological processes (Borg Galea et al. 2019). Additionally, existing monitoring systems and tools tend to be geared towards perennial rivers (Botter and Durighetto 2020; Truchy et al. 2023), such as gauging stations designed to measure discharge, which may not accurately measure no- or low-flow conditions (Zimmer et al. 2020). They are also not made to collect data about other streambed conditions such as standing water or elevated moisture content in the streambed. Furthermore, the unpredictable distribution of flowing areas along temporary streams adds complexity to the implementation of measurements. Various methods to collect data on temporary headwater streams are being tested, including aerial imagery, different sensors, field mapping, interviewing the local population, and citizen science. Nevertheless, each of these approaches has inherent limitations and challenges (van Meerveld et al. 2020).

### 1.2.3 Implications for resource management

Having a thorough understanding of streamflow generation processes in headwater streams is essential in making informed decisions for managing water resources at all spatial levels (Jung et al. 2021). However, the inclusion of temporary headwater streams into protection measures is currently not always ensured. For instance, in Europe, management frameworks vary considerably across countries and the incorporation of temporary streams still has considerable room for improvement (Leone et al. 2023). This underscores the need for additional research on the hydrology of temporary streams and their effects on downstream rivers (Assendelft and van Meerveld 2019; Swenson et al. 2023). Protecting temporary streams is crucial not only for downstream streamflow but also because they provide critical ecosystem services and support high biodiversity themselves (Acuña et al. 2014). Temporary streams are sometimes considered less aesthetically pleasing and less valuable compared to perennial reaches by the public. Nevertheless, they provide essential ecosystem services, such as flood attenuation, biogeochemical cycling, and habitats for diverse species (Jensen et al. 2017; Truchy et al. 2023).

### 1.2.4 Flowing stream network dynamics

Temporary steams include a large diversity of flow regimes across various climatic and geographic settings, encompassing streams that only dry up during severe drought periods to ephemeral streams that remain dry most of the time and only become active after intense precipitation events (van Meerveld et al. 2020; Shanafield et al. 2021; Wohl 2017b). Three hydrological states can be differentiated in temporary streams. The streambed can be dry, have standing water, or flowing water (Gallart et al. 2017). The range between these states is infinite. Additionally,

there is not only large variability between temporary streams but also along each individual stream itself (Tramblay et al. 2021). The extent of active streambeds with flowing water has a close association with climatic factors. It expands and retracts based on the moisture content of the watershed (Botter and Durighetto 2020; Whiting and Godsey 2016). In temperate humid climates, headwater streams often display seasonal flow patterns that are most pronounced during wet seasons or when evapotranspiration rates are low (Kampf et al. 2021). Climatic factors, specifically precipitation and temperature (evapotranspiration), are key factors in whether there is enough water in the system to generate surface runoff and thus explain much of the variability in the discharge dynamics of temporary streams (Hammond et al. 2021; Price et al. 2021). Nevertheless, climate cannot fully account for the considerable variations in the flow patterns of neighboring streams. Therefore, drying characteristics at the local or regional scale must be influenced by additional factors (Datry et al. 2023; Price et al. 2021; Sauquet et al. 2021; Tramblay et al. 2021; Warix et al. 2021; Whiting and Godsey 2016). For instance, persistent springs (Warix et al. 2021), changing interactions between surface water and groundwater, natural or human-induced discharge losses (Price et al. 2021; Tramblay et al. 2021), ground permeability, geological differences in bedrock and topographical characteristics including slope, curvature, and catchment area size (Hammond et al. 2021; Prancevic and Kirchner 2019) were identified as key determinants of flow regimes. However, there is still limited understanding of their full impact (Hammond et al. 2021; Whiting and Godsey 2016). The volume of runoff at a given location and time results from the balance between upstream flow and downstream drainage capacity (Godsey and Kirchner 2014). The subsequent Chapter 1.3 further explores the impact of various factors on streamflow.

## 1.3 Runoff generation processes

### 1.3.1 Dynamics of different water sources

The mechanisms responsible for runoff generation in headwater catchments are highly complex and nonlinear, posing significant challenges for researchers attempting to comprehend and model them (Sauquet et al. 2021). In simplified terms surface streamflow arises when incoming discharge from upstream areas exceeds the sediment and bedrock's ability to transport water underground (Godsey and Kirchner 2014; Prancevic and Kirchner 2019). However, the knowledge in the scientific community concerning the various sources and factors that affect streamflow generation in headwater catchments is limited, in part due to inadequate data (Barua et al. 2022; Gutierrez-Jurado et al. 2021). The sources of streamflow in headwater catchments are diverse, including surface runoff, soil water, shallow groundwater, and deeper groundwater (Barua et al. 2022; Hatley et al. 2023; Zhou et al. 2022). The higher permeability of the upper soil layers compared to bedrock at larger depth causes most of the precipitation that infiltrates into the ground to flow through these shallow depths and therefore contribute to streamflow at a

relatively young age of just a few months (Li et al. 2021). The sources control the timing of streamflow initiation and the duration of flow in temporary streams (Barua et al. 2022).

### 1.3.2 Factors affecting the occurrence of flow along the stream network

The duration that a stream receives water from groundwater sources varies significantly, resulting in varied durations of flow (Costigan et al. 2016). Runoff sources are expected to fluctuate seasonally and at different stages of flow, causing diverse flow patterns (Barua et al. 2022). However, many aspects of short-term source variations at different flow conditions in headwater streams remain unresolved (Barua et al. 2022; Hatley et al. 2023; Zhou et al. 2022). Groundwater is a crucial stable source for streamflow, not only for large perennial streams but also for smaller temporary headwater streams (Hatley et al. 2023; Sauquet et al. 2021; Warix et al. 2021). The contribution of groundwater to the streamflow is expected to be more stable compared to sources of soil water and shallow groundwater (Warix et al. 2021). However, temporary streams differ from perennial streams as they change between losing and gaining systems seasonally according to their location relative to the groundwater table, whereas perennial streams stay well connected to groundwater aquifers year-round. If the streambed is located above the groundwater table, water infiltrates into the ground, causing the stream to lose water. Contrarily, during times of elevated groundwater table, the stream gains water from groundwater storages (Barua et al. 2022). This bidirectional flow of local groundwater storages to and from the stream has major impacts on the flow permanence in temporary streams, both temporally and spatially (Swenson et al. 2023). Seasonal climate patterns generally cause groundwater levels to be at their lowest point by the end of summer (Barua et al. 2022). Throughout the fall and winter months, storages are gradually replenished due to a decrease in evapotranspiration, and an increase in runoff amounts is generally observed as the stream network expands in length (Swenson et al. 2023; Costigan et al. 2016). Once the groundwater storages are filled, precipitation and runoff amounts are linked, meaning the streamflow reacts to atmospheric inputs (Swenson et al. 2023).

Climate factors such as precipitation, meltwater, evapotranspiration, and their influence on groundwater aquifers, significantly impact streamflow generation. However, these factors alone are insufficient for predicting streamflow extent. While climatic factors may be assumed to be relatively consistent across headwater catchments due to their small size, spatio-temporal variations in the streamflow in headwater streams suggest that other factors must be influencing runoff generation as well. Other characteristics of the watersheds, such as topography, geology, and land cover impact runoff generation and water storage in soils and aquifers at various spatial and temporal scales (Costigan et al. 2016; Floriancic et al. 2019). Therefore, catchment features significantly influence flow dynamics variation within a headwater catchment (Floriancic et al. 2021).

One distinguishing factor between catchments is their topography, which has been found to impact the drying patterns of temporary headwater streams via variations in hydraulic heads that drive flow towards or away from groundwater (Prancevic and Kirchner 2019; Warix et al. 2021; Whiting and Godsey 2016). Additionally, slope has been found to contribute to variations in runoff generation. Steeper gradients lead to a more rapid flow of water towards the stream and thus faster draining (Costigan et al. 2016; Floriancic et al. 2021; Simon et al. 2022). This can lead to the concentration of water in the upper layers of soil and impeding percolation into deeper groundwater reservoirs (Hare et al. 2021). Deeper incised streams are more likely to intersect groundwater reservoirs (Floriancic et al. 2021), creating a hydraulic gradient that drives groundwater into the stream (Costigan et al. 2016). In headwater streams that are less deeply incised, the probability of the groundwater table lying below the streambed is higher, resulting in a greater chance of the hydraulic gradient being from the stream towards groundwater (Costigan et al. 2016). Alternatively, a lower slope may mean that infiltrating water does not drain as quickly and accumulates as perched groundwater. It takes more time for this process to lead to runoff in the streambed. However, once the groundwater table has reached a certain level, temporary runoff can be sustained for a longer period due to the slower flow paths, even if there is a decrease in precipitation (Gutierrez-Jurado et al. 2021; Prancevic and Kirchner 2019).

Some correlations between the size of the catchment and the runoff have also been found. Larger catchments often have a higher proportion of deeper groundwater in the streamflow during the winter season, as reported by Floriancic et al. (2019). Additionally, they found that the variability in the runoff and the streamwater chemistry decreased with the catchment size (Floriancic et al. 2019). Later, the dependence of low-flow metrics on catchment size was explored by Floriancic et al. (2021). While the relationship was somewhat unclear, there was a connection for some streams indicating increased specific discharge downstream.

Other factors than climate and topography also impact streamflow dynamics. For instance, streamheads can be strongly influenced by heterogeneities in bedrock and soil (Godsey and Kirchner 2014; Whiting and Godsey 2016). In some cases, springs can cause a streamhead to be pinned in place due to locally stable outflow, which is primarily caused by faults in lithology rather than the topography (Prancevic and Kirchner 2019; Whiting and Godsey 2016). Additionally, the geological characteristics of the watershed also impact precipitation infiltration. A higher permeability leads to high infiltration rates during the wet period, and potentially increased streamflow in the dry seasons and ultimately decreasing flow cessation. On the other hand, geology that is less permeable has a limited capacity for storing infiltrated precipitation, thus preventing sustained streamflow for extended periods during dry conditions (Costigan et al. 2016). During periods of low flow, the mechanisms responsible for groundwater storage and release significantly affect streamflow dynamics (Carlier et al. 2018). A significant proportion of runoff in low-flow conditions originates from specific layers of geological units or geomorphic

features. For instance, Quaternary deposits or sandstone provided the majority of streamflow alpine catchments and the Swiss Plateau region, respectively when conditions were generally dry (Carlier et al. 2018; Floriancic et al. 2022). However, it remains unclear whether these findings can be extended to other headwater catchments. Overall, there are still many uncertainties regarding the impact of geology on streamflow generation in headwater catchments (Floriancic et al. 2022).

Flow in temporary streams may be interrupted in their longitudinal extent and may not continuously carry surface flow (McDonough et al. 2011), due to differences in underlying geology or changing topography along a stream, which can result in different specific discharge and surface flow permanence patterns along a stream (Costigan et al. 2016; Floriancic et al. 2021). This suggests that streamflow is also conducted underground. This can occur either directly in the layers beneath the streambed or at greater depth, depending on the geological and soil characteristics (Floriancic et al. 2021)

Groundwater is widely recognized as a key source of streamflow during low-flow periods. Nevertheless, the precise impact of geology and topography on the dynamics of temporary headwater streams remains incomplete (Floriancic et al. 2021). The mechanisms governing the diverse water storage types and their respective contributions to streamflow across seasons remain elusive (Floriancic et al. 2019; Zimmer and McGlynn 2017). This is further exacerbated by the highly variable characteristics of streamflow over time and space, which adds a high degree of complexity to the nexus of precipitation, storage, and streamflow generation (Correa et al. 2017; Whiting and Godsey 2016).

Different water sources are characterized by varying flow paths, leading to different mean transit times (MTT). MTT reflects the average time it takes for precipitation to travel from the point where it entered the catchment (i.e., infiltrated) to the time when is discharges into the stream (Zhou et al. 2022). The MTT in temporary stream water is anticipated to change at different stages of the streamflow extent (Barua et al. 2022; van Meerveld et al. 2019). A comprehensive understanding of the mixing and transport processes (MTT) can enhance the knowledge of how groundwater and surface water interact, resulting in a better understanding of water storage, sources, and flow paths (Jung et al. 2020; Zhou et al. 2022). Previous hypothetical studies have shown that runoff in extended stream networks during wet conditions will likely consist of a larger fraction of young water due to the shorter flow path lengths (van Meerveld et al. 2019). As the active network retracts, the frequency distribution of flow path length and thus travel times becomes more uniform. Furthermore, the age of the water becomes more diverse, and generally much older, under conditions of increased drying (Barua et al. 2022; Swenson et al. 2023). Due to a shift in the water source when the wetness conditions of the catchment change. During wet conditions, a larger amount of water is sourced from surface water, shallower groundwater, and soil water. Contrastingly, in dry conditions, the relative proportion of water

derived from deep groundwater increases, releasing water that has been stored in the catchment for much longer periods (Swenson et al. 2023; van Meerveld et al. 2019). The release of water from deep groundwater storage is a significant factor in contributing to streamflow during the dry season and can even result in prolonged or uninterrupted streamflow in certain headwater streams (Swenson et al. 2023). Younger water has a greater influence on headwater streams, particularly during high streamflows (Barua et al. 2022). Older streamwater in headwater catchments suggests a greater proportion of water originating from prolonged storage within the catchment (Zhou et al. 2022).

Another effect worth mentioning in headwater streams is the piston effect, which describes the phenomenon of observing old groundwater in streamflow directly after intense precipitation events (Kirchner 2003). This is explained by the input of new water from precipitation, causing an immediate displacement of older groundwater. The elevated hydrostatic pressure resulting from infiltrating water in the saturated zone expels groundwater from soil at lower elevations, thus introducing volume to streamflow (Vasconcelos 2017). The pressure signal propagates much faster than the velocity of water molecules, resulting in an immediate reaction (Li et al. 2021). Consequently, despite the influx of significant quantities of young rainwater, the age of streamflow may rise after rainfall due to groundwater displacement. Flow patterns and MTT impact biogeochemical processes of water and its surrounding environment. As water flows along its path, it interacts with the geology and soils, leading to chemical weathering, which is partially dependent on the duration of water-rock contact (Li et al. 2021). Differences in stream geochemistry can therefore indicate changes in the MTT of streamwater (Barua et al. 2022).

### 1.3.3 EC as an indicator of water sources

The electrical conductivity of water refers to its ability to conduct electricity. Pure water is inefficient at conducting electricity, resulting in low conductivity (Sarath Prasanth et al. 2012). When ions are dissolved in the water, the conductivity increases as they transport electric current. This measurement can be utilized to determine the concentration of dissolved ions in streamwater. The EC of streamwater is a reliable and easily measurable parameter (Vogt et al. 2010). Water from precipitation has low conductivity due to the lack of exposure to ionizing surfaces. Once the water comes in contact with the ground, various geochemical processes start (Schmidt et al. 2012), which is why the catchment's underlying soil and geology are major factors affecting stream water conductivity. Bedrock consisting of inert materials, such as granite, leads to lower conductivity in water due to less effective ionization, resulting in fewer ions being dissolved in the water. Streams flowing through areas with more dissolvable material have a greater concentration of dissolved ions and, as a result, higher conductivity (Bhateria and Jain 2016). Geology also affects the paths and residence times of water below the ground (Carlier et al. 2018). Different discharge sources in a stream can produce varying geochemical patterns along its course (Bhateria and Jain 2016; Zhou et al. 2022). Groundwater

stored for longer periods tends to dissolve more ions due to extended contact with bedrock, leading to higher EC values when compared to stream water with shorter flow paths (Li et al. 2021; Zhou et al. 2022). If precipitation falls as rain, it can cause discharge to increase directly and dilute the stream water, resulting in a decrease in the EC (Schmidt et al. 2012; Vogt et al. 2010). Conversely, during low flow conditions, increased evapotranspiration and increased relative importance of groundwater usually result in elevated EC values (Floriancic et al. 2019; Schmidt et al. 2012). From this, it can be inferred that higher values of EC indicate a greater influx of groundwater, while lower values suggest a greater supply of surface and soil water. Therefore, conducting systematic EC measurements to assess spatio-temporal heterogeneity can provide valuable insights into the various sources of stream flow, transit times, and particularly groundwater influxes (Floriancic et al. 2019; Schmidt et al. 2012). In brief, EC is a reliable measure of the duration that water stayed in the ground, determined by the quantity of dissolved ions.

## 1.4 Research questions and objectives

Temporary streams are crucial to river networks because they impact the water quantity and quality of downstream rivers (Cottet et al. 2023). The effects of ongoing climate change, including anticipated extended dry periods (Datry et al. 2023; Kaule and Frei 2022; Nabih et al. 2021), underscore the need for better understanding of temporary stream behavior. This knowledge is essential for effective river ecosystem management (Wohl 2017a). An increasing trend in stream intermittency has been observed globally (Sarremejane et al. 2022). However, changes are not consistent in space or time, as the impacts of climate change on the runoff regime are complemented by the impacts of land use change, which includes urbanization, deforestation or afforestation, as well as other anthropogenic alterations like water abstraction (Zipper et al. 2017). It is crucial to understand local variables that affect the flow regime and their interactions to evaluate the effects of management decisions (Hammond et al. 2021). Despite increased recognition of the importance of temporary headwater streams and a desire to be more inclusive of their unique hydrological and ecological dynamics, water resource management continues to base decisions on datasets that are biased toward perennial streams. This limits the inclusion of temporary streams in water management plans (Acuña et al. 2014; Leone et al. 2023; Swenson et al. 2023; Truchy et al. 2023). Additionally, the management faces further constraints due to the limited financial resources available (Leone et al. 2023). The limited available data hinders our understanding of the impacts that changes in land use, climate change, and stream management approaches will have on headwater streams. Acquiring more in-depth knowledge about these aspects would greatly enhance our capacity to make sustainable choices in protecting the integrity of stream networks (van Meerveld et al. 2020). A growing interest and increasing number of studies in recent years have led to advances that have already shed some light on the topic. However, our understanding of how temporary headwater streams function and their

connections within landscapes remains severely limited (van Meerveld et al. 2020).

Based on the introduced theoretical backgrounds and the identified gap in current research, the following research questions were asked:

- How does streamflow discharge and EC vary across headwater streams on Zürichberg? And can this variability be explained by topography and/or geology?
- Can the temporal variability in discharge and streamwater EC be used to identify streams that are more susceptible to falling dry during periods of low flow?

It is hypothesized that groundwater (spring) fed streams have less variable discharge and a high but relatively constant EC and are less likely to go dry in summer than streams fed by flow from shallow soil layers. Streams fed by soil water, shallow subsurface flow, or overland flow have a more variable flow regime, a lower and more variable EC, and are more likely to fall dry during certain times of the year. Furthermore, it is hypothesized that lower stream reaches with a larger contributing area have a higher specific discharge due to the contribution of deeper groundwater and are also less likely to go dry. Based on the findings by Floriancic et al. (2022) the assumption is made that stream segments underlain by Molasse are less likely to go dry compared to those flowing through moraine material. To answer these questions field surveys were conducted during winter and spring of 2022/2023 to collect spatio-temporal data about the variability in streamflow and streamwater EC for the temporary headwater streams on Zürichberg.

# 2 Study site

## 2.1 Location

The research for this thesis was conducted in the study area located on Zürichberg, a forested hill based in the northern part of the city of Zurich, Switzerland. Zürichberg is situated between the valleys of the river Limmat to the southwest and the Glatt river in the northeast, and is part of the Swiss Plateau region. Elevations range from approximately 480 to 680 meters above sea level. The research area covers about 3.35 km$^2$ and is bordered by residential areas. To the East lies the Zoo Zürich and the Sagentobel after which Adlisberg follows (Swisstopo 2023). Due to its proximity to populated areas, Zürichberg is frequently used by the local population for recreational purposes and presents a dense system of forest roads and paths (Hegelbach and Spaar 2000). Due to the elevated topography in relation to the surrounding area, Zürichberg is a headwater catchment as streams originate there and flow towards lower-lying areas. Observations have revealed that a substantial portion of these streams exhibit a temporary flow regime (CrowdWater 2023).


Figure 1: Map of the location of the study area on Zürichberg, the Meteo station at Fluntern, and the surrounding urban areas of the city of Zurich. Inset map: The location of the study area within Switzerland (red dot). (Data sources: Federal Office of Topography Swisstopo, 'swissBOUNDARIES3D'; Federal Office for the Environment FOEN, 'surface waters'; Federal Office of Meteorology and Climatology MeteoSwiss, location Meteo Station Fluntern).

## 2.2 Climate

Long-term measurements at the nearby meteorological station Fluntern (556 m a.s.l.) (see Figure 1 for the location) reveal an average annual temperature of 8.5°C and annual precipitation of 1055 mm (period 1864-2022) (MeteoSwiss 2023). The norm monthly temperature and precipitation values (reference period 1991–2020), shown in Table 1, indicate a temperate climate with a trend towards increased precipitation during the summer months. However, the temperature is also significantly higher during these months, resulting in a concurrent rise in potential evapotranspiration. By comparing the actual monthly values during the data collection period from November 2022 until May 2023 (shown in Table 1), it can be observed that November and December of 2022 received a precipitation volume that was relatively typical when compared to the reference period. January and especially February of 2023 were significantly drier. However, the subsequent months of March and April experienced above-average amounts of precipitation, whereas May was slightly below average. Monthly mean temperatures were higher compared to the norm period for each month except for April which was colder.

Table 1: Monthly average temperature and precipitation (Reference period 1991–2020) and the monthly mean measurements during the data collection period at the Meteo Station Fluntern (MeteoSwiss 2023).

| | Jul | Aug | Sep | Oct | Nov | Dec | Jan | Feb | Mar | Apr | May | Jun |
|---|---|---|---|---|---|---|---|---|---|---|---|---|
| Temp. [°C] | 19.0 | 18.6 | 14.4 | 10.0 | 4.9 | 1.7 | 0.9 | 1.8 | 5.8 | 9.6 | 13.6 | 17.1 |
| Precip. [mm] | 126 | 119 | 87 | 85 | 76 | 83 | 63 | 60 | 71 | 80 | 128 | 128 |
| 22/23 T. [°C] | - | - | - | - | 7.3 | 2.7 | 2.9 | 3.5 | 7.0 | 8.2 | 13.8 | - |
| 22/23 P. [mm] | - | - | - | - | 75 | 90 | 43 | 21 | 100 | 103 | 117 | - |

The hourly temperature and precipitation values, along with the cumulative precipitation from the start of October 2022 are illustrated in Figure 2. Stars denote the days of data collection to provide an overview of the climate conditions leading up to them. The aforementioned extended dry period from January to February 2023 is clearly visible on the plot of the cumulative precipitation.

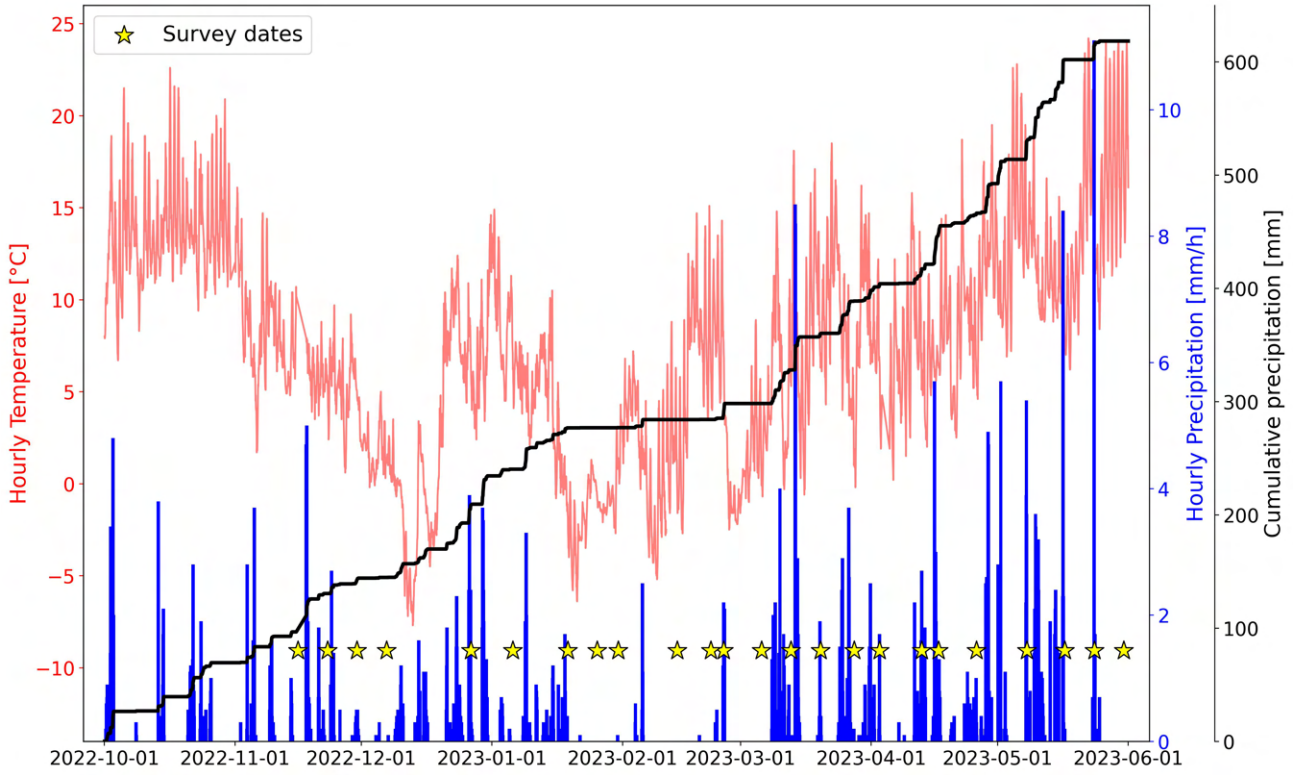


Figure 2: Climate conditions prior to and during the measurement period from November 2022 to May 2023: temperature (°C), precipitation (mm), and cumulative precipitation (mm) at the Fluntern Meteo station (MeteoSwiss 2023). Survey dates are marked with stars.

Precipitation determines the amount of water that enters the catchment system from the atmosphere. Temperature along with solar radiation, humidity, wind speed, and albedo, determine the amount of water lost back to the atmosphere through evapotranspiration and therefore unavailable for streamflow generation. To determine this potential loss that varies seasonally, the potential evapotranspiration (PET) was derived. This is an approximation of the quantity of water that may evaporate or be transpired by plants in the absence of water resource constraints. The PET calculation was based on the simplified Penman equation by Valiantzas (2006), and additional information regarding the calculation and formulas used can be found in Appendix A1.

To determine if the catchment was losing or gaining water, the balance between precipitation and PET was calculated. A positive balance indicates that precipitation input was greater than the amount of water that could potentially be evapotranspirated. Conversely, a negative balance means that potentially more evapotranspiration could have occurred, but the amount of water input on that specific day was limiting it. Surplus precipitation was observed in October, November, and December of 2022 due to the decrease in PET and the occurrence of regular precipitation. This pattern is typically observed in winter months when PET is low because of cold temperatures and short days. However, in January and February, precipitation levels were so low that the monthly precipitation surplus decreased and even became negative in February.

There was a subsequent increase in precipitation in March, however, PET also rose over the next few months. If persistent negative balances are significant as they suggest potential long-term dryness in the catchment area. Conversely, a surplus of precipitation allows for infiltration into the ground and replenishment of aquifers (Hamilton et al. 2018).

The mean annual evaporation from areas with forest cover in Switzerland over the period between 1973–1992 lies at approximately 620 mm (Spreafico and Weingartner 2005). With a calculated total of 439 mm in 248 days, it is assumed to lie in a reasonable range. The total precipitation between October 1, 2022, and June 5, 2023, was 618 mm and therefore approximately 179 mm/m$^2$ was infiltrated into the ground.

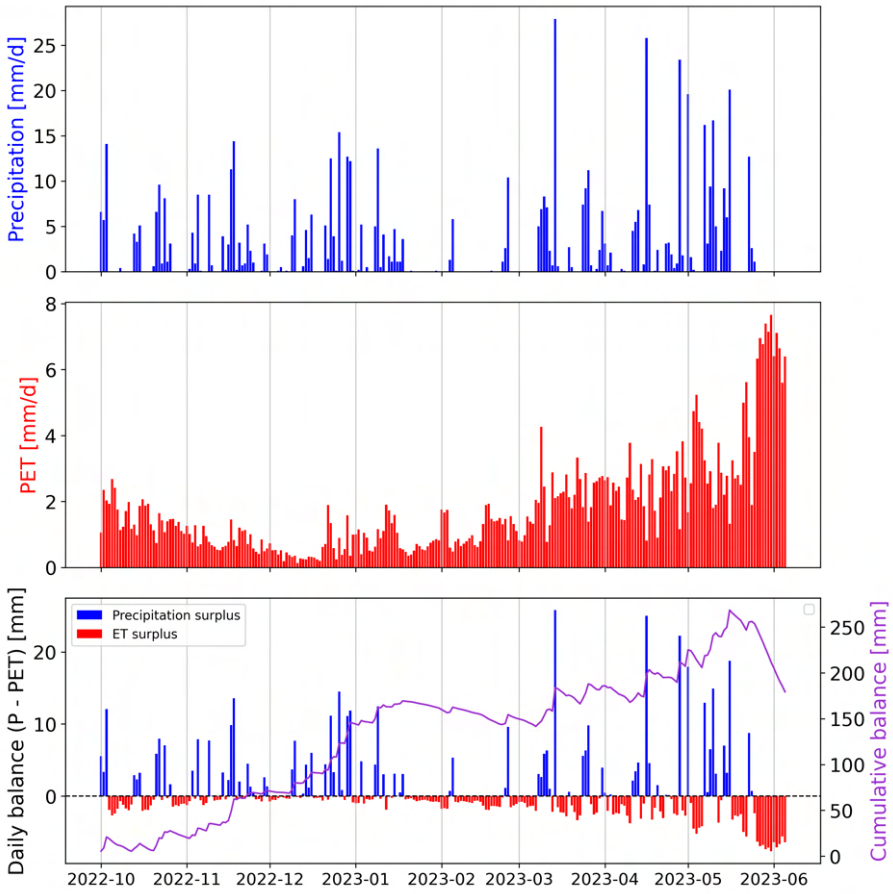


Figure 3: Time series of the precipitation, the calculated potential evapotranspiration (PET), the daily balance between the two (P - PET) indicating daily moisture deficits or surpluses, and the cumulative balance to show the development of moisture conditions during the measurement period (MeteoSwiss 2023).

Given the small size of the study area, we can assume uniform climate conditions across the entirety of Zürichberg. This allows for the investigation of the impacts of topographical and geological characteristics on the dynamics of streamflow regimes.

## 2.3 Geology and Geomorphology

Zürichberg is located in the Northern Alpine Foreland Basin, which is also referred to as the Molasse Basin (Rocholl et al. 2018). The bedrock primarily comprises Upper Freshwater Molasse, which was deposited in the Tertiary era approximately 16 to 13 million years ago. The prevalent rocks are sandstones, siltstones, and mudstones with infrequent occurrences of freshwater limestone and conglomerates (Pavoni et al. 2015; Rocholl et al. 2018). During the middle and late Pleistocene, the alpine glaciers advanced into the foreland and eroded significant portions of the Molasse Basin. The Linthglacier also covered Zürichberg during the last ice age, around 23'000 to 24'000 years ago, resulting in its rounded shape. About 18'000 years ago, during the Quaternary era, the Linthglacier retreated into the Lake Zurich Basin, leaving behind substantial amounts of glacial till in the region (Pavoni et al. 2015). The majority of Zürichberg consists of such glacial moraine material, as illustrated in Figure 4. Nevertheless, there are areas with Upper Freshwater Molasse that were not eroded by the glacial advances. Smaller areas where a thin layer of unconsolidated rock cover overlays the Upper Freshwater Molasse are also present. These areas share similar hydrological characteristics with the Upper Freshwater Molasse and are thus considered in the same category as pure Upper Freshwater Molasse according to Rocholl et al. (2018). Furthermore, Zürichberg has experienced some minor landslides, although they are not further examined in this thesis.

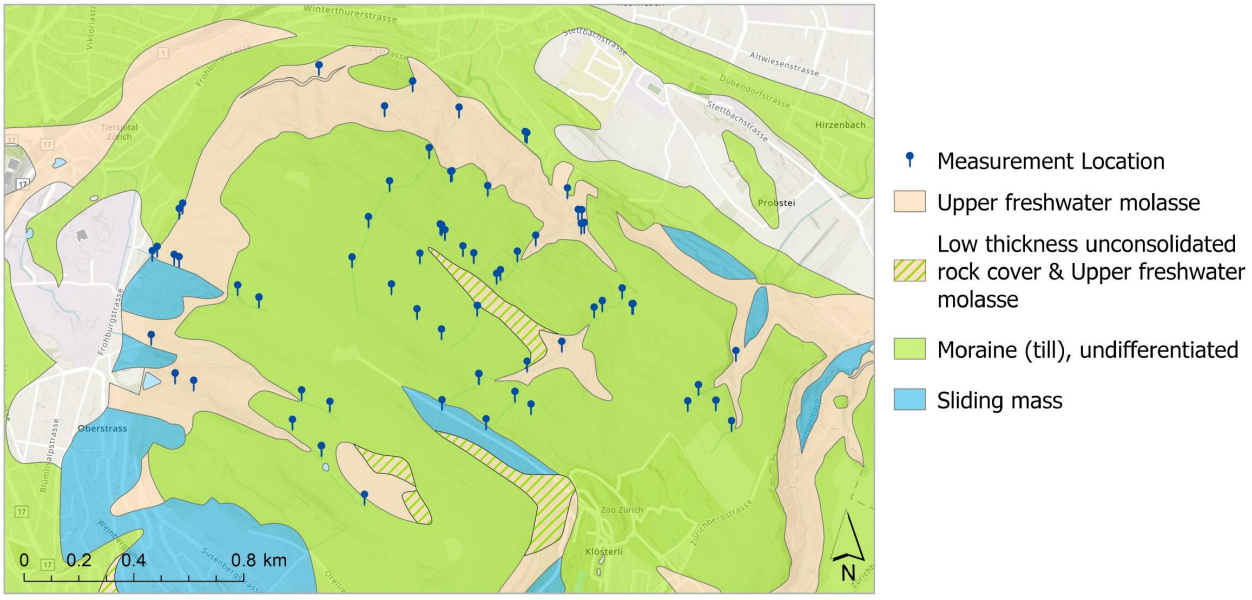


Figure 4: Geologic units present in the study area on Zürichberg with the measurement locations marked for later analyses (Data source: Swisstopo, 'GeoCover').

Zürichberg is a moderately flat hill in the Swiss Plateau area, with generally gentle slopes due to the aforementioned glacial coverage. Nonetheless, Figure 5 exposes certain regions on the hill with notably steeper slopes as a result of incised streambeds eroding in the terrain. Of particular interest are the two streambeds located on the westward-facing slope and the one in the furthest eastern part of Zürichberg that showcase steeper slopes indicated by darker color. Furthermore, the lower sections of Zürichberg display steeper slopes in contrast to the relatively flat center of the hill.

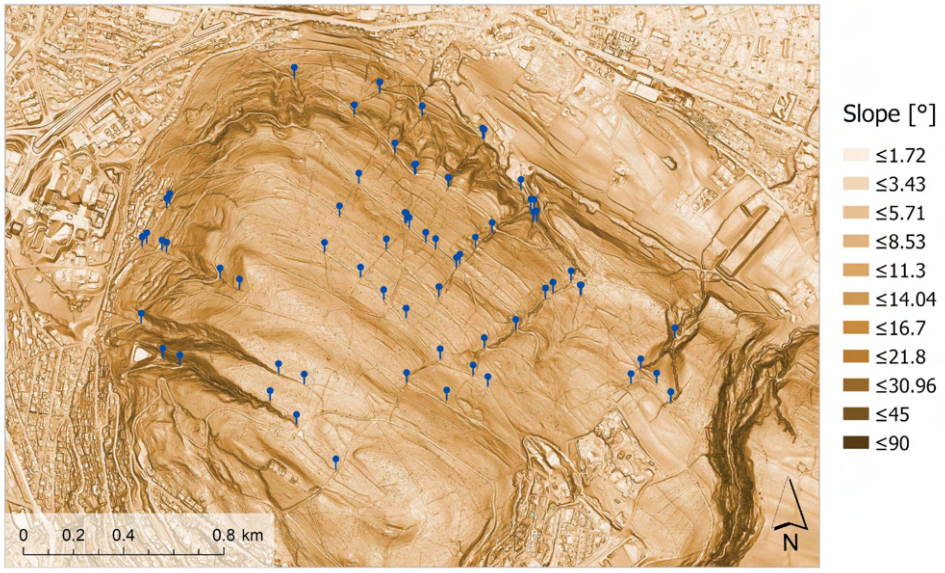


Figure 5: Topographic slope in the study site area on Zürichberg with the measurement locations marked. The slope is calculated based on the Digital Elevation Model (DEM) (Data source: Swisstopo, 'swissALTI3D').

## 2.4 Land use

Land cover refers to the physical material that covers the Earth's surface and is influenced by meteorological, geological, ecological, and anthropogenic factors (Costigan et al. 2016). In the study area part of Zürichberg, the land cover is relatively uniform, with deciduous forest coverage dominating. Land use, on the other hand, refers to how the landscape is anthropogenically managed and modified. For instance, alterations in the course of a streambed or infrastructure modifications such as culverts, weirs, and dams affecting the land use (Costigan et al. 2016). Zürichberg serves as a popular recreational area for the local population. The accessibility is remarkably good due to the well-connected network of forest roads and paths. Land use is therefore strongly influenced by human use of the area which can severely disturb the hydrological networks and ecosystems. It is integral to understand how diverse anthropogenic activities modify these systems along with concurrent natural modifications (Cooper et al. 2013; Costigan et al. 2016).

### 2.4.1 Anthropogenic alterations on Zürichberg

Due to the extensive utilization of Zürichberg for forestry and recreational purposes, human activity has significantly altered the landscape and streamflow paths. The dense network of roads and paths on Zürichberg provides convenient access to the streams; however, these roads interfere with the natural landscape and topography, resulting in various alterations of the stream network. Some streambeds are modified manually to alter the stream's course. Additionally, there are several pipes and fountains distributed throughout the study area that generate additional surface runoff. These insert significant amounts of water into the system but it is unclear whether the source of the water is natural or partly human-induced. Unpaved forest roads can function as small-scale dams in the study area as they form an obstruction to the natural streamflow direction. In order to prevent the accumulation of water, pipes have been installed underneath the roads to facilitate water flow downhill. The high alteration of the natural water flow posed a particularly large challenge in the calculation of the catchment areas. Furthermore, it was also observed that during the data collection period, streambeds were manually created or reinforced with machinery to direct water flow in a specific direction. The data collection for this study was however not affected by this, as it was in an area at the base of the hill where no measurement points were located. Additionally, there were forestry and logging operations occurring on Zürichberg during the data collection period. Due to insufficient information on the spatial extent, precise duration, and the exact impact on both the quantity and quality of streamflow, it was not taken into account in the analysis.

Zürichberg also serves as a critical site for both the extraction and storage of drinking water. The 'Strickhof' reservoir, located at the foothills of the forest above the Irchel campus of the University of Zurich, stores water which is pumped from Lake Zurich. Moreover, a building with the inscription "Quellwasserfilter Streitholz", translating to "Spring Water Filter Streitholz", indicates that spring water is also collected on Zürichberg. This is supported by the dataset of springs, visualized in the map in Figure 6, which shows many natural springs as well as tapped springs throughout the study area. These findings have a substantial impact on the hydrological characteristics of Zürichberg, specifically modifying the interactions between groundwater and surface water, which can greatly affect the flow patterns of temporary streams (Tramblay et al. 2021). The abstraction of water can lower the groundwater table (Costigan et al. 2016), and exert pressure on the flow intermittency in temporary streams.

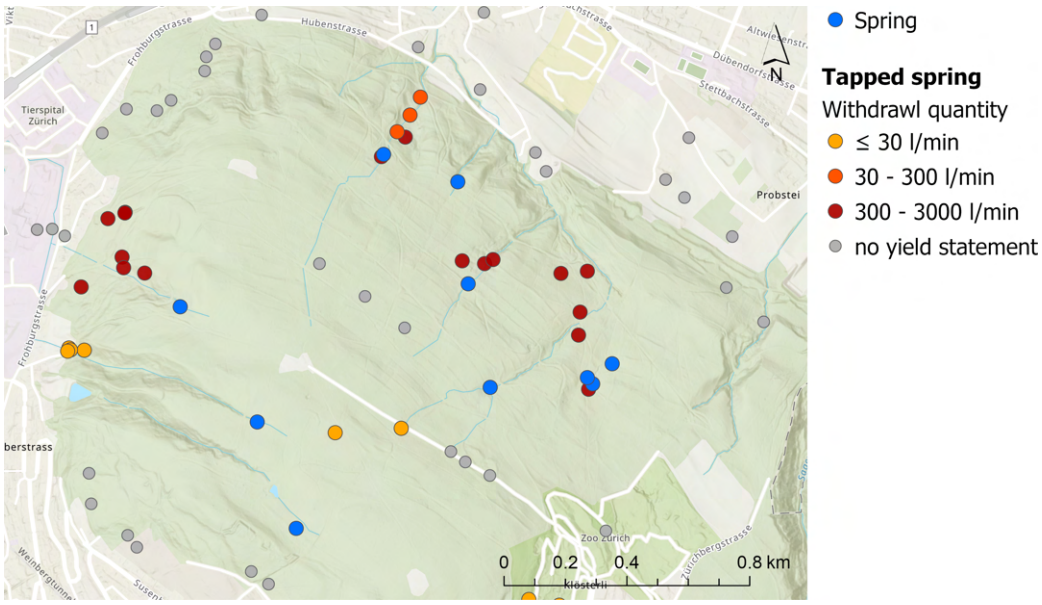


Figure 6: Distribution of natural (blue) and tapped springs in the study area. For the tapped springs the approximated amount of withdrawn water is indicated as well (Stadt-Zürich 2023a; Stadt-Zürich 2023b).

## 2.5 Stream network

Streams are commonly represented on standard topographic maps. However, there are considerable disparities in the extent of the stream network that is shown on those maps, and temporary headwater streams are frequently underrepresented or depicted inaccurately, as stated in Chapter 1.2.2. In the first map in Figure 7, the study area is presented in Google Maps. Streams are depicted as light blue lines, but not comprehensively. Numerous stream segments are either not mapped at all or are incomplete. For instance, at location 1, a portion of the stream is absent. In addition, the stream in the northeast corner (location 2), terminates halfway down the slope, although in reality, it continues downhill as a reasonably substantial stream. Other streams are completely absent on the map (locations 3). This map therefore reveals that there are examples where commonly used and widely known mapping services inadequately depict temporary headwater streams. The Swisstopo map by the Federal Office of Topography uses the dataset swissTLM3D to visualize streams. In comparison to Google Maps, the stream network is significantly more extensive, exhibiting elongated streams and featuring numerous streams not depicted on Google Maps. Consequently, the map provided by Swisstopo was utilized for various tasks during the fieldwork of this thesis. Nonetheless, it was observed in the field that the Swisstopo map is also incomplete, as it does not display several streambeds, some of which are dry while others did have flowing water at least for some time. The Swisstopo map was expanded to include new streambeds discovered on Zürichberg. In addition to field observations, a slope map created in ArcGIS Pro was utilized to locate streambeds in the terrain. The bottom map in Figure 7 presents the enhanced stream network, where stream segments were

added in light blue to the existing dark blue network by Swisstopo. In certain streams, it was noted that their length slightly exceeded the length indicated by the map. Additionally, some stream reaches, for example, the two streams located near the red X, are completely missing on the official map. Some stream segments had surface water or flow near the roads for a period of time, but due to visibility obstructions and difficulty of access, there is uncertainty as to where the surface flow continued. The streambed can be traced to some extent in ArcGIS Pro, but in some cases, the streambeds ended or it was not entirely clear from the map where they continued. Accordingly, it should be noted that this map is incomplete as well but it shows that temporary headwater streams are in fact often omitted from maps. Because of the sheer abundance of headwater streams on Zürichberg, field mapping proves to be time-intensive. Other methods, like determining them from aerial images, cannot be used due to their small size and location in a forested area. Additionally, their placement in the forest makes accurate field mapping challenging, as following the stream through the dense bushed and sometimes steep terrain is difficult.

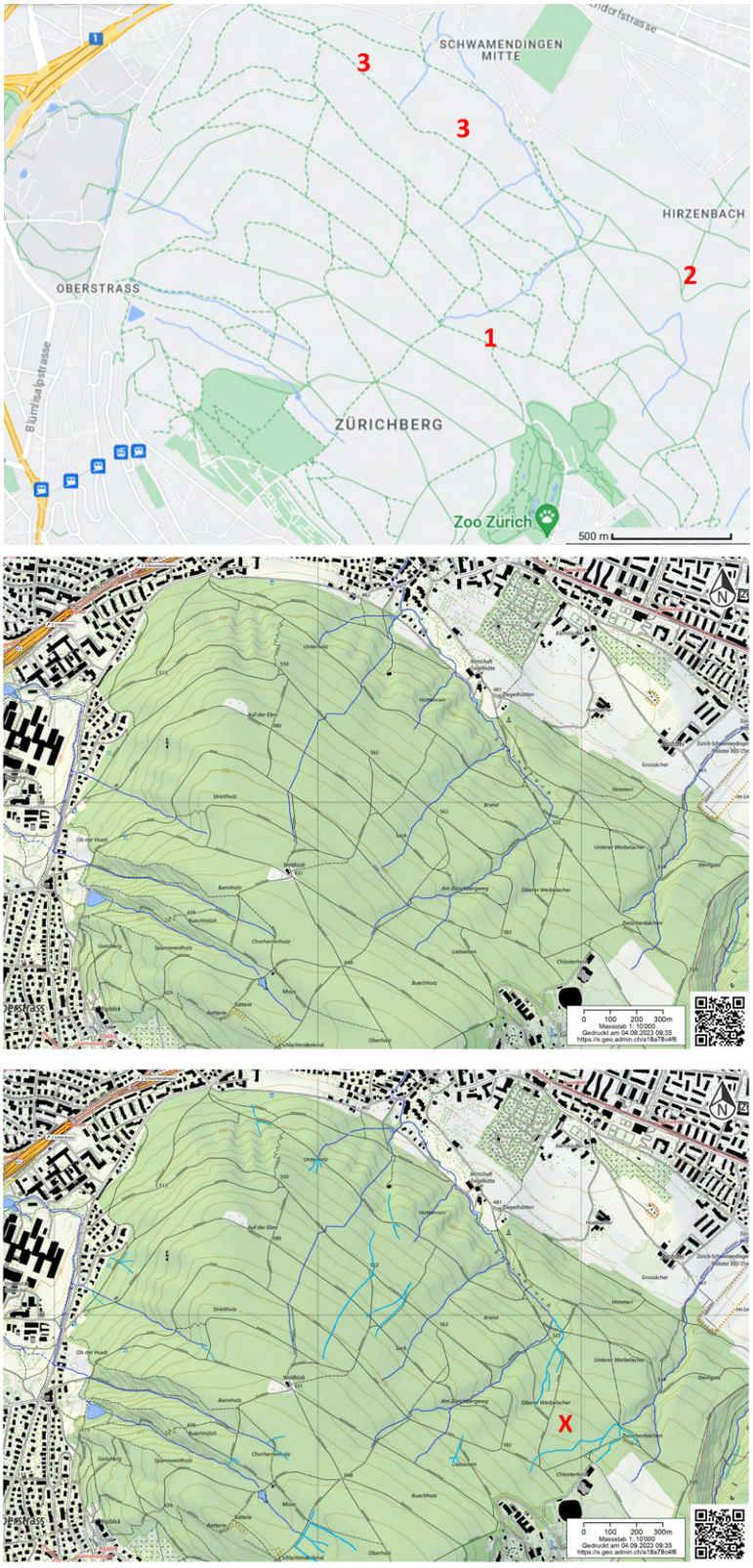


Figure 7: Top: Stream network mapped in Google Maps (global map service). Map source: Google Maps (04.09.2023). The labels (1-3) indicate missing streams or stream segments (see text); Middle: Stream network mapped by Swisstopo based on the dataset 'swissTLM3D'. Map source: Federal Office of Topography Swisstopo, National Map 1:25 000; Bottom: Stream network mapped by swisstopo, extended with additional stream segments observed in the field. The red X marks an area where two streams were completely missing.

# 3 Methods

The objective of this thesis is to investigate the variability in streamflow and streamwater electrical conductivity (EC) within the headwater stream network on Zürichberg, and to examine how topography and geology can explain this variability. The possibility of using runoff and EC measurements to predict dry periods during the summer months will also be investigated. In order to achieve this, extensive fieldwork was carried out to collect data on runoff and streamwater EC. The precise methods will be discussed in greater detail below. All programming related to the statistical analysis and visualization of the data was conducted in Python. For generating maps and performing the watershed analysis, ArcGIS Pro was used.

## 3.1 Measurement design

As an initial step, sampling locations were selected based on the factors of accessibility from paths and stream characteristics for specific measurement methods, including pipes for the bucket method and suitable stream segments for the salt dilution method. The number of measurements was restricted by time, as all measurements had to be taken in one day. A variability of streams with flow and without flow at the beginning of the data collection in the fall was selected with the expectation that some would begin producing runoff later on in the measurement period. Additionally, the full elevation range of the forested area and sites spanning all geologic units were included to study the influence of topography and geology. Furthermore, ensuring an even distribution of measurements throughout the entire study area proved difficult due to challenges such as unidentifiable streambeds and lack of visible surface runoff in certain areas at the time of site selection. For instance, in the northwestern region, neither field observations nor the topographical maps based on the DEM from Swisstopo provided clear identification of streambeds. This also did not change later on, despite the observed increase in surface runoff in other areas. The study excluded pipes and fountains with unknown water sources from the analysis due to the inability to calculate their catchment areas and the uncertainty of their runoff production being influenced by natural or human-related factors. Figure 8 displays the location of all sampling points and their ID number.

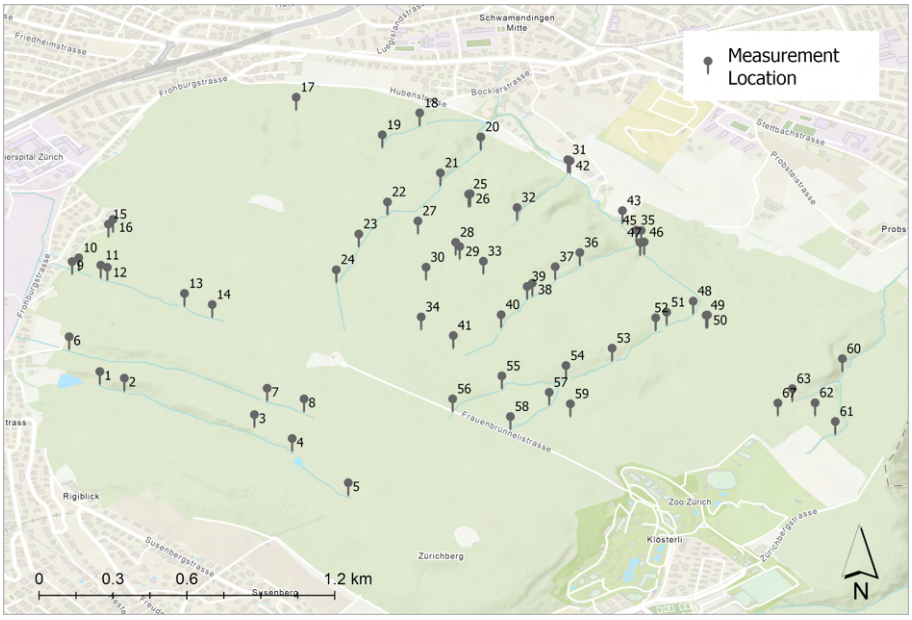


Figure 8: Distribution of measurement locations on Zürichberg. For identification purposes in following analyses, the ID numbers are shown as well.

Data was collected through field surveys, in which all locations were sampled in a single day. Measurements were taken approximately once a week, but scheduling and weather conditions caused irregularities. Dates were planned ahead of time to ensure a randomized set of meteorological conditions. Exceptions were made for days with heavy irregular rainfall which were rescheduled. This was done to avoid any lack of comparability between measurements from one day due to the influence of precipitation as immediate input to streamflow. In contrast, measurements were conducted as scheduled during days of continuous light precipitation, as this did not significantly impact the measurement's accuracy. A total of 24 field surveys were conducted during a 28-week period from November 2022 to May 2023. Originally, measurements were planned from November to March. However, due to the prolonged dry period in January and February, and the desire to collect data about the variability during the wet season, the data collection period was extended through May. The order of the measurements was carefully planned to ensure that the runoff measurements with salt tracer did not influence the downstream measurements. This was achieved by measuring downstream reaches before upstream locations or allowing sufficient time to elapse between measurements to avoid any impact. Further information regarding all measurement locations and watershed characteristics is summarized in Table A2 in the Appendix.

## 3.2 EC measurements

Electric conductivity (EC) was measured at all locations with sufficient water to submerge the conductivity measuring cell of the WTW Multi 3320 meter. As the EC is also impacted by temperature, this device displays the EC compensated for temperature at 25°C (Correa et al.

2017). To ensure reliable measurements, turbulent segments were avoided because they affect the measured EC value due to air bubbles (Merz and Doppmann 2006). Furthermore, the probe was kept in the water until the value stabilized. Another measure taken to enhance data quality was to conduct the measurement in an upstream direction from the standing location to minimize the potential impact of the soil water being pressed into the stream due to the author's weight, which might have altered the EC value.

## 3.3 Runoff measurement

The runoff (Q) measurement method for each site was determined during the initial visits to the study area. The chosen methods to measure the runoff include the bucket method, salt dilution, and estimations, which are further elaborated in the following sections.

### 3.3.1 Bucket method

Runoff was measured using the bucket method at selected sites with pipes carrying moderate to low outflow and where it was feasible to collect the complete streamflow. A 10-liter bucket with 4- and 5-liter markings was used for this purpose. However, the bucket method could be applied to fewer sites than initially planned. On one hand, several pipes on Zürichberg are positioned at ground level, making it impossible to place a bucket underneath them. On the other hand, it became increasingly challenging to take precise time measurements as the runoff increased. As a consequence, adjustments needed to be implemented to the measurement method for certain locations during the measurement period. For instance, the salt dilution method described in Section 3.3.2 was used to replace the bucket method where feasible, but at some locations, the runoff measurement was stopped because there was no reliable alternative. These sites were then excluded from the statistical analyses of the runoff, but the EC was still continuously measured.

### 3.3.2 Salt dilution method

The salt dilution method is used to calculate runoff in small streams with turbulent flow or shallow depth. It involves introducing a tracer solution into the stream and monitoring its dilution over time at a downstream location through EC measurements. These measurements can be integrated over time to determine stream runoff (Sappa et al. 2015). Regular table salt (NaCl) was used as a tracer at concentrations that did not harm the environment. The selected stream segments for this methodology must meet certain requirements. These include achieving complete horizontal and vertical tracer mixing with streamwater within a short distance. Furthermore, the accumulation of water in areas with low flow velocities must be avoided to prevent prolonging the tracer's passage time (Moore 2003; Moore 2005). The distance between the injection and the measurement location depends on how well the water is mixed, which

relies on stream morphology (Moore 2003).

For every measurement, the necessary salt amount was estimated based on the targeted EC peak values (at least 150% of the background concentration), estimated runoff volume, and prior measurement evaluations (Moore 2005). After dissolving the salt in a specific amount of water, the relationship between the NaCl concentration and the EC was calibrated through eight measurements of 0.2 ml salt solution in 250 ml of "pure" stream water. Subsequently, the value of k is established through the slope of the correlation between the relative concentration and the measured EC (Bronge and Openshaw 1996). Additionally, the background EC was measured at the point of injection. Downstream, the EC meter was positioned in the main section of the streamflow, avoiding turbulent areas with substantial air bubbles that can affect EC measurements. The measurements were automatically recorded every five seconds. The salt solution was injected into the stream in a slug injection and EC was continuously monitored until it returned to the initial concentration. Typically, the salt concentration measured over time produces a curve resembling Figure 9. From these data, discharge was calculated using the mass balance equation 1 (Moore 2003; Moore 2005).

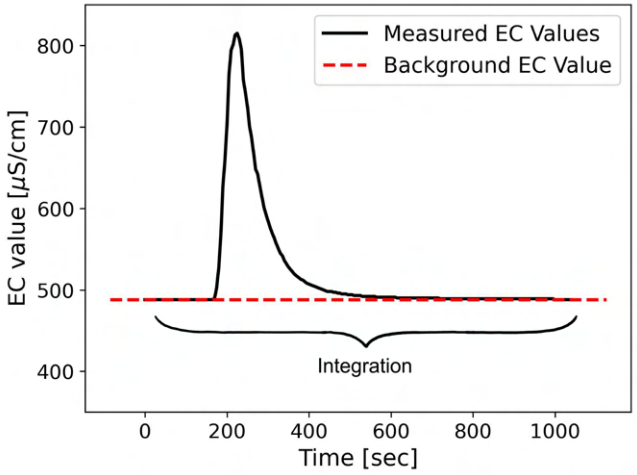


Figure 9: Exemplary breakthrough curve showing the change in EC in response to the instantaneous injection.

$$Q = \frac{V}{k \cdot \int_0^{t_{end}} (EC(t) - EC_0)dt} \tag{1}$$

where: Q [l/s] is the runoff, V [l] is the volume of injected tracer solution, k is the slope of the relationship between the conductivity and the salt concentration, EC(t) [$\mu$S/cm] is the EC value at time t, $c_0$ is the background EC value [$\mu$S/cm], and dt [s] is the time interval between EC measurements.

As the measurement period progressed, the runoff in numerous streams increased, resulting in more stream segments that were suitable for salt tracer measurements. Consequently, some sites that were initially measured using the bucket or estimation method at lower runoff were measured with the salt tracer method at higher runoff levels. However, it should be noted that the salt dilution method is more time-consuming than the other methods, which restricts its practicality. Therefore, the increase in salt dilution measurements was limited, even if there were additional streams with sufficient streamflow in appropriate reaches.

### 3.3.3 Estimation

At sites where both the bucket and the salt tracer measurements were not feasible due to obstructions, larger pools, low flow rates, or other reasons, the runoff was estimated to the best of the author's ability. Many of these estimated streams had little to no runoff at the beginning of the measurement period, making it easier to estimate the discharge compared to streams with higher runoff. Nevertheless, such estimations come with a significant margin of error. Due to challenges in estimating higher streamflow quantities, the locations that continuously had estimated runoff values higher than 80 liters per second were excluded in retrospect.

## 3.4 Data analysis

### 3.4.1 Watershed analysis

The measured and estimated runoff values required normalization by the catchment area to obtain specific discharge (q) values. To achieve this, a watershed analysis was necessary to determine the catchment size for each measurement location. The catchment areas were also required for determining the mean catchment slope variable for the correlation analysis later on. The analysis was conducted using the Spatial Analyst toolbox and the Hydrology toolset within ArcGIS Pro. The Digital Elevation Model (DEM) from swissALTI3D (Swisstopo), with a resolution of 0.5 m, formed the basis for the calculation. The approach is based on the simplified assumption that runoff follows the surface topography, even though subsurface flow does not always follow the suggested directions by topography and may change over time, based on water table gradients (van Meerveld et al. 2019).

The aforementioned dense road network on Zürichberg posed a challenge for the watershed analysis because streets act like dams for surface runoff. Therefore, pipes have been installed to drain the water underneath the streets to prevent them from flooding. However, the DEM does not include these pipes, and the program fails to recognize water flow through them. For this reason, each pipe had to be manually breached in the following process. To start, the pipe locations were mapped in the field. The precise coordinates of the beginning and end points of the pipes were then determined with the help of the slope map (see Figure 5) and the DEM. It was essential to ensure that the starting pixel had the lowest elevation in the vicinity and

that the pixel at the end of the pipe had a lower elevation to guarantee the correct downhill flow direction. For each pipe, a line was created between the two coordinate points. Each line was then converted into a raster format and assigned the minimum value of the corresponding pixels on the DEM layer. Subsequently, the line layer was superimposed on the DEM. Next, any potential sinks up to 1 m deep in the DEM, where water would accumulate, were filled. Such sinks may be either natural sinkholes or result from errors in the data set. The next step in the process involved determining the flow direction, where for each pixel the steepest descent to the D-8 neighborhood was calculated. With the flow direction layer and the coordinate points of the measurements, the number of pixels that drain into each specific site was determined. Since multiple measurements were taken in one stream the catchments were interleaved. Therefore, the analysis had to be segmented into groups of points that do not share any common catchment area. The area in square meters was calculated based on the count of pixels per watershed. For the analysis of potential correlations with topographical factors, the mean slope for each of the catchments was calculated by creating polygons from the raster data in the first step. Next, using the 'Zonal Statistics as Table' tool with the slope layer, the average slope per watershed was determined. The summarized results can be viewed in Table A2 in the Appendix.

### 3.4.2 Statistical analysis

For the statistical analysis of the data collected, sites with less than five measurements were excluded. This decision was made due to the significant uncertainty that arises when calculating statistical variables from a limited number of measurements. However, by setting the threshold higher, a bias towards streams with less pronounced intermittency would be introduced. As a compromise, the cut-off was chosen at five values. The coefficient of variation (CV) was calculated to analyze the variability of discharge and EC values over time. This is a measure of the dispersion of values around the mean and was used in maps to show spatial variation, as well as in correlation analyses. The Pearson correlation coefficient was calculated in order to identify possible linear relationships between stream measurements and catchment attributes such as site elevation, mean catchment slope, and the presence of Molasse bedrock, using either the CV or the mean. For statistical analysis, the two large outliers in the mean discharge dataset were excluded. The streambed wetness data was analyzed to determine the percentage of dry, wet, and flowing conditions. This analysis will aid in comparing dry measurements across locations and with CrowdWater data. Additionally, a ternary plot will be generated to graphically represent the proportion of the three states of streambed conditions.

### 3.4.3 Comparison with CrowdWater data

CrowdWater is a project of the Department of Geography at the University of Zurich, whereby citizen scientists collect hydrological data via a smartphone application. One category of data collection is temporary streams, where qualitative data on flow conditions can be collected using

the classes flowing, trickling water, standing water, isolated pools, damp or wet streambed, or dry streambed. On Zürichberg, extensive efforts have been made to inform the public about the project with signs. Therefore, there has been relatively dense data collection ongoing since the beginning of 2021. In order to compare my data to that collected by the CrowdWater app, locations from Zürichberg were downloaded from the CrowdWater website (CrowdWater 2023). To prepare the data, both datasets of observations on streambed conditions, were filtered for common points. Two time frames were selected for comparison purposes. The first one covers November 2022 to May 2023, which is the same period as the survey period. The second one spans two entire years from June 2021 to May 2023, encompassing all seasons of the year. These time frames were chosen to compare the collected data with citizen scientists' data for the same period and for a period that also covers dry seasons. For statistical stability, locations with less than 30 observations during the CrowdWater two-year period and less than 10 observations during the six-month period were excluded. Since the CrowdWater data for temporary streams only covers the flow state, dry observation percentages during two different time periods were mapped and visually compared. Furthermore, a correlation analysis was performed to determine the possibility of predicting the likelihood of a stream drying up during summer by examining discharge and EC variability and its relation to the percentage of dry observations made through CrowdWater during the months of July, August, and September of 2021 and 2022. These three months were chosen based on the expectations that they represent the driest conditions of the year due to generally high evapotranspiration rates during the summer and depleted groundwater storages at the end of summer (MeteoSwiss 2023). Pearson's correlation coefficient was used to determine whether there is a statistically significant relationship between the variability in runoff and EC and the dryness of a stream during the dry period.

# 4 Results

## 4.1 Spatio-temporal variation in streamflow

The stacked bar chart in Figure 10 provides a first overview of the temporal course of the normalized discharge measurements during the data collection period. Due to a significant number of missing data points from November 16, 2022, data from this day was excluded from further analysis. Furthermore, some values from November 23, 2022, are also missing. The yellow bars denote locations where no surface flow was measured. Conditions were particularly dry in the beginning, with over 30 streambed locations being dry for the first three measurements. A significant shift in discharge was observed on December 27, 2022, when the number of sites lacking streamflow had decreased by half (from 35 to 17 locations) and the number with runoff in all three categories increased remarkably. Over the ensuing six survey dates, a consistent increase in dry measurements can be observed. Meanwhile, the class ranging from 0 to 0.1 mm/day exhibited only a minor decline in the number of measurements, dropping from 27 to 23. Conversely, the highest two classes (0.1 to $>$ 1 mm/day) decreased from 13 to only 2 measurements. Notably, February 22, 2023, represents the driest day recorded, which will be further analyzed in Figure 11. A shift towards more discharge was observed thereafter, except for March 6, 2023. Especially the number of high discharge values ($>$ 0.1 mm/day) increased again. This coincides with the observed increase in precipitation in the months of March, April, and May (Figure 2). March exhibited a rising trend of streamflow, while in April and May, the trend no longer continued and the conditions varied more among measurement days. Two days, April 17 and May 17, 2023, saw particularly high discharge, with only a limited number of locations showing no flow (8 and 5 locations, respectively). By the end of May, an indication of a drying trend was observed again, but field surveys were stopped.

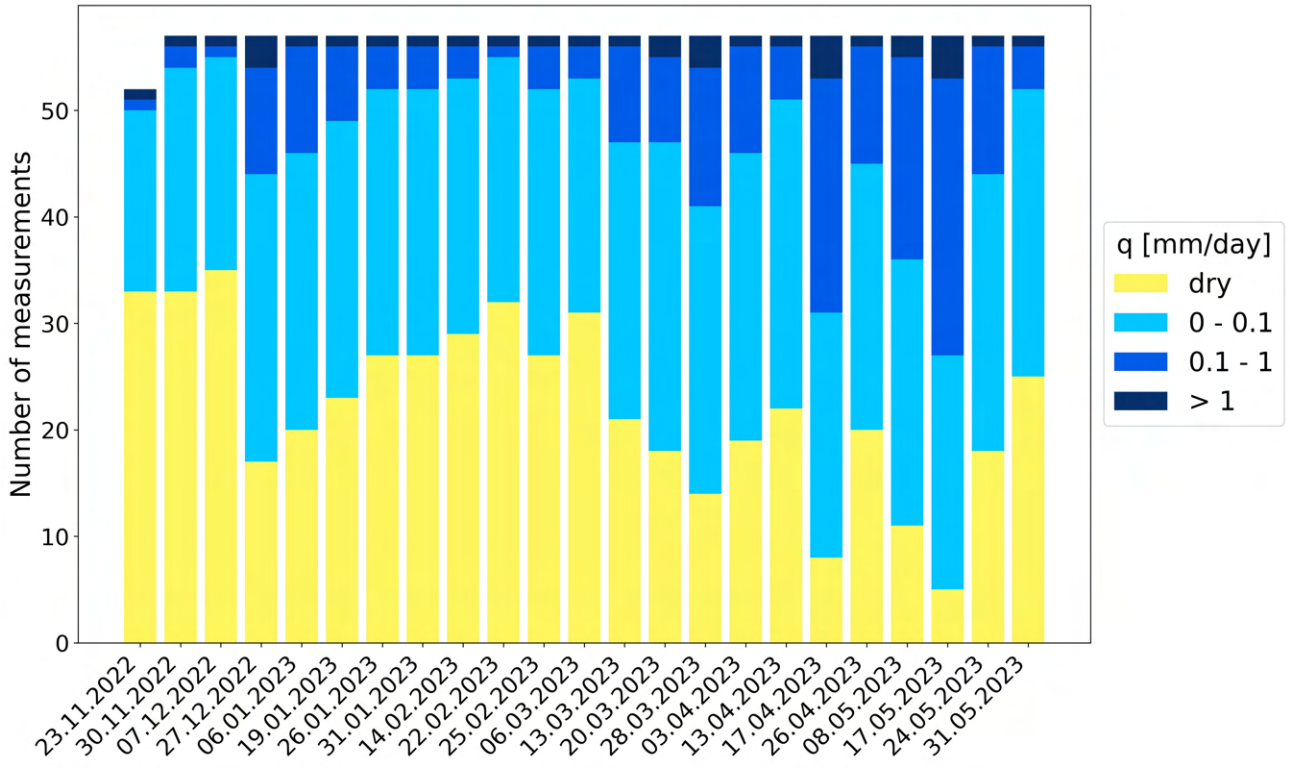


Figure 10: Stacked bar chart displaying the absolute number of classified discharge (q) values for each survey in the measurement period from November 23, 2022, until May 31, 2023 (the measurements from November 16, 2022, are missing due to incompleteness and a few locations are also missing on November 23, 2022).

After analyzing the course of streamflow measurements over time, three specific days were selected for further examination in terms of spatial analysis. These days were chosen to compare variations in discharge amounts. Based on the cumulative discharge measurement for each day, the maximum, minimum, and median of the daily total discharge were selected. The map from February 22, 2023, features the driest measured conditions, following the extended dry period in January and February of 2023. On that particular day, only four locations had a discharge exceeding 0.05 mm, while many streams showed no runoff at all. An interesting observation is that the two locations to the northeast of the zoo (in the lower right corner of the map, ID 61 and 67) exhibit very high discharge even on the overall driest day in the measurement series. However, further downstream at location 60, the specific discharge was significantly smaller. The other two locations that showed increased discharge on February 22, 2023, are located at the bottom of the hill on the northeastern slope (ID 20 and 31). Besides the stream north of the zoo, the first stream northwest of the zoo also exhibits a quite large extent of flowing stream (ID 43–54). The discharge values there are all consistently in the low range.

January 19, 2023, represents the day with median discharge conditions. The map presented demonstrates that, while the conditions over the whole data collection period were predominantly dry, more locations generated runoff or exhibited increased discharge values in comparison

to minimal discharge conditions. A rise in discharge can be observed in streams that retained flowing water throughout the driest conditions generally located at lower elevations. Most of the medium and high elevation sites with flow during the driest conditions did not elevate a category. However, several locations in the medium elevation range were dry on February 22, 2023, but had flow on January 19, 2023, while many of the sites at higher elevations remained dry even during median wetness conditions.

The third map presents the date when the highest volume of total discharge within the study area was recorded, which was on May 17, 2023. Only a small number of stream sites showed dry conditions on that specific day. Nearly all the sites that had flowing conditions at the median state, exhibited increased discharge on the day when the wettest conditions occurred. A few locations increased by one class, whereas locations 8 and 11 in the western part of the study area shifted three classes from dryness to more than 0.1 mm/day. One measurement even increased from being dry to over 1 mm/day (ID 26). Out of the five locations that remained dry, four never exhibited streamflow during all measurements. However, there is no clear trend in the location of these dry measurements. Three of them are located at a lower elevation, while the other two are located at the highest point of their streambed.

Overall, a trend is observed for higher specific discharge at lower elevations in these three maps, particularly in the streams on the northeastern slope, except for the stream below the zoo. This pattern is also evident in the maps of all other survey days, which are accessible in Appendix A3.


Figure 11: Specific discharge (q) on three selected days. Top: Measurements during the day of lowest cumulative discharge (February 22, 2023). Middle: Day of median cumulative discharge (January 19, 2023). Bottom: Highest cumulative discharge per day (May 17, 2023). For the maps for all other survey dates, see Figure A1 - A4 in Appendix A3

### 4.1.1 Coefficient of Variation in discharge

The mean discharge, calculated for each location on Zürichberg over the measuring period, varied between 0.001 and 11.026 mm/day. The location with mean discharge of 11 mm/day as well as another with 2.6 mm/day are outliers as all other locations present values below 0.5 mm/day. Qualitative assessment showed that the amount of discharge varies greatly both spatially and temporally in the temporary streams on Zürichberg. The coefficient of variation (CV) gives further insight into the variability at each measurement site and allows for a quantitative assessment. Therefore, the CV is calculated for each location and visualized in the map in Figure 12, allowing for an examination of possible spatial patterns of discharge variability. Removing sites with less than five measurements from the statistical analysis resulted in the exclusion of many streams at higher elevations. Some locations at lower elevations were also excluded due to imprecise discharge measurements. For locations where the CV could be calculated, a higher value indicates a greater dispersion of the data around the mean and therefore a higher variability of the data. Across all locations, the CV ranged from 62.372% to 148.152%. Refer to Table A2 for the precise values at each location. The highest value is found at ID 5 in the stream situated on the western side of Zürichberg. The three streams on this side have several other locations with substantial variability, and only one location has a CV below 82%. On the northeastern side, there are also numerous locations with high variability, but more sites have variability ranges in the lower end as well. These sites with less variability are predominantly situated at the foot of the hill. The patterns within the streams are not as apparent, although the stream with locations 20, 21, and 22 exhibits a trend of decreasing variability downstream. This downstream trend is also observed in the stream with locations 35, 36, 37, and 38. A noteworthy observation is the four measurements in the stream northeast of the zoo, which show rather low variability.

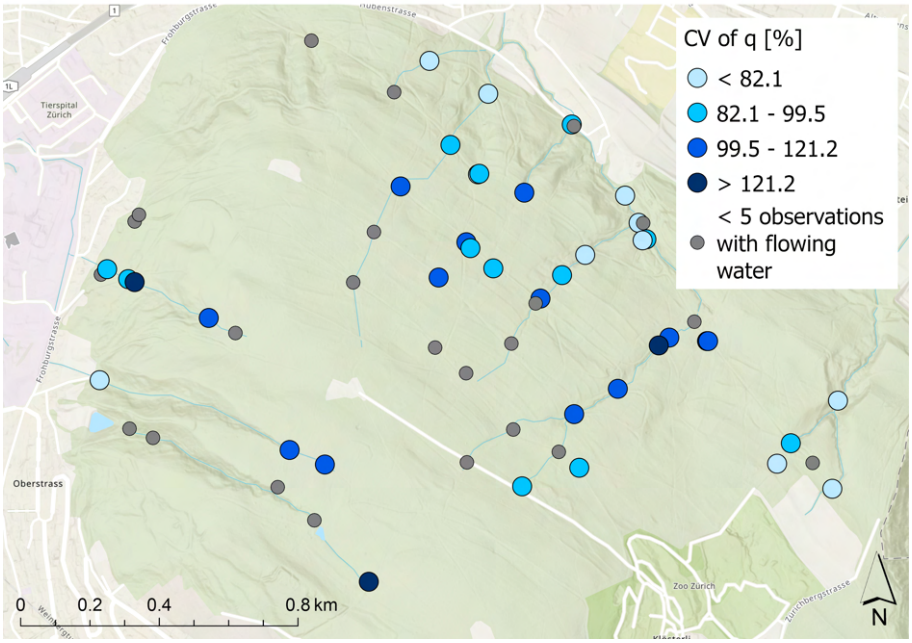


Figure 12: Spatial pattern of the coefficient of variation (CV) calculated based on the discharge measurements between November 2022 and May 2023 across Zürichberg. The CV was only calculated for the days for which there was flowing water.

### 4.1.2 Patterns of flow states

Because numerous points in the CV have insufficient flow measurements and therefore a CV could not be calculated for them, the percentage of times each site was recorded to be dry is also illustrated as an additional value that is available for all locations. This is visualized in the map in Figure 13. Dry conditions are defined as streambed conditions that do not have an elevated moisture content compared to the surrounding soils. Thus, if the streambed was wetter than the surrounding area or standing water was present, it is no longer considered dry. The spatial distribution of the number of dry measurements at each stream location shows that, generally, there are more dry measurements at higher elevations than at lower ranges of Zürichberg. However, this is only a trend, and not all locations follow it. In the northwestern part of Zürichberg, there is an area where locations at the bottom of the hill have comparatively high levels of dry measurements. Furthermore, there are also points at the top of Zürichberg, particularly in the southwest (ID 4, 5, and 7), that exhibit a relatively low rate of dry measurements. Distinct patterns can be observed among individual streams, which vary from one to another.

To examine this more closely, four streams (labeled A, B, C, and D in Figure 13) were selected and their patterns of dry measurements along the distance of the streambed are displayed in Figure 14. The trend indicates that streams located farther from the first location, and therefore at lower elevations, have a lower proportion of no flow measurements compared to those situated closer to the beginning of the streambed. However, several locations defy this

trend. In stream A, ID 58 exhibits a significantly lower percentage of no-flow measurements compared to both the upstream and the two locations at lower elevations (ID 55 and 57). Whenever measurements were taken, ID 54 downstream had flowing water. In a reach between locations 54 and 53, observations showed that the streambed was dry most of the time, although streamflow was present upstream at ID 54 and reappeared just before ID 53. This information is not shown in the graph because, by ID 53, the surface flow had already reappeared in most of the measurements. At ID 48, surface flow was not maintained at the beginning of the measurement period, resulting in an increase in no-flow measurements. There were no measurements without flowing water downstream of this point. Stream B exhibited very dry conditions for the first three locations. However, followed by a location (ID 38) that had flow measured every time. Surface runoff disappeared again for some of the measurements at ID 37, but constant flowing conditions were measured thereafter. The shape of the curve in stream C most closely follows the trend of increasing no-flow measurements at higher elevations, with the exception of location ID 23, which shows slightly higher no-flow measurements than the upstream location (ID 24). Lastly, in stream D, no-flow decreases at the first three locations (ID 14, 15, and 16), however, the two locations a the bottom of the stream (ID 10 and 11) have more instances where surface water did not flow.

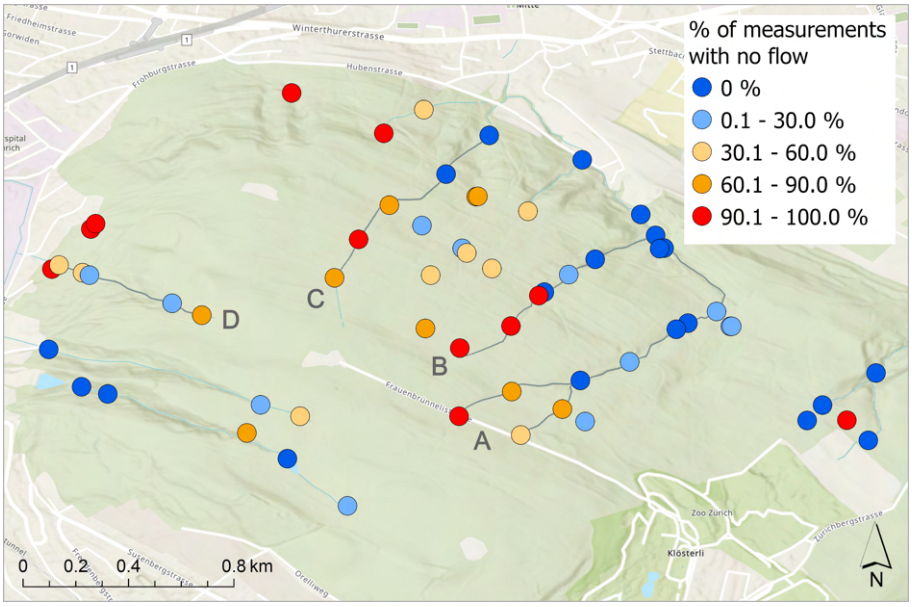


Figure 13: Map showing the percent of measurements where no flow was observed for each of the measurement locations. No flow includes conditions with dry streambed, wet streambed, and standing water. The values of selected streams A-D are plotted as a function of stream length in Figure 14.

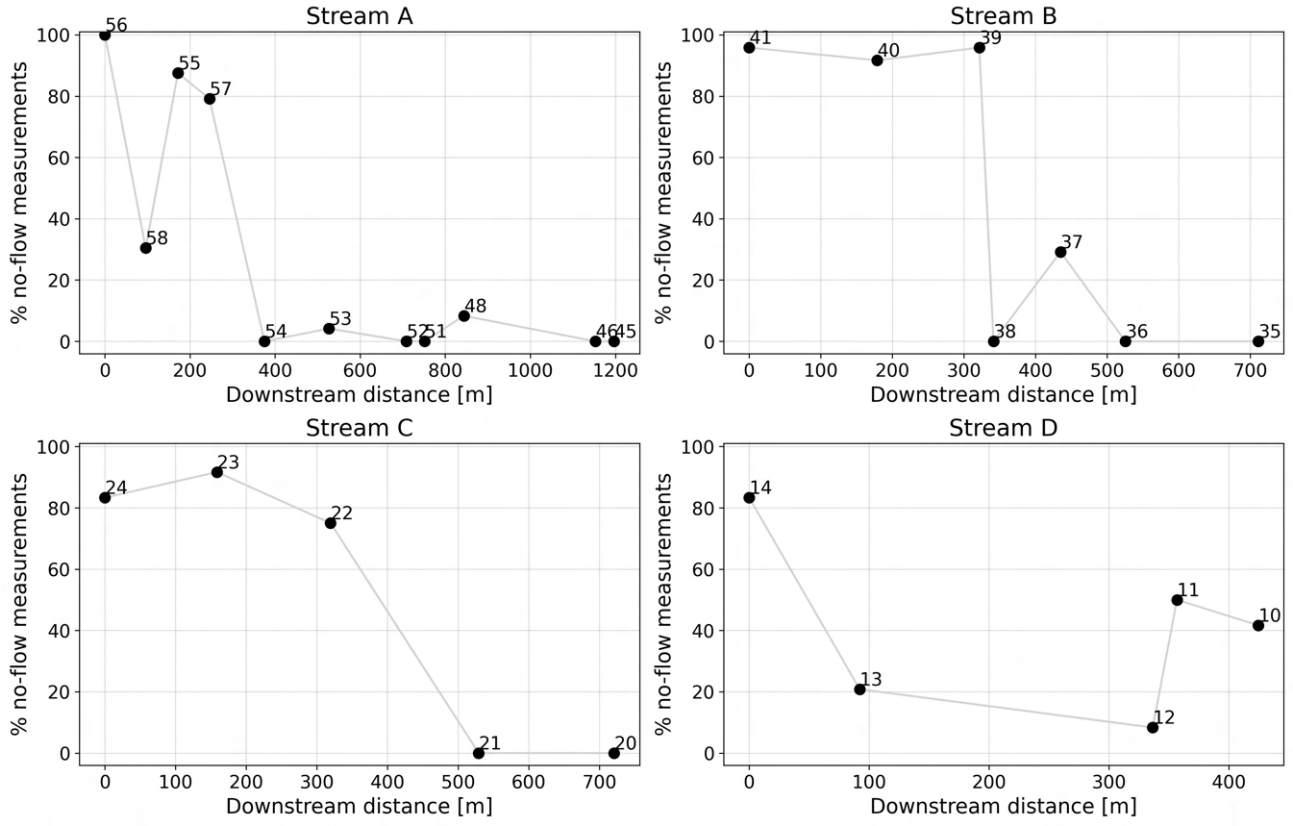


Figure 14: Plots for the streams A, B, C, and D as marked in Figure 13 as a function of the downstream distance. 0 meters does not represent the streamhead, but rather the location of the first measurement in each stream. Distances from downstream locations are measured to this first site.

After looking at the spatial patterns of dry measurements, the patterns of all streambed conditions are now considered. Therefore, to assess the distribution of streambed conditions at each monitoring site and to identify potential patterns, a ternary plot in Figure 15 shows the proportions of flowing, wet, and dry streambed. The wet streambed condition includes the full range between dry and flowing states. Some of the points are overlapping and those measurement points where only one or two of the three possible states were ever measured are located on the border and are partly cut off. The plot illustrates that there were no stream locations predominantly featuring wet streambed conditions, as the points are clustered in the right part of the graph. Two loosely defined clusters are identifiable - one in the triangle's lower right corner, representing streams that were primarily dry with occasional instances of wet streambed and flow. The second cluster in the upper corner indicates streams that typically had flowing water and occasionally experienced dry or wet conditions during data collection.

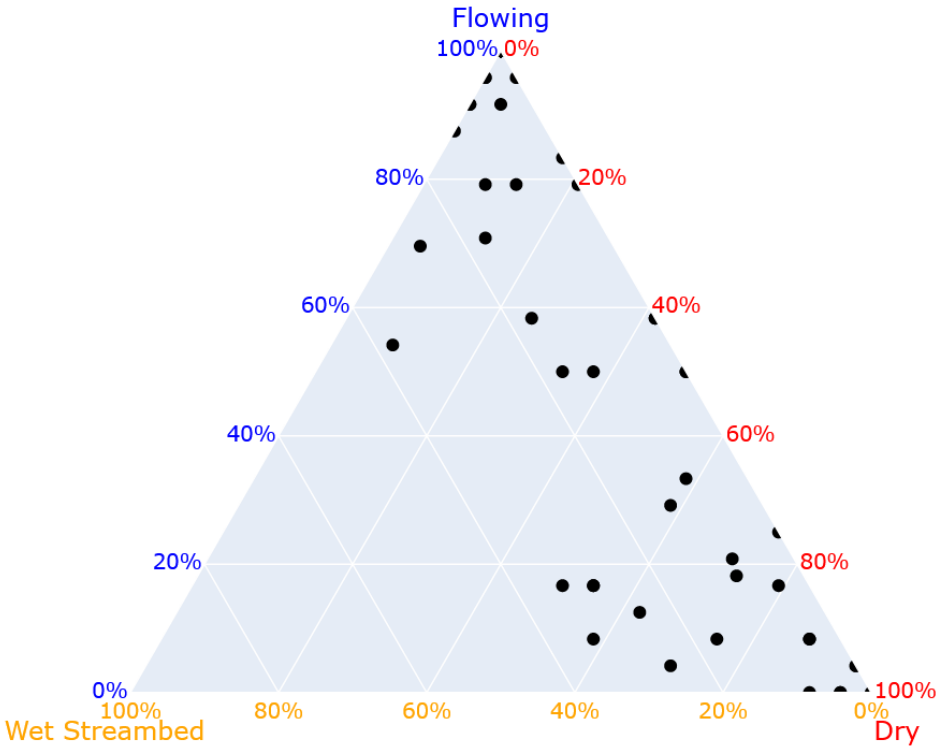


Figure 15: Ternary graph showing for each location the percentage measurements with dry streambed, wet streambed and flowing water for all measurements taken between November 2022 and May 2023.

## 4.2 Spatio-temporal variation in EC

At each location where surface water was present, an EC measurement was recorded as well. However, the number of EC measurements fluctuated significantly over time due to the varying number of streams with measurable water quantities. To provide an overview of the EC values during the data collection period, a stacked bar chart similar to the one for discharge was generated and is shown in Figure 16. The variable number of measurements was standardized to 100 to reflect the percentage for each day and category. The Jenks natural break optimization classified all EC measurements for each day throughout the measurement period. Notably, there is a consistent occurrence of high EC values ranging from 584 to 950 $\mu$S/cm. Exceptions are the two outliers, on November 23, 2022, with a significantly higher proportion of measurements in this class, and the other on April 17, 2023, with a considerably lower proportion of this class compared to an otherwise relatively uniform trend. The low number of high EC values measured on April 17, 2023, coincides with high discharge measurements on that day. However, the same cannot be observed for May 17, 2023. All other three classes present much more pronounced variability. When looking at the second-highest class (red), a noticeable peak is seen on January 19, 2023, followed by a decline. However, the percentage of the second-lowest class (orange) experienced a significant increase after the peak, until there was again a sudden

rise in the percentage of the red EC class with higher values. From then on the classes remain more constant compared to the measurements taken in the first half of the measurement period, with the exception of the measurements taken on April 17, 2023. Simultaneously, the percentage of lower values (yellow) exhibited a small increase before subsequently decreasing again as of April 17, 2023.

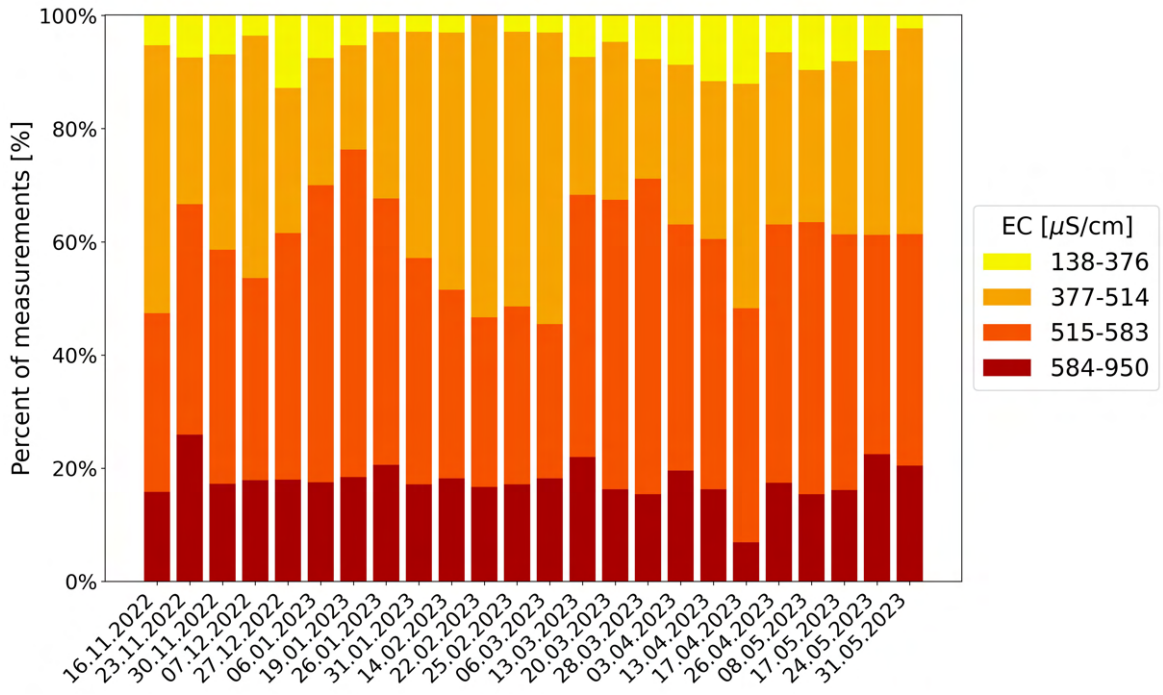


Figure 16: Stacked bar chart of the percentage of EC values for each survey day during the measurement period from November 16, 2022, until May 31, 2023.

Extreme value days for EC measurements were identified based on the daily mean. The lowest values were measured on April 17, 2023, while the highest values were taken on January 19, 2023. The map from February 15, 2023, shows the values closest to the median. Missing data points are indicated in gray to signify locations where runoff was not available or not sufficient for measurement. When comparing the three maps, it is evident that on the day with the lowest EC values, there are significantly fewer locations without measurements than in the other two maps. Additionally, on January 19, 2023, when the overall highest mean EC was recorded, more measurements were obtained compared to median conditions on February 25, 2023. There are some streams with similar EC values across all measured locations, leading to the same classification. This was observed in two of the three streams on the western slope on April 17, 2023. However, on the day with the highest mean EC values, greater variability was observed across the different sites for these streams. Furthermore, several sites maintained their EC classification between the highest and lowest EC days. For instance, location 5 consistently displayed low EC levels, while the values at locations 20, 51, 52, and 54 were consistently between 515 $\mu$S/cm and 583 $\mu$S/cm across all three maps. On April 17, 2023, the streams located on

the western side showed lower EC values compared to the rest of the study area. Among the three streams located in the western part, two of them also exhibited lower EC measurements on the other two days while the third showed a stronger increase. Visual patterns are difficult to assess on the northeastern side. High EC measurements were observed both at the bottom and top of the hill. The stream section located at IDs 48 and 51–54 indicates comparable values on both the days with the highest and lowest total EC values. However, other streams show more significant variations between the two days. On January 19, 2023, the stream with IDs 38, 37, 36, and 35 displays a trend of lower EC values downstream. This inclination is less pronounced in median conditions and absent in low EC circumstances.

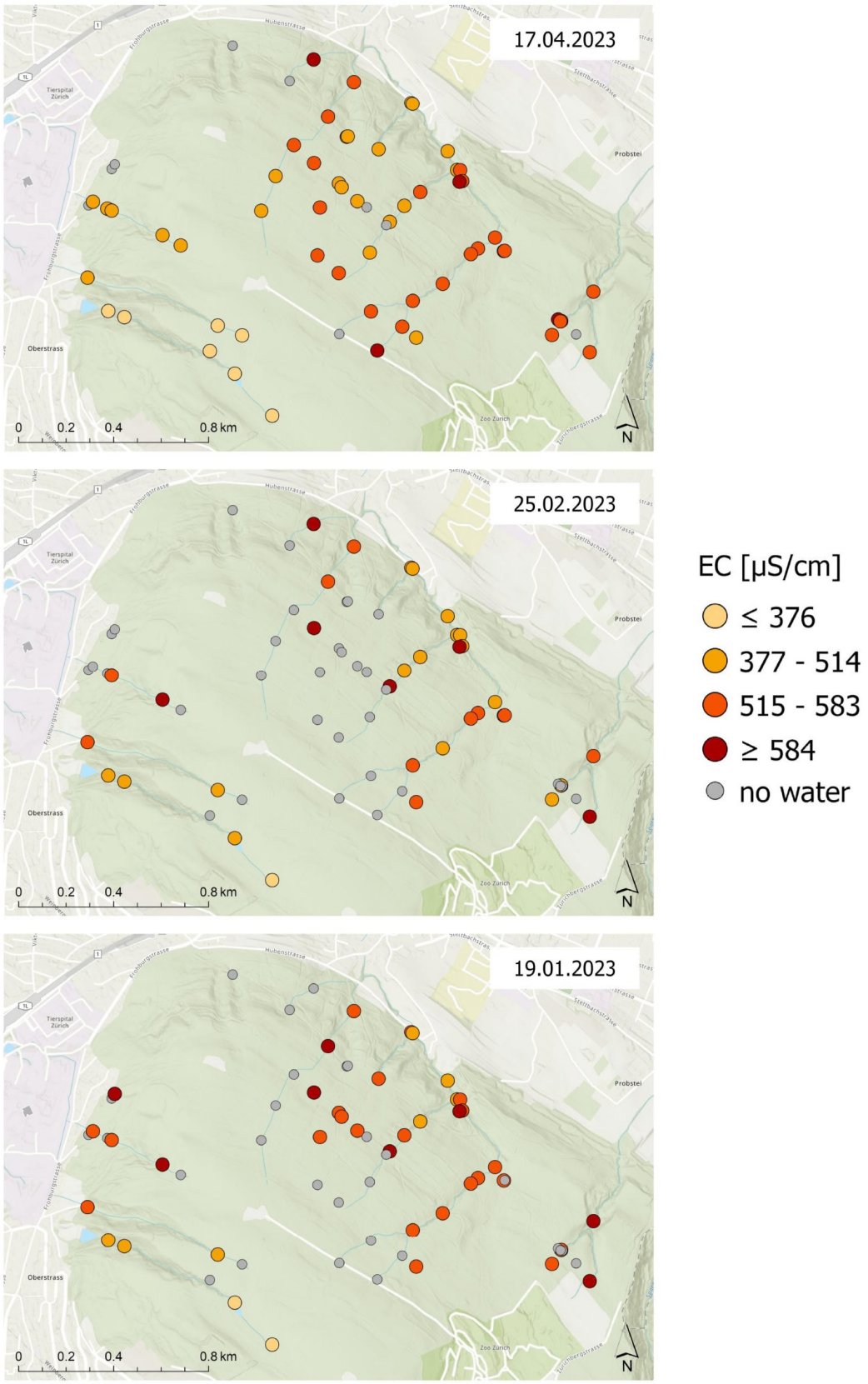


Figure 17: Map showing the measured variation in streamwater EC on three selected days. Top: Lowest mean EC (April 17, 2023). Middle: Median mean EC value (February 25, 2023). Bottom: Highest mean EC (January 19, 2023).

The spatial distribution of the coefficient of variation of the EC is illustrated in Figure 18. Like the CV in the discharge, the CV in EC also exhibits high values in the streams on the western slope of Zürichberg, particularly at the higher elevation locations. The four locations in the stream north of the zoo all exhibit high CV values in the class between 6.364 and 13.609%. The EC variability in streams on the northeastern side is generally low, except for a few instances of elevated variability, which tend to occur at medium elevations on this side of Zürichberg. All other sites demonstrate variability values lower than 3.5% in this area. From the visual analysis of the classified values, the differences in the variability appear to be greater between the streams than within them. Overall it is noticeable that the CV for the EC is significantly lower in comparison to that of the discharge measurements. The site exhibiting the greatest variability in EC has a CV of 21.436% while for the discharge the highest CV is 148.152% (see Table A5 for the detailed values at each measurement site).

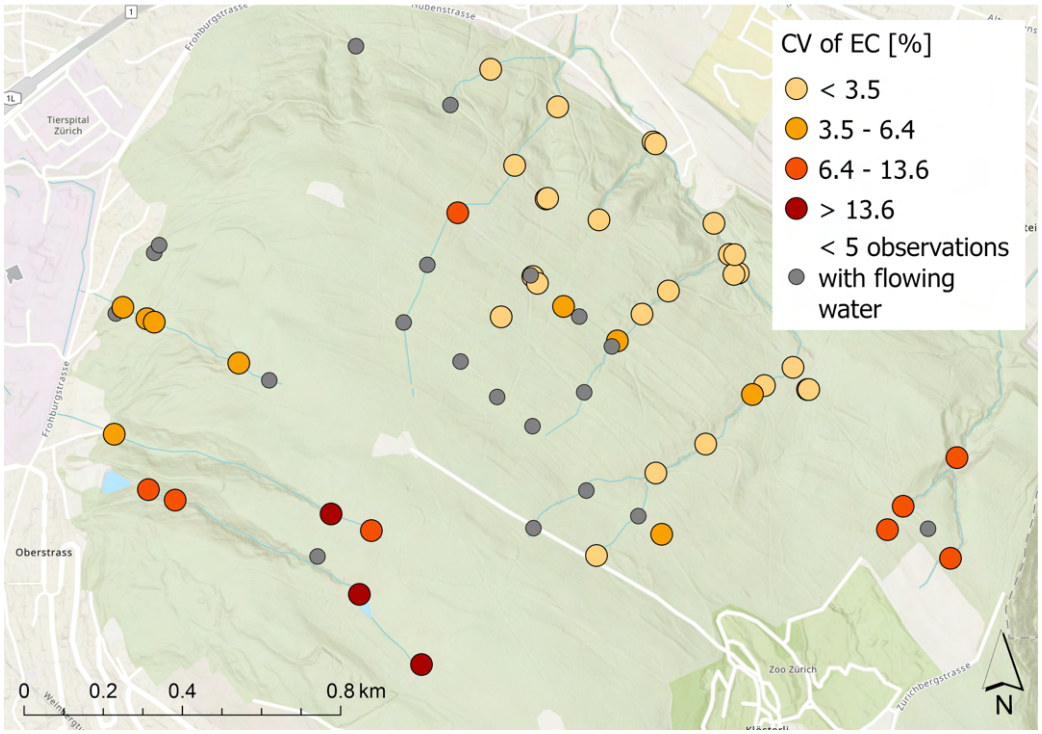


Figure 18: Map showing the spatial distribution of the coefficient of variation (CV) of the EC for all measurements taken during the measurement period.

### 4.2.1 Variability of stream EC responses to precipitation inputs

To analyze how streams react to precipitation inputs, the EC measurements were grouped based on their reaction to the heavy precipitation event on April 16, 2023. The grouped temporal patterns are then visualized in Figure 19 in combination with the precipitation data of the Meteo station Fluntern and the cumulative balance of Precipitation - PET. The upper EC plot (1) shows locations with a clear decrease in the measured EC value after heavy precipitation events. This pattern is particularly evident following the rainfall event on April 16, 2023, as the

EC values measured on April 17, 2023, significantly decreased from the pre-event measurement on April 13, 2023. The measurements on December 27, 2022, and on May 17, 2023, are similar but the decrease is less pronounced. Furthermore, this group of measurements can be further subdivided into two groups. The lowest five to six locations display lower EC values than the cluster of locations above them. Moreover, they exhibit a greater variability over time compared to the more stable IDs in the higher EC range. The high variability measurements are all located in the two southern streams on the western side of Zürichberg (IDs 1, 2, 4, 5, 6, and 7). The stable cluster includes the IDs 10, 11, 12, 13, 18, 21, 27, 28, 32, 33, 38, 47, 51, 52, 54, 59, and 63 which are located across all other streams, at sites of generally lower to medium elevations. Graph (2) illustrates the changes in EC values at locations experiencing significant increases in EC after heavy precipitation. This is particularly evident in the values obtained on April 17, 2023, and May 17, 2023, and slightly less pronounced on December 27, 2022. The line ID numbers for plot 2 include 20, 31, 35, 36, 37, 42, 43, 44, 45, and 46. These numbers are located on the northeastern side of Zürichberg and, with the exception of 37, are located in the lowest part of the hill. An additional factor that distinguishes plots 1 and 2 is the range of EC values. The measurements in plot 1 display a significantly wider range spanning from under 200 $\mu$S/cm to nearly 700 $\mu$S/cm, compared to the more concentrated lines in plot 2, which range approximately from 460 to 560 $\mu$S/cm. Additionally, the second plot demonstrates a decreasing trend throughout the measurement period, which is not evident from visual inspection in the first plot.

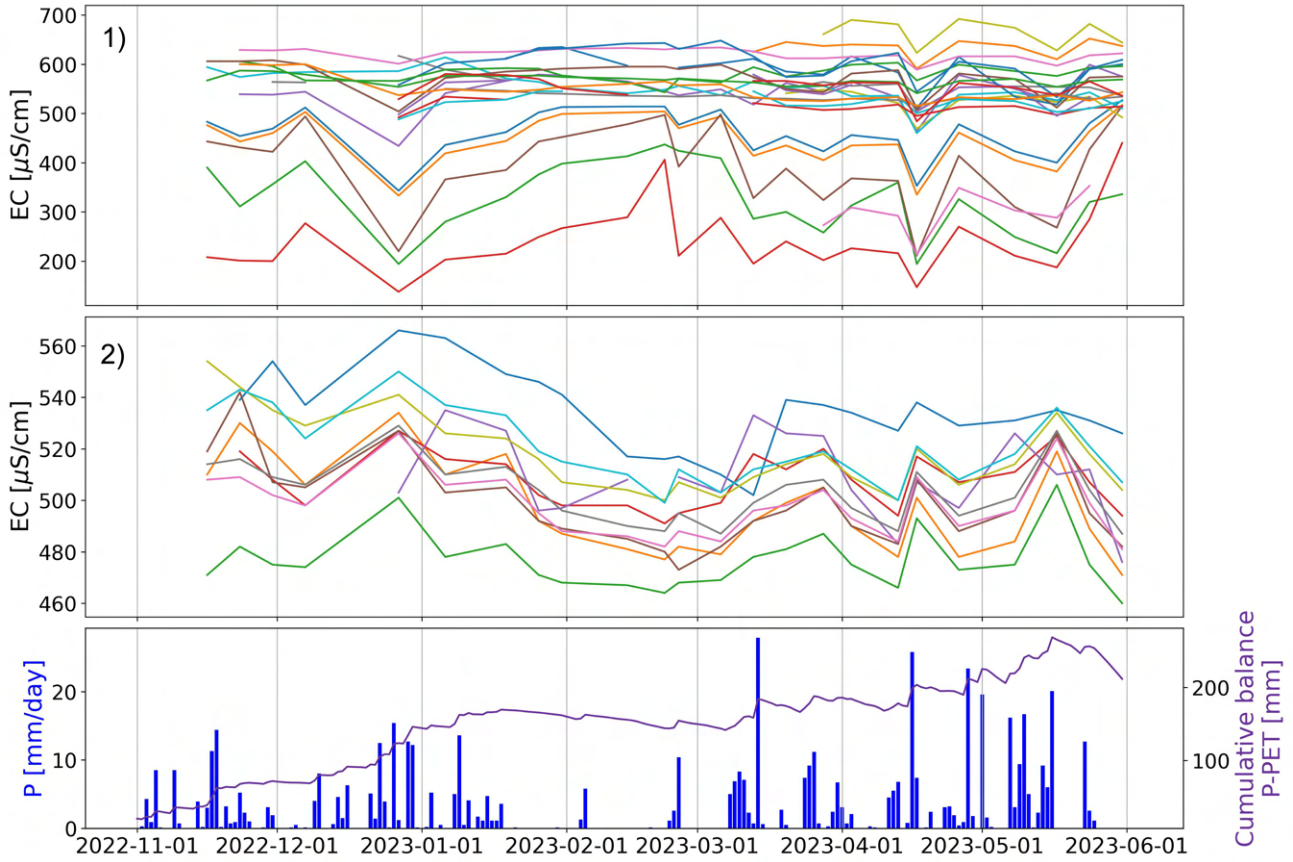


Figure 19: Time series of the EC for locations with similar patterns in the upper two plots and measured precipitation and calculated cumulative daily moisture balance in the bottom plot. 1) Locations showing a (sharp) decrease in response to heavy precipitation. 2) Locations with a (sharp) increase in EC after heavy precipitation (e.g., 17.04.2023 or 17.05.2023).

## 4.3 Correlation between discharge and EC

To analyze possible correlations between the CV and the mean values of the measured discharge and EC values at individual streambed locations, Pearson's correlation coefficient was calculated. Significant correlations were found for four out of the six analyses.

Between the mean discharge and the variability in q, a moderately negative correlation was found (r-value: -0.391, p-value: 0.015). A moderately positive correlation was found between the variabilities of EC and q (r-value: 0.331, p-value: 0.037). A robust negative correlation (r-value: -0.685, p-value: 1.5e-07) was discovered between the mean and variability in EC. This indicates that a higher average EC generally corresponds to a lower temporal variability. This pattern was also evident in the graph (1) shown in Figure 19, where the group with the higher EC values appeared to be more stable than the cluster with lower EC values. Meanwhile, the mean EC and variability in discharge show a barely significant moderate negative correlation (r-value: -0.314, p-value: 0.049). All other analyses with the mean discharge resulted in non-significant p-values.

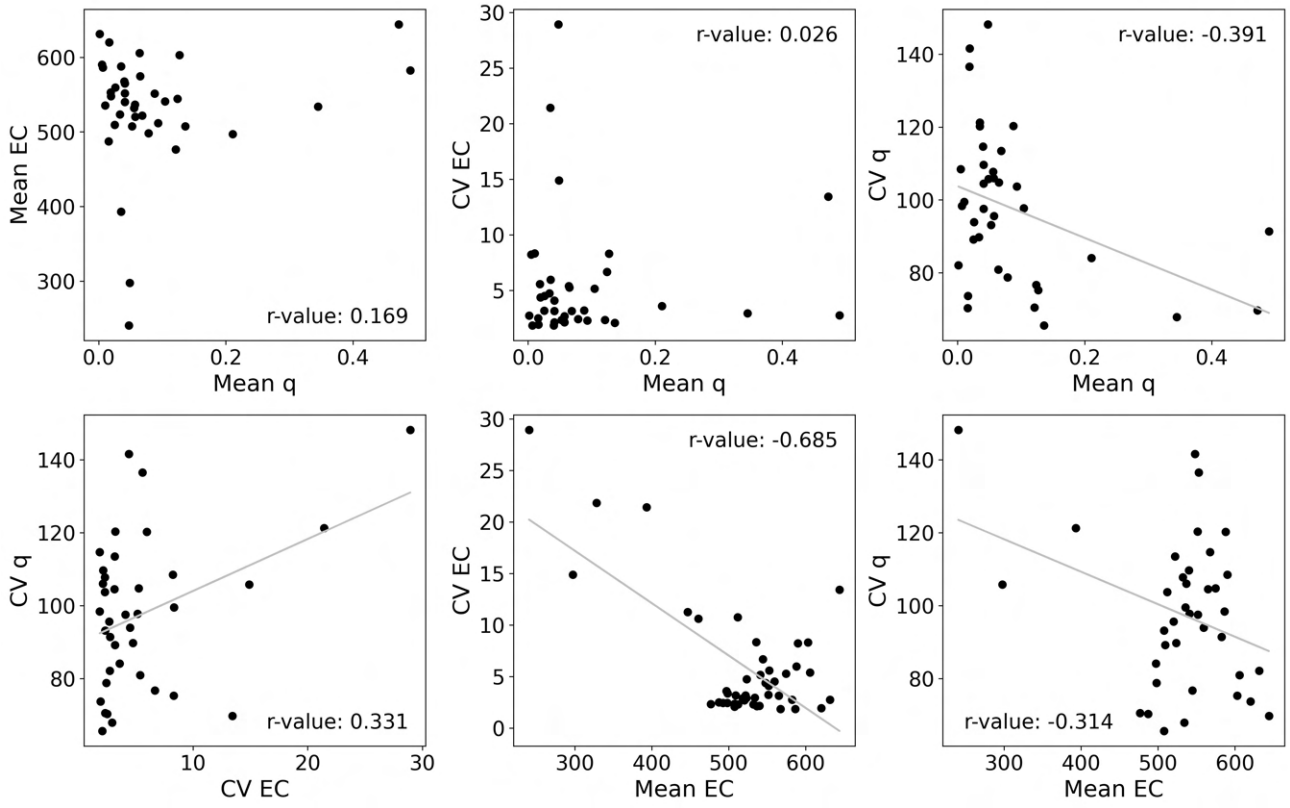


Figure 20: Scatter plots comparing the mean and CV of discharge and EC with each other. Regression lines are only shown for significant correlations.

## 4.4 Factors impacting variability in headwater streams

Further correlation analyses were conducted on factors that are expected to have an influence on the runoff and EC values of headwater streams. The first section investigates topographical relationships. A strong positive correlation (r-value: 0.673, p-value: 2.984e-07) was identified between the CV of EC and the elevation, indicating a tendency for streams at higher elevations to exhibit higher variability in EC values. At the same time, there is a significant, strong negative correlation (r-value: -0.502, p-value: 3.81e-04) between the mean EC and elevation, indicating that streams at higher elevations generally have lower EC values. For the discharge, there was a significant strong positive correlation between the variability in discharge and the elevation (r-value: 0.537, p-value: 3.52e-04), but no significant correlation was found between the mean discharge and elevation.

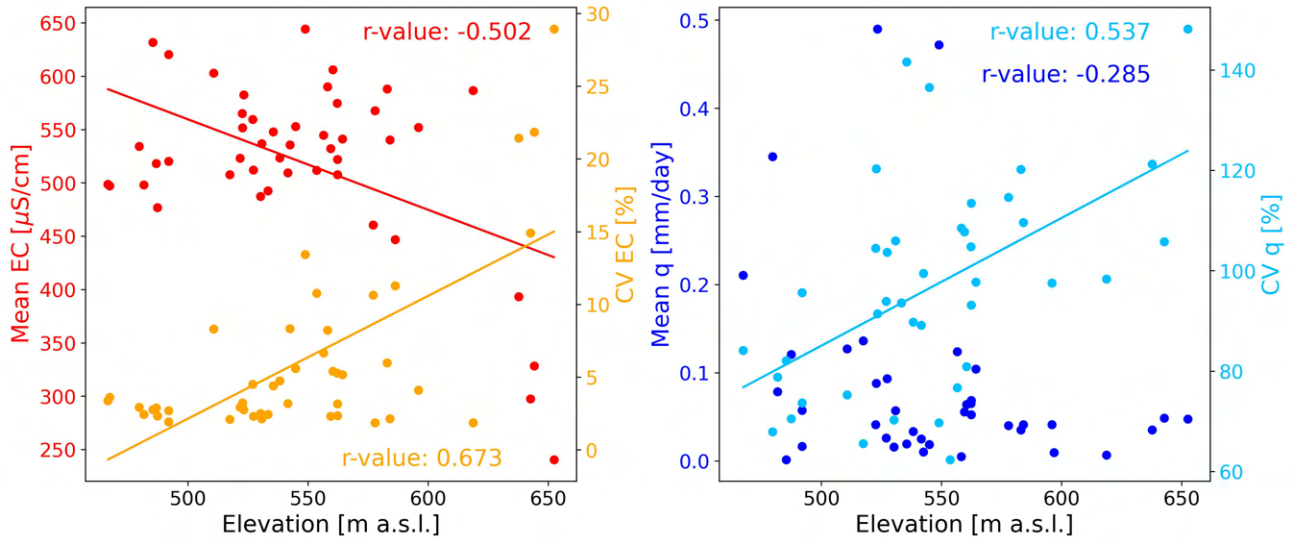


Figure 21: Scatter plot comparing the elevation of the measurement location to the mean and CV of EC (left plot) and to the mean and CV of the discharge (right plot). Regression lines are only shown for significant correlations.

The analysis of the mean catchment slope at each location served as the second topographical variable. The mean EC exhibits a moderate positive correlation (r-value: 0.325, p-value: 0.027), while the CV of EC demonstrates a strong negative correlation (r-value: -0.505, p-value: 3.44e-04). This suggests that streams in steeper catchments typically have greater EC values and lower variability than those in comparably flat regions. No significant correlation was found between either the mean or the CV of discharge and the catchment slope.

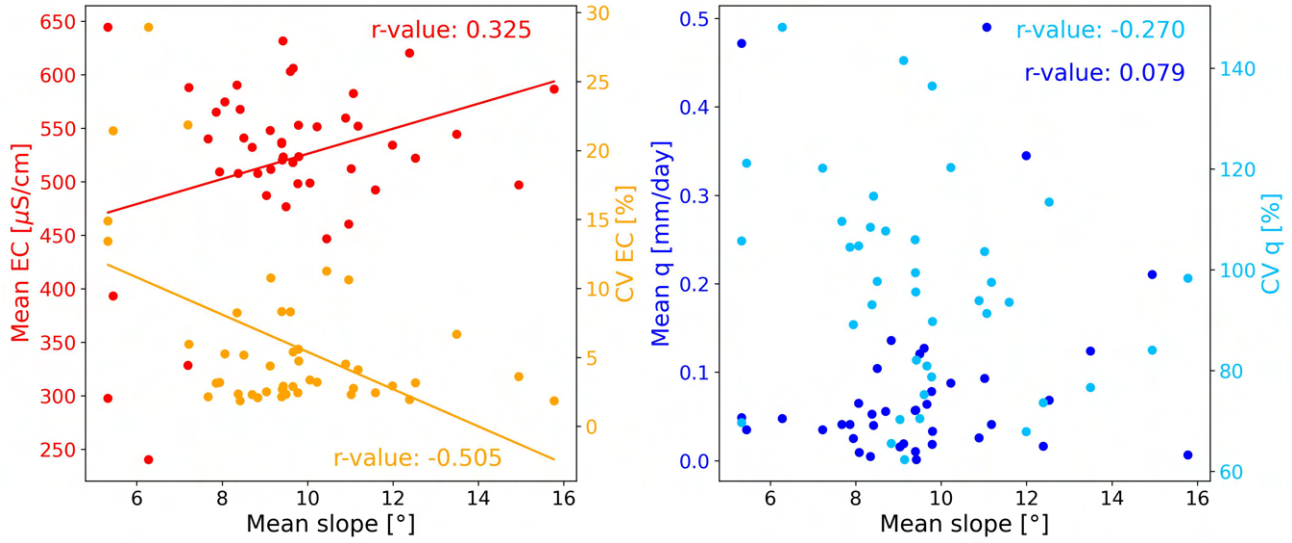


Figure 22: Scatter plot comparing the mean slope of the catchment to the mean and CV of EC (left plot) and to the mean and CV of the discharge (right plot). Regression lines are only shown for significant correlations.

Based on the hypothesis that a Molasse bedrock enhances flow continuity, this analysis investigates the correlation among geology, discharge, and EC. The objective is to determine whether a relationship exists between streams located in or directly below Molasse areas and the variability and mean values of discharge and EC. A value of 1 represents the presence of Molasse and 0 stands for the absence of Molasse. The findings reveal that neither the mean nor the CV of discharge displays any significant correlation. However, the variability in the EC values exhibits a moderate negative correlation (r-value: -0.322, p-value: 0.029) with the presence of Molasse, indicating that the variability tends to be lower in catchments partially underlain by Molasse. The correlation between the mean EC and the presence of Molasse is not significant.

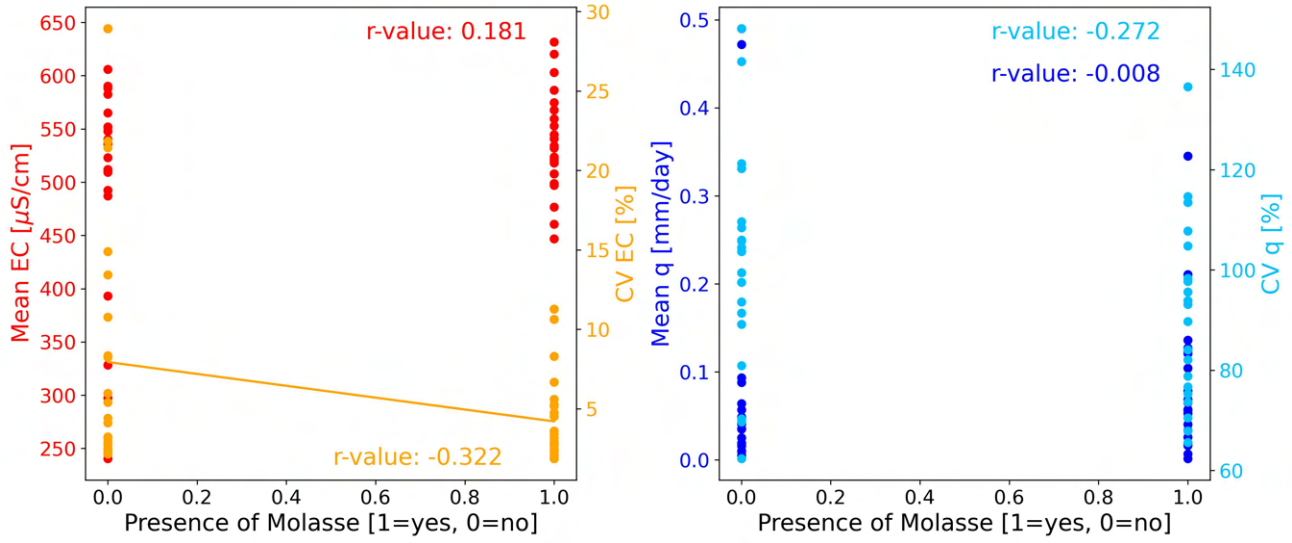


Figure 23: Scatter plot comparing the presence (1) or absence (0) of Molasse geology at or right above the measurement location to the mean and CV of EC (left plot) to the mean and CV of the discharge (right plot). Regression lines are only shown for significant correlations.

To summarize, the only significant correlation for the discharge is the positive correlation between the CV of discharge and the elevation. Despite the apparent visual trend of higher discharge values in lower locations depicted in Figure 11, the statistical analysis indicates that this correlation is not significant. Moreover, all other correlation analyses conducted between the discharge and slope and geology were determined to be statistically insignificant. Significant correlations with EC were observed among all variables and the EC, except for mean EC and the presence of Molasse. Catchments with higher elevations and flatter mean slopes display increased variability in EC. Conversely, the presence of Molasse in the catchment leads to lower variability in EC. Moreover, the mean of EC tends to decline with increasing elevation and rise with steeper catchment slopes.

## 4.5 Comparison with CrowdWater data

The data collected in the fieldwork for this thesis is restricted to the time between November 2022 and May 2023 and therefore is limited to the meteorologically defined seasons of winter and spring, with the exception of the initial measurements in November (National Centers for Environmental Information NOAA 2016). There is a network of data collection points utilizing the CrowdWater app on Zürichberg, where increased data collection by citizen scientists began around 2021. First, field measurements are compared to data from the same time period obtained by CrowdWater, which shows that the author's measurements tend to have a higher percentage of dry measurements compared to the CrowdWater data. For instance, at location 27, the stream was never observed to be dry in the CrowdWater data, while in the author's measurements, it was dry for at least 33% of the measurements. Though some locations show a greater level of agreement, the author's measurements were either similar or drier than the observations made by the Citizen scientists.

Moreover, the map of CrowdWater data from June 2021 to May 2023 shows an increased number of locations with more dry observations. In fact, the map of this time period more closely resembles the dryness patterns map of my observations. However, there are still some locations that had proportionally more flowing observations in the map incorporating all seasons compared to my observations during the six months of winter and spring observations.

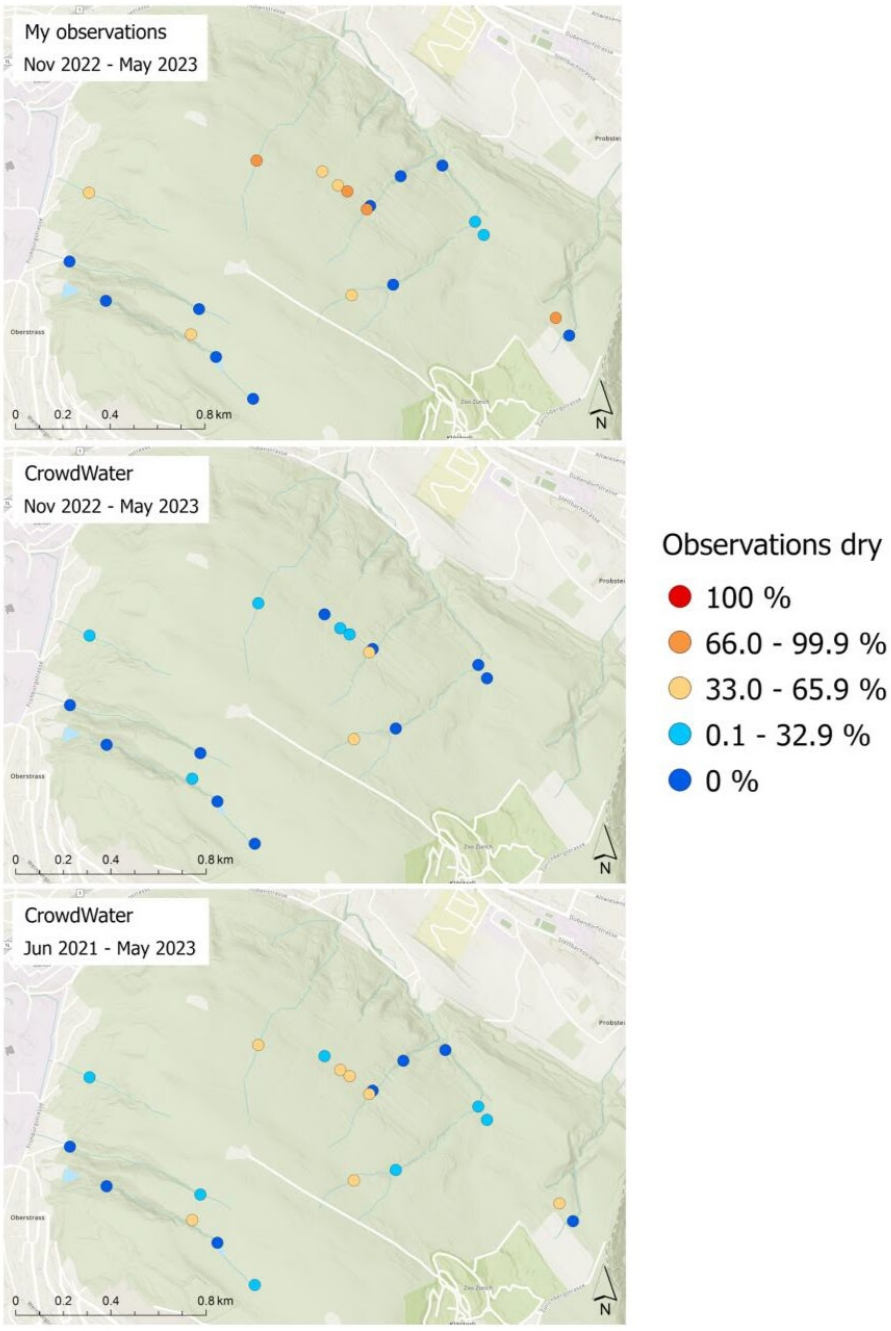


Figure 24: Three maps showing the frequency of dry streambed observations for streams on Zürichberg. The first one shows the observations made during the fieldwork for this thesis, the second one visualizes the observations made with the CrowdWater app during the same time period, and the third map is also based on CrowdWater data but calculated based on the data from two full years.

To investigate the relationship between the variability and the probability of stream drying at the end of the summer, Pearson's correlation coefficient was determined for the CV of EC and discharge, and the percentage of dry observations from CrowdWater during the months of July, August, and September in 2021 and 2022. A weak negative correlation for the CV of EC and a weak positive correlation for the CV of discharge were calculated, however, not significant.

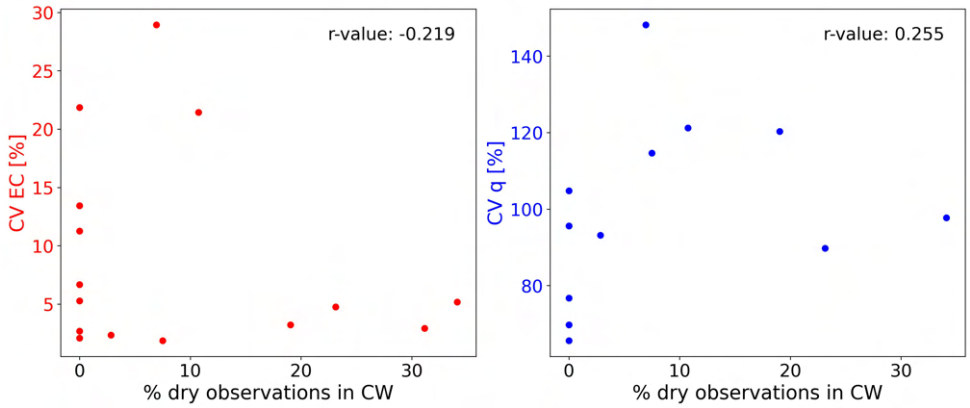


Figure 25: Scatter plot comparing the variability in streamwater EC and discharge and the percent of dry observations in the months of July, August, and September of 2021 and 2022. There were no significant correlations.

The analysis was extended to the percentage of dry observations made during field surveys with more data points available from the surveys and a measured dry period in winter 2023 due to persistent dry conditions. However, no correlations were found between the percentage of dry measurements made during the measurement period of this thesis and the variability of discharge and EC.

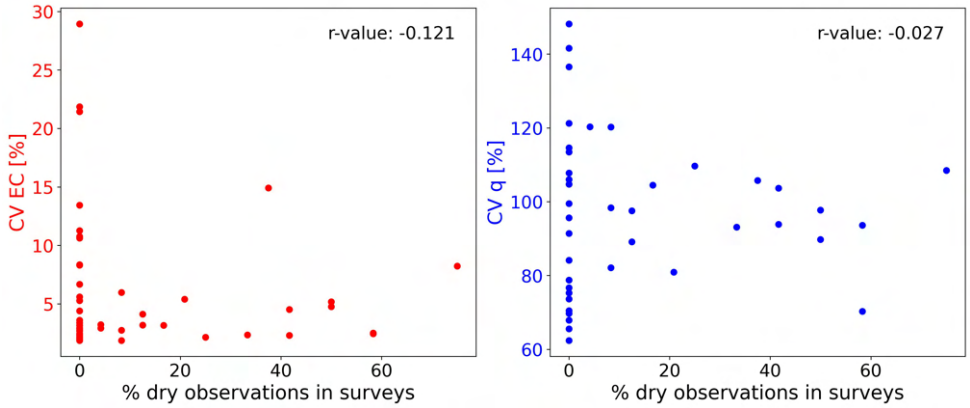


Figure 26: Scatter plot comparing the variability in streamwater EC and discharge and the percent of dry observations made in the field surveys between November 2022 and May 2023. There were no significant correlations and r-values are indicated in the plots.

The streams with continuous streamflow in both the CrowdWater and the survey data exhibit significant variability in the CV of discharge and EC. However, streams that were temporarily dry have relatively low EC variability, with the exception of two outliers in the CrowdWater plot and one outlier in the surveys. Conversely, the variability in discharge for temporary streams falls within the medium range in the survey data and the upper range in the CrowdWater data. They also exhibit a wider range of variability values compared to the EC. Moreover, there is no discernible trend in the extent of dryfall and its variability.

# 5 Discussion

The thesis's main objective was to determine the variability in discharge and streamwater EC. The research question aked whether topography and geology would be able to explain the variability in streamwater EC and runoff across temporary headwater streams on Zürichberg and if this variability can predict a stream's likelihood or duration of falling dry.

## 5.1 Patterns and variability across headwater streams on Zürichberg

Increased runoff was expected during the winter months as they generally tend to be wetter due to the lower evapotranspiration rates caused by the decreased temperature (see Chapter 2.2). The objective was to measure the variability of runoff during this wetting period following the dry fall conditions and subsequently during the period of elevated runoff. At the beginning of the measuring period, conditions were excessively dry, possibly due to the exceptionally high mean temperatures of +3.7°C for October and +2.4°C for November in contrast to the monthly averages in the period 1991-2020 (MeteoSwiss 2023). The snowfall in December and its subsequent melting resulted in a significant reduction in dry measurements and an increase in discharge throughout Zürichberg on December 27, 2022. On that same day, an increase in EC measurements was observed in the second-highest class, which coincided with a rise in the percentage of measurements in the lowest EC class. The latter might be attributed to the melting snow that increased the contribution of young water in the streams. As shown in Figure 2 and Table 1, the winter months of 2023 experienced low precipitation levels causing the stream conditions to be drier than predicted. The impact of this dry period from mid-January to February is also noticeable in the discharge measurements. Throughout January and February, conditions gradually became drier until achieving a peak of dry measurements on February 22, 2023. During this progressive drying in the streams the EC measurements reveal that over the first three survey days, the EC increased. After January 19, 2023, the discharge continued to decrease but in the EC values there was a shift from the third highest class to the second highest class, therefore an overall decrease. There was no clear correlation observed between the patterns of discharge and EC over time. Contrary to the negative correlation trend between discharge and EC values that was discovered by Zhou et al. (2022) no significant correlation was found between the mean discharge and mean EC on Zürichberg. It is worth noting that the snowfall in mid-January did not lead to increased discharge, and conditions continued to become drier until reaching the driest point on February 22, 2023. On that day, there were slightly fewer dry measurements compared to the initial three measurements from November and December. Nonetheless, the total amount of discharge was lower than at the start of the measurement period.

The consistent share of high EC values in Figure 16 suggests that groundwater exerted a sustained impact on the streamflow on Zürichberg throughout the data collection period. This

category shows two distinct outliers, with the November 23, 2022 data showing a higher proportion of sites featuring high EC levels in streamwater. The second occurrence was measured on April 17, 2023, potentially due to the increased number of streams with discharge on that day. This led to a higher number of EC measurements taken. This additional data likely had lower EC values, resulting in a proportional decrease in the highest-value class.

Until early March, the three classes below the highest class exhibited significantly greater variability. Initial losses during the transition from dry to wet catchment conditions, as water infiltrates and recharges the groundwater aquifers, may have contributed to increased variability in water sources during the first half of the survey period. The soil's hydraulic properties and storage differences have significant effects on the distribution of contributing streamflow sources (Gutierrez-Jurado et al. 2021). In March, after experiencing some heavier precipitation events, the proportions of each EC category appeared to stabilize over time. With the increasing saturation of soils and aquifers, it is possible that this contributed to a more consistent streamflow chemistry from then on (Gutierrez-Jurado et al. 2021).

During this same period of more constant EC values, there appears to be a rise in the discharge variability amongst survey dates. It can be assumed that the refilling of groundwater storage has the opposite effect on discharge compared to the EC measurements. If precipitation input increases and water is no longer lost to underground storage, it could directly affect streamflow by contributing to it as fast flow paths or by increasing the pressure on storage, causing displacement of older groundwater and resulting in less buffering through intake into storage. This linkage of rainfall and discharge once groundwater storages are full was also shown by Swenson et al. (2023). Another possible explanation is that the heavier rainfall events during March, April, and May led to more significant and immediate water inputs, as opposed to the lower and slower input resulting from snow melting in December and January. Additionally, the increase in dry streambed conditions observed during the last three measurements in May is most likely due to the temperature rise and the subsequent negative balance between precipitation and evapotranspiration (refer to Figures 2 and 3). Concurrently, there was a decrease in low EC values during the same three measurement days.

The comparison of the two maps featuring extreme measurement days and the median discharge and EC conditions demonstrates that though the survey day with the lowest EC measurements (April 17, 2023) does not coincide with that of the highest discharge measurements (May 17, 2023), it still occurred on a day with discharge measurements nearly as high. The significant rainfall occurring on April 16, 2023, one day ahead of the EC measurements on April 17, 2023, caused a significant decline in EC values. This can be attributed to the increased input of young water from precipitation, which subsequently also increased the amount of discharge. Although similar rainfall events occurred during the measurement period, they were not mea-

sured immediately the day after, and by the time measurements were taken, the discharge had already decreased. Further, the number of EC and flowing runoff measurements were significantly higher on both April and May 17, 2023, especially at higher elevations, in comparison to the other maps. The increase in runoff, specifically at higher elevation sites, led to a rise in the number of measurements in streams that are primarily influenced by shorter flow paths. Consequently, the stream water was younger, with lower EC values. Contrary to Floriancic et al. (2019) who found a weak positive correlation between the mean elevation and the EC, in the streams on Zürichberg a strong negative correlation was found, therefore indicating a trend of decreased EC values at higher elevations.

The median discharge conditions recorded on January 19, 2023, confirm relatively dry conditions overall. Many streams at higher elevations in the center of Zürichberg lacked surface flow under these conditions. However, in comparison to the driest recorded day, most locations at lower elevations experienced increased discharge. Additionally, some mid-elevation locations that were dry on February 22, 2023, exhibited flowing water. Hence, the driest day cannot be considered an extreme outlier. On January 19, 2023, the highest average EC measurements were recorded. Preceding these measurements, snowfall occurred and temperatures remained below 1°C throughout the day. As a result, the snow precipitation was not directly added into the system as water and could not dilute the streamwater with low conductivity water, as rain would have.

On January 19, 2023, one stream exhibited a decreasing trend of EC values downstream across locations 38, 37, and 36. This survey exhibited numerous dry measurements due to recent snowfall that did not immediately add to streamflow. The presence of a spring directly above site 38 (refer to Figure 6) and the limited contribution of fresh precipitation implies that the discharge mainly comprises of older water. This hypothesis is supported by the absence of any surface flow at site 39, directly above the spring. This implies that the vast majority of water sampled at site 38 originated from the spring. Further downstream, the decrease in EC values may indicate a higher proportion of young water from shallow groundwater or soil water. On April 17, 2023, with the lowest mean EC, the same pattern for the three locations does not exist. The EC at location 36 is higher than at 38. One possible explanation for the reduced EC at 38 is the higher proportion of young water from recent precipitation diminishing the effect of the spring. According to Figure 19, it is evident that location 36 shows increased EC following precipitation inputs. This phenomenon can likely be attributed to the piston effect. The infiltration of rainfall water into the aquifer one day prior leads to elevated pressure that displaces older groundwater to contribute to streamflow. A similar contribution of springs during periods of low flow was illustrated in a study by Correa et al. (2017). The study showed that spring water becomes more important during dry conditions and declines as younger sources of water become more significant. Furthermore, it was observed that sites 13, 21, and 54 also located downstream of springs experienced increased EC levels on February 25, 2023 (three days

after the driest recorded day) as demonstrated in Figure 11. On April 17, 2023, exhibiting wetter conditions, it was observed that their values were grouped comparably with both upstream and downstream sites. This reinforces the assumption that older spring water (with a higher EC) has a weaker effect during high-flow conditions. However, this trend is less pronounced for site 7, which is also situated downstream of a spring. Though its absolute value is low, it is still higher compared to the wetter conditions on April 17, 2023. Furthermore, as illustrated in Figure 11, the stream beneath the zoo (ID 61 and 67) displays unusually high discharge rates even during dry conditions. This may be attributed to a miscalculation of a too small catchment area, leading to unnaturally high normalized discharge values. Alternatively, it is plausible that unnatural water input from the zoo could be responsible for these heightened values, as a pipe emerging from the zoo area was observed discharging water into a streambed. EC values in these streams are also rather high, and substantial changes in background EC concentration up to 10 $\mu$S/cm were observed during salt tracer measurements.

Another notable area is in the northwest of Zürichberg (ID 15 to 19), where there was either no discharge or very minimal discharge even during the wettest conditions. In comparison to other similar elevated sites, these sites exhibit significantly reduced discharge. Additionally, Figure 13 indicates that these areas were predominantly dry. There is no significant water abstraction in this area as shown in Figure 6, however, all locations are situated in Molasse bedrock. According to Floriancic et al. (2019), it was hypothesized that Molasse would result in a more consistent flow. However, this was not observed at these sites or across the entire study area. No significant correlation was found between the mean or CV of discharge and the presence of Molasse.

The CV in the discharge presented in Figure 12 generally exhibits significantly large values, which is expected. Headwater streams tend to display higher variability in their discharge compared to perennial streams due to their catchment characteristics and their rapid response to short-term changes in precipitation and temperature (Tramblay et al. 2021). The variability of EC on the other hand is much lower than the one in the discharge measurements. The positive correlation between the CV of EC and discharge that was found in Chapter 4.3, indicates that locations with higher variability in discharge tend to also present higher EC variability and vice versa, which could indicate that higher variability in the source of streamflow also causes larger variabilities in the discharge amount. It was hypothesized that streams with more soil water and shallow groundwater, and therefore generally younger water, would display higher variability. The locations presenting high variability in EC partly correspond with locations that show lower absolute EC values in Figure 17, especially the two streams on the western slope (ID 1,2,4,5,6,7, and 8). This relationship was also significantly negatively correlated over the whole study area as shown in the correlation analysis in Figure 20. Locations 4, 5, 7, and 8 which show the highest values in the CV of EC over the study area, are located in an area with a very flat slope

as well as at high elevation, indicating a strongly reduced impact of groundwater sources on the streamflow. The spatial pattern of the CV in discharge reveals that the majority of sites with low variability are situated in the lower elevation range. The significant positive correlation between the runoff variability and elevation supports the notion that groundwater exerts a stabilizing effect on discharge amounts at lower elevations. Conversely, at higher elevations, younger water sources, which are more influenced by atmospheric conditions, have a greater impact on discharge. This results in greater variability than what is observed in groundwater-fed streams.

This trend of decreased CV of discharge downstream is evident in two streams (1: 20,21,22 & 2: 35, 36, 37, 38). In those streams, the trend in the variability of EC measurements is not as clear in Figure 18, but Appendix A5 demonstrates that the trend is approximately present for the CV of EC as well. Overall, a strong positive correlation was observed between the variability in EC and elevation, while a strong negative correlation was found for the mean EC and elevation across all sites. These findings support the hypothesis that decreasing elevation leads to an increase in the influence of groundwater, which in turn has a more balanced effect on discharge and water source variability compared to higher-elevation stream segments that are primarily fed by younger runoff sources (Warix et al. 2021). Despite the assumption that the specific discharge would increase at lower elevations and the observed trend of increased runoff at lower elevations in the maps shown in Figure 11, the weak negative correlation found between the mean discharge and the elevation is not statistically significant. Additionally in contrast to the findings on Zürichberg, Simon et al. (2022) found a greater groundwater contribution in upstream segments of headwater streams. Furthermore, Abbott et al. (2018) discovered no significant correlation between the variability of water chemistry and elevation. However, in their research, they looked at longer stream sections, across headwater streams as well as perennial reaches. This demonstrates that the impact of groundwater varies across different study areas. It appears that there is no generally applicable correlation between elevation and groundwater influence. Instead, other factors must also be considered. For instance, in the study area investigated by Simon et al. (2022), the topography displayed steeper slopes at higher elevations and was flatter in the lower elevation range. This suggests that in this case, slope had a greater impact than elevation on groundwater contribution to streamflow. In contrast, the study area on Zürichberg has a flatter hilltop and generally steeper slopes at the base. The strong negative correlation between the variability in EC and the mean catchment slope indicates that water sources in steeper catchments are more stable. Meanwhile, the moderate positive correlation between the mean EC and the mean slope suggests that groundwater has a stronger impact in steeper catchments. However, there were no significant correlations found for the discharge and slope on Zürichberg.

Additionally, one noticeable trend is again the locations north of the zoo. The lower variability in discharge at three of the four sites could possibly be explained by an unnatural and constant

water input. The relatively high variability observed in the EC measurements contradicts the positive correlation between the variabilities in discharge and EC. Despite a strong assumption of the influence of the zoo, it cannot be ruled out that this phenomenon is naturally controlled. Other than the stream below the zoo, the three streams on the western slope also exhibit significantly higher variability in EC measurements compared to the other streams situated on the northeast-facing slope. Although these streams also contain some sites with increased variability, these are isolated, individual points, and not the entire stream. For instance, at locations 22, 33, 38, 52, and 59. This indicates more constant water sources on this side of Zürichberg.

As previously discussed in the example of site 36, the response of EC to precipitation can be divergent, as illustrated in Figure 19. The decline in EC subsequent to increased precipitation may be attributed to a higher proportion of young precipitation water in the runoff, leading to dilution of the streamwater with lower EC levels. This is a common phenomenon in streams where deep groundwater has little or no effect, making them more sensitive to precipitation events. Figure 18 indicates some correlation between the decreasing EC after precipitation and higher EC variability, particularly in the three streams on the western slope. This is consistent with a pattern of lower mean EC values in these streams. These factors suggest minimal groundwater impact. In contrast, the second graph in Figure 19 reflects the opposite EC pattern when significant precipitation events occur. The substantial increase in EC on April 17 and May 17, 2023, probably indicates the piston effect, where the input of precipitation displaces older groundwater, leading to increased age of streamwater at such locations. This requires the streambed to be connected to the groundwater table, which explains why sites showing this behavior are generally located at the bottom of the hill on the northeastern slope of Zürichberg. This suggests that the impact of groundwater in these regions outweighs that of additional surface runoff from precipitation, as evident in the streams from the first plot.

The extended dry period measured during winter led to a pattern of varying percent of measurements where no surface flow was observable. Constantly flowing water was observed predominantly at the base of the hill, which is consistent with the observed increasing importance of deeper groundwater in other analyses. However, there are also sites at higher elevations that have never dried up in the measurement period. As well as the opposite, streams at the base of the hill that had very limited to no flowing occurrences. Therefore, it can be said that the trend of lower no-flow occurrences at lower elevations observed in Figures 13 and 14 is a general trend and many exceptions can be observed. Possible explanations for the occurrence or non-occurrence of this trend in the four streams A through D at individual points are now examined in more detail.

Stream A maintained relatively consistent flowing conditions at the lower 7 sites and showed a

marked increase in dry conditions upstream. Figure 6 illustrates the presence of a spring just above site 54. Sites uphill from this spring do not receive the same water input, and as a result, exhibit a greater frequency of dry conditions. Notably, there are differences in the geology along the stream. Sites 53 and 54, as well as 45 and 46, are located in upper freshwater Molasse, while the remaining sites are situated on moraine material. It is assumed that the steady influx of water from the spring significantly affects location 54. Additionally, site 53 displays a decrease in flowing measurements, contradicting expectations given its Molasse geology, which was shown to have higher low-flow magnitudes (Floriancic et al. 2019). Surface flow was frequently observed to cease below site 53 and re-emerge at varying distances upstream of site 52, with sustained flow occurring only after periods of high precipitation. Similar patterns have been described by Kampf et al. (2021) where variations in the geologic underground or changes in channel slope can facilitate patterns of flow cessation along a stream. Upstream site 58 displays a significant outlier (approximately 30% of flow observations) in contrast to the other three sites with no flow observations ranging between 80 and 100%. There is a lack of a clear explanation for this increase in flow observation resulting from any natural springs or geological variations. It is worth noting that tapped springs are situated above sites 56 and 58, which could possibly contribute to a decrease in surface streamflow. Furthermore, it is possible that the narrow area of thin unconsolidated rock cover and Molasse, situated above location 58 and ending right before site 56, may have an impact. In the lower section of this stream observations of dry conditions at site 48 were noted. Sites 52 and 51, which lacked any dry observations, exhibit no geological disparity. Nonetheless, water extraction from two nearby tapped springs may be the cause of reduced surface flow. As shown by Costigan et al. (2016), this practice can result in increased intermittent flow.

Stream B displays a significant rise in the percentage of no-flow measurements from sites 38 to 39. While water flow was evident on each survey date at site 38, none of the three upstream sites showed streamflow in over 90% of the observations. As previously discussed, this is likely attributable to the spring situated between the two sites. A possible explanation for the emergence of this spring is the area of low-thickness unconsolidated rock cover and Upper Freshwater Molasse geology above it. Despite being located below the geologic area, location 39 may remain dry as the water in this area could infiltrate and only resurface through this spring directly beneath it.

In stream C, a considerable amount of no-flow observations were recorded in the top three sites. However, none of them were consistently dry. Surface flow was consistently present below site 22 and could be attributed to the spring located above site 21. The tapped springs between sites 21 and 20 did not significantly affect the flow at site 20 and did not cause the stream to run dry, as flow was consistently present at that location.

Compared to the other three streams, Stream D displays an interesting trend in the two bottom

locations, indicating a rise in no-flow observations. A plausible explanation for the increase in measurements with flow at site 13 is the presence of a spring directly above it. Although surface flow persists at location 12 for the majority of survey days, the two downstream locations show a significant increase in no-flow measurements. They are located in Molasse geology, as is location 12, which is nearby. Although the springs tapped above 12 could help explain some of the decrease in surface flow, it still does not account for why site 12 has not been impacted. The two clusters depicted in the ternary plot in Figure 15 show a lack of streams predominantly exhibiting wet streambed conditions indicating that this is not a typical condition over extended periods. Instead, it is a state that occurs during the transition between dry and flowing conditions.

## 5.2 Probability of stream drying

The presented map in Figure 13 and the individual stream plots in Figure 14 have shown that higher elevations on Zürichberg exhibit a trend of increased stream drying. Dry streambeds were frequently observed during the particularly dry conditions of January and February 2023, as indicated in Figure 10. The trend for a higher percentage of dry observations during surveys, as opposed to those made through the Crowdwater app within the same timeframe, is apparent in Figure 24. Interestingly, some locations show an even greater prevalence of dry streambed conditions than the CrowdWater data across all seasons for two years. This finding is surprising given that with the inclusion of the summer months, which tend to be drier, a higher proportion of dry observations was expected. Dry measurements were primarily taken in January and February surveys when low temperatures might have discouraged some of the citizen scientists from collecting data. Additionally, the definition of a dry streambed can vary between individuals. For classification purposes, the author defined dry streambeds as those with no discernible increase in moisture compared to adjacent surfaces. Consequently, after rain events when the surroundings were wetter than normal, comparable moisture conditions in the streambed and next to it were also counted as a dry streambed. It is possible that, due to alternative definitions by contributors in the CrowdWater app, fewer dry streambed occurrences were observed. Comparing the two time periods of CrowdWater data, the higher dry measurements during the full year period, as opposed to just November through May, support the idea that there is typically more streamflow during the winter season and the dry measurements assumed during summertime and early fall contribute to reducing the overall proportion of dry measurements.

Based on the significant negative correlations found on Zürichberg between the mean EC and the CV of EC as well as the mean EC and the CV of discharge, it was concluded that sites with a higher groundwater content (higher mean EC) exhibit less variability in both EC and discharge. This implies that the contribution of older groundwater to a headwater stream has a balancing effect on both discharge and streamwater sources. The correlation analysis of elevation and slope also revealed a contradictory trend in the mean EC and the CV of EC.

It was hypothesized that a steady supply of groundwater would provide sustained streamflow, thus reducing the occurrence of dry conditions in temporary headwater streams. A positive correlation was hypothesized between the variability in discharge/EC observed during field surveys, and the percentage of dry observations in the CrowdWater data from July, August, and September. However, the results of the correlation analysis did not show any statistically significant correlations. The expected direction of the correlation was observed with a weak positive correlation for discharge variability. However, if it was significant, the CV for EC exhibits a weak negative correlation, suggesting a larger proportion of dry observations with lower variability. The additional correlation analysis with the percent of dry observations in the surveys revealed correlations so weak that they are more or less irrelevant. The scatter plot in Figure 26 indicates that surveyed streams that were always flowing display greater variability compared to those that experienced temporary dry spells, which exhibit rather low variability in EC and moderate variability in discharge, albeit with greater scatter. Notably, no significant differences were observed between streams with varying percentages of dry observations. Based on the variability in discharge and streamwater EC in this dataset, it was not possible to predict the likelihood or the extent of a headwater stream falling dry during July, August, and September of 2021 and 2022.

## 5.3 Limitations of this study and future work

The methodology employed in this thesis required extensive fieldwork to manually collect data on the runoff and EC in headwater streams across an area of 3.35 $km^2$. Although labor-intensive, the presence of a well-connected road network as well as the close proximity to Zurich made accessibility to the study site and the respective stream sites easy. Additionally, further field visits were necessary to determine the coordinates of pipes, facilitating the watershed analysis. However, this was an exceptional circumstance as Zurichberg has experienced substantial modifications as a result of its proximity to the city of Zurich, a phenomenon not typically expected in more remote areas. The lack of significant correlations between the discharge and most catchment characteristics could stem from the presence of measurement uncertainties that hinder correlation assessment. The salt tracer and bucket measurements were conducted with care, but minor inaccuracies may occur. The increased runoff in March and the following months likely increased inaccuracies in runoff estimations, which led to the decision to reject them at some sites. Although less precise, the author conducted these estimates weekly, which enabled the estimation of relative differences in runoff from memory. However, it is feasible that these approximations were imprecise and led to the lack of correlations.

To normalize the runoff values, the catchment areas needed to be calculated for each measuring site. The Zürichberg study area is relatively compact, covering a total of 3.35 $km^2$. At certain sites, the catchment area is quite small, which makes minor errors significant, especially because the DEM needed to be corrected manually due to the high-density network of roads, posing

considerable risk for inaccuracies. Additionally, it is important to consider that water flow in the deeper groundwater aquifer may not always align with surface topography. However, this is the basis for calculating catchments, but necessary information on underground flow remains unavailable.

Measuring the EC of streamwater has been proven to be a highly effective method for determining both its age and source. This approach requires minimal time and effort and eliminates the need for laboratory analysis compared to for example the analysis of isotopic compositions (Swenson et al. 2023) or radioactive hydrogeological tracers for water residence times (Li et al. 2021). The EC meter is lightweight and portable, making it easier to transport. Despite its usefulness, it should be noted that there are some limitations associated with using EC as an indicator of water age. The electric conductivity of water is influenced by not only ions from subsurface weathering processes but also by other factors that may lead to EC variations. For instance, aquatic organisms can also alter the EC of streamwater (Vogt et al. 2010). Additionally, different lithologies impact the concentration of dissolved ions in water due to the varying weathering rates of different types of rocks. Geological formations composed of inert materials demonstrate a lower ionization rate and therefore decreased conductivity. Conversely, materials like clay display a higher ionization rate, resulting in increased electrical conductivity, even after a shorter storage period (Bhateria and Jain 2016). One alternative to field measurements has already been presented and utilized in this thesis, namely the collection of data through citizen scientists using the CrowdWater app. This method is becoming increasingly popular in mapping the extent of temporary streams and their spatial and temporal variability of flow states in temporary streams (Borg Galea et al. 2019). As an alternative, Assendelft and van Meerveld (2019) presented a technique to automatically record surface water presence and absence as a description of flow states in temporary streams. However, these methods are limited to streambed conditions data and do not measure flow quantity or stream chemistry.

In the future, conducting the analysis of variability in a study area with less human influence could enhance the quality of data and the analysis of thereof. By improving the precision of the catchment area calculations, it would make more sense to determine the proportion of the catchment that is underlain by Molasse, rather than solely assessing the presence of absence of Molasse. However, remote locations may have limited CrowdWater data, creating limitations for comparing variability to citizen scientist data on streambed conditions. To mitigate labor intensity during data collection, automatic water level loggers could be utilized to assess streamflow variability. Automatic data collection would enable greater study area coverage and continuous data collection compared to the data collected during the surveys in this study. As studies have demonstrated varied results regarding the influence of different catchment characteristics, more research is necessary on the extent and strength of this influence and how it links to other factors.

# 6 Conclusion

This study analyzed the discharge and streamwater EC variability on Zürichberg and investigated possible correlations between streamflow characteristics and catchment variables. Additionally, the study determined whether this data could predict the occurrence or magnitude of dryfall during low flow periods in CrowdWater data.

Collectively the findings have shown that an elevated impact of groundwater on streamflow has a balancing effect on both the discharge rate and the EC of streamwater. Stream sites with a lower mean water age reveal more variation in both water sources and the amount of discharge. Thus, a greater input of older groundwater to the stream leads to a more consistent discharge. Additionally, the study found correlations between the water source and topographical catchment variables. On Zürichberg, lower mean EC and higher EC variability were observed at higher elevations and in catchments with flatter slopes. Additionally, the discharge variability displayed a positive correlation with increasing elevation. Nonetheless, these relationships cannot be generalized to all headwater catchments as other studies have discovered opposing findings. The interaction of the various factors can have different influences depending on the catchment characteristics. The hypothesis that increased variability could predict flow cessation was not supported by the data in this study.

Nonetheless, the detected correlations and observations at distinct stream locations or patterns along streams suggest a major role of water source in the generation of streamflow, affecting both the rate of discharge and streamwater EC. Additionally, a significant variation in conditions was noted throughout the rather small Zürichberg headwater catchment, underscoring the significance of catchment characteristics in temporary headwater streams. Furthermore, the prolonged dry period measured in January and February impressively showed the impact of an extended period with low precipitation input, also during winter months, when wetter conditions are expected.

The combination of these findings reinforces the need for more investigations on the complex patterns of streamflow generation and spatio-temporal variability thereof in temporary headwater streams. Having a more thorough understanding of streamflow sources could help understand patterns of flow cessation and therefore predict changes in streamflow contribution to larger perennial streams under future climate and land use changes and improve management strategies.

# References


Abbott, B. W., Gruau, G., Zarnetske, J. P., Moatar, F., Barbe, L., Thomas, Z., Fovet, O., Kolbe, T., Gu, S., Pierson-Wickmann, A.-C., Davy, P. and Pinay, G. (2018). "Unexpected spatial stability of water chemistry in headwater stream networks". In: *Ecology letters* 21.2, pp. 296–308.

Acuña, V., Datry, T., Marshall, J., Barceló, D., Dahm, C. N., Ginebreda, A., McGregor, G., Sabater, S., Tockner, K. and Palmer, M. A. (2014). "Why should we care about temporary waterways?" In: *Science* 343.6175, pp. 1080–1081.

Allen, G. H., Pavelsky, T. M., Barefoot, E. A., Lamb, M. P., Butman, D., Tashie, A. and Gleason, C. J. (2018). "Similarity of stream width distributions across headwater systems". In: *Nature communications* 9.1, pp. 1–7.

Assendelft, R. S. and van Meerveld, H. J. (2019). "A low-cost, multi-sensor system to monitor temporary stream dynamics in mountainous headwater catchments". In: *Sensors* 19.21, pp. 1–28.

Barradas, V. L. and Adem, J. (1992). "Albedo model for a tropical dry deciduous forest in western Mexico". In: *International journal of biometeorology* 36, pp. 113–117.

Barua, S., Cartwright, I., Dresel, P. E., Morgenstern, U., McDonnell, J. J. and Daly, E. (2022). "Sources and mean transit times of intermittent streamflow in semi-arid headwater catchments". In: *Journal of Hydrology* 604, pp. 1–13.

Bhateria, R. and Jain, D. (2016). "Water quality assessment of lake water: a review". In: *Sustainable Water Resources Management* 2, pp. 161–173.

Borg Galea, A., Sadler, J. P., Hannah, D. M., Datry, T. and Dugdale, S. J. (2019). "Mediterranean intermittent rivers and ephemeral streams: Challenges in monitoring complexity". In: *Ecohydrology* 12.8, pp. 1–11.

Botter, G. and Durighetto, N. (2020). "The stream length duration curve: A tool for characterizing the time variability of the flowing stream length". In: *Water Resources Research* 56.8, pp. 1–21.

Botter, G., Vingiani, F., Senatore, A., Jensen, C., Weiler, M., McGuire, K., Mendicino, G. and Durighetto, N. (2021). "Hierarchical climate-driven dynamics of the active channel length in temporary streams". In: *Scientific reports* 11.1, pp. 1–12.

Bronge, C. and Openshaw, A. (1996). "New instrument for measuring water discharge by the salt dilution method". In: *Hydrological processes* 10.3, pp. 463–470.

Busch, M. H., Costigan, K. H., Fritz, K. M., Datry, T., Krabbenhoft, C. A., Hammond, J. C., Zimmer, M., Olden, J. D., Burrows, R. M., Dodds, W. K., Boersma, K. S., Shanafield, M., Kampf, S. K., Mims, M. C., Bogan, M. T., Ward, A. S., Rocha, M. P., Godsey, S., Allen, G. H., Blaszczak, J. R., Jones, C. N. and Allen, D. C. (2020). "What's in a name? Patterns, trends, and suggestions for defining non-perennial rivers and streams". In: *Water* 12.7 (1980), pp. 1–19.

Carlier, C., Wirth, S. B., Cochand, F., Hunkeler, D. and Brunner, P. (2018). "Geology controls streamflow dynamics". In: *Journal of Hydrology* 566, pp. 756–769.

Cooper, S. D., Lake, P. S., Sabater, S., Melack, J. M. and Sabo, J. L. (2013). "The effects of land use changes on streams and rivers in mediterranean climates". In: *Hydrobiologia* 719, pp. 383–425.

Correa, A., Windhorst, D., Tetzlaff, D., Crespo, P., Célleri, R., Feyen, J. and Breuer, L. (2017). "Temporal dynamics in dominant runoff sources and flow paths in the Andean Páramo". In: *Water Resources Research* 53.7, pp. 5998–6017.

Costigan, K. H., Jaeger, K. L., Goss, C. W., Fritz, K. M. and Goebel, P. C. (2016). "Understanding controls on flow permanence in intermittent rivers to aid ecological research: Integrating meteorology, geology and land cover". In: *Ecohydrology* 9.7, pp. 1141–1153.

Cottet, M., Robert, A., Tronchère-Cottet, H. and Datry, T. (2023). ""It's dry, it has fewer charms!": Do perceptions and values of intermittent rivers interact with their management?" In: *Environmental Science & Policy* 139, pp. 139–148.

CrowdWater (2023). CrowdWater. URL: https://crowdwater.ch/de/daten/ (Accessed: 05.06.2023).

Datry, T., Truchy, A., Olden, J. D., Busch, M. H., Stubbington, R., Dodds, W. K., Zipper, S., Yu, S., Messager, M. L., Tonkin, J. D., Kaiser, K. E., Hammond, J. C., Moody, E. K., Burrows, R. M., Sarremejane, R., DelVecchia, A. G., Fork, M. L., Little, C. J., Walker, R. H., Walters, A. W. and Allen, D. (2023). "Causes, responses, and implications of anthropogenic versus natural flow intermittence in river networks". In: *BioScience* 73.1, pp. 9–22.

Djodjic, F., Bieroza, M. and Bergström, L. (2021). "Land use, geology and soil properties control nutrient concentrations in headwater streams". In: *Science of the Total Environment* 772, pp. 1–8.

Floriancic, M. G., Berghuijs, W. R., Molnar, P. and Kirchner, J. W. (2021). "Seasonality and drivers of low flows across Europe and the United States". In: *Water Resources Research* 57.9, pp. 1–17.

Floriancic, M. G., Fischer, B. M. C., Molnar, P., Kirchner, J. W. and van Meerveld, H. J. (2019). "Spatial variability in specific discharge and streamwater chemistry during low flows: Results from snapshot sampling campaigns in eleven Swiss catchments". In: *Hydrological Processes* 33.22, pp. 2847–2866.

Floriancic, M. G., Spies, D., van Meerveld, H. J. and Molnar, P. (2022). "A multi-scale study of the dominant catchment characteristics impacting low-flow metrics". In: *Hydrological Processes* 36.1, pp. 1–18.

FOEN (2023). Basic monitoring network: water levels and discharge in surface waters. URL: https://www.bafu.admin.ch/bafu/en/home/topics/water/state/water–monitoring-networks/basic-monitoring-network–water-levels-and-discharge-in-surface-.html (Accessed: 02.08.2023).

Gallart, F., Cid, N., Latron, J., Llorens, P., Bonada, N., Jeuffroy, J., Jiménez-Argudo, S.-M., Vega, R.-M., Solà, C., Soria, M., Bardina, M., Hernández-Casahuga, A.-J., Fidalgo, A., Es-

trela, T., Munné, A. and Prat, N. (2017). "TREHS: An open-access software tool for investigating and evaluating temporary river regimes as a first step for their ecological status assessment". In: *Science of the Total Environment* 607, pp. 519–540.

Godsey, S. E. and Kirchner, J. W. (2014). "Dynamic, discontinuous stream networks: Hydrologically driven variations in active drainage density, flowing channels and stream order". In: *Hydrological Processes* 28.23, pp. 5791–5803.

Goodrich, D. C., Kepner, W. G., Levick, L. R and Wigington Jr, P. J. (2018). "Southwestern intermittent and ephemeral stream connectivity". In: *JAWRA Journal of the American Water Resources Association* 54.2, pp. 400–422.

Gutierrez-Jurado, K. Y., Partington, D. and Shanafield, M. (2021). "Taking theory to the field: streamflow generation mechanisms in an intermittent Mediterranean catchment". In: *Hydrology and Earth System Sciences* 25.8, pp. 4299–4317.

Hafen, K. C., Blasch, K. W., Rea, A., Sando, R. and Gessler, P. E. (2020). "The influence of climate variability on the accuracy of NHD perennial and nonperennial stream classifications". In: *JAWRA Journal of the American Water Resources Association* 56.5, pp. 903–916.

Hamilton, S. K., Hussain, M. Z., Lowrie, C., Basso, B. and Robertson, G. P. (2018). "Evapotranspiration is resilient in the face of land cover and climate change in a humid temperate catchment". In: *Hydrological Processes* 32.5, pp. 655–663.

Hammond, J. C., Zimmer, M., Shanafield, M., Kaiser, K., Godsey, S. E., Mims, M. C., Zipper, S. C., Burrows, R. M., Kampf, S. K., Dodds, W., Jones, C. N., Krabbenhoft, C. A., Boersma, K. S., Datry, T., Olden, J. D., Allen, G. H., Price, A. N., Costigan, K., Hale, R., Ward, A. S. and Allen, D. C. (2021). "Spatial patterns and drivers of nonperennial flow regimes in the contiguous United States". In: *Geophysical Research Letters* 48.2, pp. 1–11.

Hare, D. K., Helton, A. M., Johnson, Z. C., Lane, J. W. and Briggs, M. A. (2021). "Continental-scale analysis of shallow and deep groundwater contributions to streams". In: *Nature Communications* 12.1, pp. 1–10.

Hatley, C. M., Armijo, B., Andrews, K., Anhold, C., Nippert, J. B. and Kirk, M. F. (2023). "Intermittent streamflow generation in a merokarst headwater catchment". In: *Environmental Science: Advances* 2.1, pp. 115–131.

Hegelbach, J. and Spaar, R. (2000). "Saisonaler Verlauf der Gesangsaktivität der Singdrossel (Turdus philomelos), mit Anmerkungen zum nachbrutzeitlichen Gesangsschub". In: *Journal für Ornithologie* 141.4, pp. 425–434.

Jensen, C. K., McGuire, K. J. and Prince, P. S. (2017). "Headwater stream length dynamics across four physiographic provinces of the Appalachian Highlands". In: *Hydrological Processes* 31.19, pp. 3350–3363.

Jung, Y.-Y., Koh, D.-C., Lee, J., Tsujimura, M., Yun, S.-T. and Lee, K.-S. (2020). "Mean transit time and subsurface flow paths in a humid temperate headwater catchment with granitic bedrock". In: *Journal of Hydrology* 587, pp. 1–14.

Jung, Y.-Y., Koh, D.-C., Shin, W.-J., Kwon, H.-I., Oh, Y.-H. and Lee, K.-S. (2021). "Assessing seasonal variations in water sources of streamflow in a temperate mesoscale catchment with granitic bedrocks using hydrochemistry and stable isotopes". In: *Journal of Hydrology: Regional Studies* 38, pp. 1–14.

Kampf, S. K., Dwire, K. A., Fairchild, M. P., Dunham, J., Snyder, C. D., Jaeger, K. L., Luce, C. H., Hammond, J. C., Wilson, C., Zimmer, M. A. and Sidell, M. (2021). "Managing nonperennial headwater streams in temperate forests of the United States". In: *Forest Ecology and Management* 497, pp. 1–16.

Kaplan, N. H., Blume, T. and Weiler, M. (2020). "Predicting probabilities of streamflow intermittency across a temperate mesoscale catchment". In: *Hydrology and Earth System Sciences* 24.11, pp. 5453–5472.

Kaule, L. and Frei, S. (2022). "Analysis of drought conditions and their impacts in a headwater stream in the Central European lower mountain ranges". In: *Regional Environmental Change* 22 (82), pp. 1–15.

Kirchner, J. W. (2003). "A double paradox in catchment hydrology and geochemistry". In: *Hydrological processes* 17.4, pp. 871–874.

Krabbenhoft, C. A., Allen, G. H., Lin, P., Godsey, S. E., Allen, D. C., Burrows, R. M., DelVecchia, A. G., Fritz, K. M., Shanafield, M., Burgin, A. J., Zimmer, M. A., Datry, T., Dodds, W. K., Jones, C. N., Mims, M. C., Franklin, C., Hammond, J. C., Zipper, S., Ward, A. S., Costigan, K. H., Beck, H. E. and Olden, J. D. (2022). "Assessing placement bias of the global river gauge network". In: *Nature Sustainability* 5.7, pp. 586–592.

Leone, M., Gentile, F., Lo Porto, A., Ricci, G. F. and De Girolamo, A. M. (2023). "Ecological flow in southern Europe: Status and trends in non-perennial rivers". In: *Journal of Environmental Management* 342, pp. 1–16. ISSN: 0301-4797.

Li, L., Sullivan, P. L., Benettin, P., Cirpka, O. A., Bishop, K., Brantley, S. L., Knapp, J. L. A., van Meerveld, H. J., Rinaldo, A., Seibert, J., Wen, H. and Kirchner, J. W. (2021). "Toward catchment hydro-biogeochemical theories". In: *Wiley Interdisciplinary Reviews: Water* 8.1, pp. 1–31.

MacDonald, L. H. and Coe, D. (2007). "Influence of headwater streams on downstream reaches in forested areas". In: *Forest Science* 53.2, pp. 148–168.

McDonough, O. T., Hosen, J. D. and Palmer, M. A. (2011). "Temporary streams: the hydrology, geography, and ecology of non-perennially flowing waters". In: *River Ecosystems: Dynamics, management and conservation*, pp. 259–290.

Merz, J. and Doppmann, G. (2006). "Measuring mountain stream discharge using the salt dilution method". In: pp. 1–12.

Messager, M. L., Lehner, B., Cockburn, C., Lamouroux, N., Pella, H., Snelder, T., Tockner, K., Trautmann, T., Watt, C. and Datry, T. (2021). "Global prevalence of non-perennial rivers and streams". In: *Nature* 594.7863, pp. 391–397.

MeteoSwiss (2023). Messwerte und Messnetze. URL: https://www.meteoschweiz.admin.ch/service-und-publikationen/applikationen/messwerte-und-messnetze.htmllang=deparam=messwerte - lufttemperatur-10min (Accessed: 27.09.2023).

Moore, R. D. (2003). "Introduction to salt dilution gauging for streamflow measurement: Part 1". In: *Streamline Watershed Management Bulletin* 7.4, pp. 20–23.

Moore, R. D. (2005). "Slug injection using salt in solution". In: *Streamline Watershed Management Bulletin* 8.2, pp. 1–6.

Nabih, S., Tzoraki, O., Zanis, P., Tsikerdekis, T., Akritidis, D., Kontogeorgos, I. and Benaabidate, L. (2021). "Alteration of the ecohydrological status of the intermittent flow rivers and ephemeral streams due to the climate change impact (case study: Tsiknias river)". In: *Hydrology* 8.1 (43), pp. 1–26.

National Centers for Environmental Information NOAA (2016). Meteorological Versus Astronomical Seasons. URL: https://www.ncei.noaa.gov/news/meteorological-versus-astronomical-seasons. Accessed: 24.08.2023.

Pavoni, N., Schindler, C., Freimoser, M. and Haldimann, P. (2015). "Blatt 1091 Zürich". In: *Geol. Atlas schweiz 1:25 000, Erläut.* 90.

Prancevic, J. P. and Kirchner, J. W. (2019). "Topographic controls on the extension and retraction of flowing streams". In: *Geophysical Research Letters* 46.4, pp. 2084–2092.

Price, A. N., Jones, C. N., Hammond, J. C., Zimmer, M. A. and Zipper, S. C. (2021). "The drying regimes of non-perennial rivers and streams". In: *Geophysical Research Letters* 48.14, pp. 1–12.

Rocholl, A., Schaltegger, U., Gilg, H. A., Wijbrans, J. and Böhme, M. (2018). "The age of volcanic tuffs from the Upper Freshwater Molasse (North Alpine Foreland Basin) and their possible use for tephrostratigraphic correlations across Europe for the Middle Miocene". In: *International Journal of Earth Sciences* 107, pp. 387–407.

Sappa, G., Ferranti, F. and Pecchia, G. (2015). "Validation of salt dilution method for discharge measurements in the upper valley of aniene river (central italy)". In: *13th International Conference on Environment, Ecosystem and Development (EED'15).*

Sarath Prasanth, S. V., Magesh, N. S., Jitheshlal, K. V., Chandrasekar, N. and Gangadhar, K. (2012). "Evaluation of groundwater quality and its suitability for drinking and agricultural use in the coastal stretch of Alappuzha District, Kerala, India". In: *Applied Water Science* 2, pp. 165–175.

Sarremejane, R., Messager, M. L. and Datry, T. (2022). "Drought in intermittent river and ephemeral stream networks". In: *Ecohydrology* 15.5, pp. 1–25.

Sauquet, E., Beaufort, A., Sarremejane, R. and Thirel, G. (2021). "Predicting flow intermittence in France under climate change". In: *Hydrological Sciences Journal* 66.14, pp. 2046–2059.

Schmidt, C., Musolff, A., Trauth, N., Vieweg, M. and Fleckenstein, J. H. (2012). "Transient analysis of fluctuations of electrical conductivity as tracer in the stream bed". In: *Hydrology and Earth System Sciences* 16.10, pp. 3689–3697.

Shanafield, M., Bourke, S. A., Zimmer, M. A. and Costigan, K. H. (2021). "An overview of the hydrology of non-perennial rivers and streams". In: *Wiley Interdisciplinary Reviews: Water* 8.2, pp. 1–25.

Simon, N., Bour, O., Faucheux, M., Lavenant, N., Le Lay, H., Fovet, O., Thomas, Z. and Longuevergne, L. (2022). "Combining passive and active distributed temperature sensing measurements to locate and quantify groundwater discharge variability into a headwater stream". In: *Hydrology and Earth System Sciences* 26.5, pp. 1459–1479.

Spreafico, M. and Weingartner, R. (2005). "The hydrology of Switzerland". In: *Selected aspects and results. Reports, Bundesamt f. Wasser u. Geologie (BWG) Water Series* 7.

Stadt-Zürich (2023a). Quelleninventar (OGD) (kantonaler Datensatz). URL: https://www.-zuerich.ch/geodaten/download/532. Accessed: 05.08.2023.

Stadt-Zürich (2023b). Wasserfassungen (OGD) (kantonaler Datensatz). URL: https://www.-zuerich.ch/geodaten/download/317. Accessed: 05.08.2023.

Swenson, L., Zipper, S., Peterson, D. M., Jones, C. N., Burgin, A. J., Seybold, E., Kirk, M. F. and Hatley, C. (2023). "Changes in water age and source during dry-down of a non-perennial stream". Manuscript submitted for publication.

Swisstopo (2023). Maps of Switzerland. URL: https://map.geo.admin.ch/ (Accessed: 13.07.2023).

Tramblay, Y., Rutkowska, A., Sauquet, E., Sefton, C., Laaha, G., Osuch, M., Albuquerque, T., Alves, M. H., Banasik, K., Beaufort, A., Brocca, L., S., Camici, Csabai, Z., Dakhlaoui, H., DeGirolamo, A. M., Dörflinger, G., Gallart, F., Gauster, T., Hanich, L., Kohnová, S., Mediero, L., Plamen, N., Parry, S., Quintana-Seguí, P., Tzoraki, O. and Datry, T. (2021). "Trends in flow intermittence for European rivers". In: *Hydrological Sciences Journal* 66.1, pp. 37–49.

Truchy, A., Csabai, Z., Mimeau, L., Künne, A., Pernecker, B., Bertin, W., Pellizzaro, F. and Datry, T. (2023). "Citizen scientists can help advance the science and management of intermittent rivers and ephemeral streams". In: *BioScience* 73.7, pp. 513–521.

Valiantzas, J. D. (2006). "Simplified versions for the Penman evaporation equation using routine weather data". In: *Journal of Hydrology* 331.3-4, pp. 690–702.

van Meerveld, H. J., Kirchner, J. W., Vis, M. J. P., Assendelft, R. S. and Seibert, J. (2019). "Expansion and contraction of the flowing stream network alter hillslope flowpath lengths and the shape of the travel time distribution". In: *Hydrology and Earth System Sciences* 23.11, pp. 4825–4834.

van Meerveld, H. J., Sauquet, E., Gallart, F., Sefton, C., Seibert, J. and Bishop, K. (2020). "Aqua temporaria incognita". In: *Hydrological Processes* 34.26, pp. 5704–5711.

Vasconcelos, V. V. (2017). "What maintains the waters flowing in our rivers? Rethinking hydrogeology to improve public policy". In: *Applied water science* 7.4, pp. 1579–1593.

Vogt, T., Hoehn, E., Schneider, P., Freund, A., Schirmer, M. and Cirpka, O. A. (2010). "Fluctuations of electrical conductivity as a natural tracer for bank filtration in a losing stream". In: *Advances in Water Resources* 33.11, pp. 1296–1308.

Ward, A. S., Wondzell, S. M., Schmadel, N. M. and Herzog, S. P. (2020). "Climate change causes river network contraction and disconnection in the HJ Andrews Experimental Forest, Oregon, USA". In: *Frontiers in Water* 2, pp. 1–10.

Warix, S. R., Godsey, S. E., Lohse, K. A. and Hale, R. L. (2021). "Influence of groundwater and topography on stream drying in semi-arid headwater streams". In: *Hydrological Processes* 35.5, pp. 1–18.

Whiting, J. A. and Godsey, S. E. (2016). "Discontinuous headwater stream networks with stable flowheads, Salmon River basin, Idaho". In: *Hydrological Processes* 30.13, pp. 2305–2316.

Wohl, E. (2017a). "Connectivity in rivers". In: *Progress in Physical Geography* 41.3, pp. 345–362.

Wohl, E. (2017b). "The significance of small streams". In: *Frontiers of Earth Science* 11, pp. 447–456.

Zhou, Z., Cartwright, I. and Morgenstern, U. (2022). "Sources and mean transit times of stream water in an intermittent river system: the upper Wimmera River, southeast Australia". In: *Hydrology and Earth System Sciences* 26.17, pp. 4497–4513.

Zimmer, M. A., Kaiser, K. E., Blaszczak, J. R., Zipper, S. C., Hammond, J. C., Fritz, K. M., Costigan, K. H., Hosen, J., Godsey, S. E., Allen, G. H., Kampf, S., Burrows, R. M., Krabbenhoft, C. A., Dodds, W., Hale, R., Olden, J. D., Shanafield, M., DelVecchia, A. G., Ward, A. S., Mims, M. C., Datry, T., Bogan, M. T., Boersma, K. S., H., Busch M., Jones, C. N., Burgin, A. J. and Allen, D. C. (2020). "Zero or not? Causes and consequences of zero-flow stream gage readings". In: *Wiley Interdisciplinary Reviews: Water* 7.3, pp. 1–25.

Zimmer, M. A. and McGlynn, B. L. (2017). "Bidirectional stream–groundwater flow in response to ephemeral and intermittent streamflow and groundwater seasonality". In: *Hydrological Processes* 31.22, pp. 3871–3880.

Zipper, S. C., Soylu, M. E., Kucharik, C. J. and Loheide II, S. P. (2017). "Quantifying indirect groundwater-mediated effects of urbanization on agroecosystem productivity using MODFLOW-AgroIBIS (MAGI), a complete critical zone model". In: *Ecological Modelling* 359, pp. 201–219.

# Appendix

## A1 Potential evpapotranspiration – Penman equation

The calculations for the PET were based on the simplified version of the Penman equation that uses data that is usually available from weather stations (Valiantzas 2006). For the albedo values, the measurement period was subdivided into the leafed season in November and May and the leafless season in December until April. A value of 0.15 was chosen for the leafed period, and 0.22 for the leafless months (Barradas and Adem 1992).

$$E_{PEN} = E_{radS} - E_{radL} + E_{aero} \tag{2}$$

$$E_{radS} = 0.051(1-\alpha) * Rs * \sqrt{T+9.5} \tag{3}$$

$$E_{radL} = 0.188(T+13)(\frac{Rs}{RA} - 0.194) * (1 - 0.00015(T+45)^2\sqrt{\frac{RH}{100}}) \tag{4}$$

$$E_{aero} = 0.048(T+20)(1-\frac{RH}{100})(a_u + b_u u) \tag{5}$$

where $\alpha$ is 0.15 for November and May (leafed period) and 0.22 for December to April (leafless period), T is the temperature in °C, Rs is the incoming solar radiation $[MJ\ m^{-2}\ day^{-1}]$, RA is the extraterrestrial solar radiation $[MJ\ m^{-2}\ day^{-1}]$, RH is the mean relative humidity [%], $a_u$ is a factor 1, $b_u$ is a factor 0.536 and u is the wind speed at 2 m above ground [m/s] (MeteoSwiss 2023; Valiantzas 2006).

## A2 Location Characteristics

Table A1: Table summarizing all specifications for each measurement location ID (coordinates and elevation of the sampling location, size of the catchment, the mean slope of the catchment, the presence(1) of absence(0) of Molasse at or above the location, and the method of runoff measurement).

| ID | Longit. | Latitude | m a.s.l. | Area[$m^2$] | $\overline{\text{slope}}$[°] | Molasse | Method |
|---|---|---|---|---|---|---|---|
| 1 | 8.5544279 | 47.3919715 | 577.1 | 222221.8 | 10.961 | 1 | EC only |
| 2 | 8.5553224 | 47.3917301 | 586.3 | 213921.3 | 10.448 | 1 | EC only |
| 3 | 8.5600644 | 47.3904012 | 642.6 | 6132.0 | 4.215 | 0 | Estimation |
| 4 | 8.5614419 | 47.3895285 | 644.2 | 150433.0 | 7.197 | 0 | EC only |
| 5 | 8.5634884 | 47.3879172 | 652.5 | 74485.0 | 6.275 | 0 | Estimation |
| 6 | 8.5533088 | 47.3932423 | 556.5 | 108481.8 | 13.494 | 1 | Tracer |
| 7 | 8.5605360 | 47.3913591 | 637.7 | 30953.3 | 5.443 | 0 | Estimation |
| 8 | 8.5618759 | 47.3909733 | 642.7 | 13378.0 | 5.323 | 0 | Estimation |
| 9 | 8.5534141 | 47.3959882 | 526.0 | 12048.8 | 15.279 | 0 | Estimation |
| 10 | 8.5536591 | 47.3961211 | 527.0 | 121919.0 | 10.888 | 1 | Estimation |
| 11 | 8.5544625 | 47.3958525 | 538.2 | 97520.3 | 9.794 | 1 | Bucket/Estim. |
| 12 | 8.5546996 | 47.3957785 | 544.9 | 97352.8 | 9.787 | 1 | Estimation |
| 13 | 8.5575152 | 47.3948207 | 583.0 | 68258.5 | 7.219 | 0 | Tracer |
| 14 | 8.5585255 | 47.3944149 | 614.0 | 53481.0 | 6.721 | 0 | Estimation |
| 15 | 8.5547401 | 47.3973477 | 529.3 | 41359.8 | 11.442 | 1 | Estimation |
| 16 | 8.5549090 | 47.3975214 | 530.4 | 61105.8 | 10.613 | 1 | Estimation |
| 17 | 8.5615867 | 47.4019771 | 488.2 | 28309.0 | 17.493 | 1 | Estimation |
| 18 | 8.5661257 | 47.4014291 | 485.4 | 160808.5 | 9.417 | 1 | Estimation |
| 19 | 8.5647286 | 47.4006065 | 510.9 | 139958.0 | 8.645 | 1 | Estimation |
| 20 | 8.5683198 | 47.4005303 | 479.7 | 63397.0 | 11.989 | 1 | Tracer |
| 21 | 8.5668469 | 47.3992174 | 523.3 | 14467.5 | 11.067 | 0 | Tracer |
| 22 | 8.5649172 | 47.3981572 | 558.2 | 67309.3 | 8.341 | 0 | Bucket/Estim. |
| 23 | 8.5638722 | 47.3969893 | 583.2 | 23441.0 | 7.593 | 0 | Estimation |
| 24 | 8.5630503 | 47.3956840 | 598.7 | 21273.5 | 7.597 | 0 | Estimation |
| 25 | 8.5678709 | 47.3984568 | 530.2 | 54616.5 | 9.033 | 0 | Estimation |
| 26 | 8.5679039 | 47.3984611 | 533.3 | 95.5 | 11.589 | 0 | Estimation |
| 27 | 8.5660288 | 47.3974632 | 560.4 | 26036.3 | 9.662 | 0 | Estimation |
| 28 | 8.5674021 | 47.3966853 | 562.3 | 30548.8 | 12.524 | 1 | Estimation |
| 29 | 8.5675527 | 47.3965668 | 562.3 | 43767.3 | 8.376 | 1 | Estimation |
| 30 | 8.5663240 | 47.3957781 | 584.1 | 31512.3 | 7.672 | 0 | Estimation |
| 31 | 8.5714953 | 47.3997305 | 467.4 | 40311.3 | 14.942 | 1 | Tracer |

| | | | | | | | |
|---|---|---|---|---|---|---|---|
| 32 | 8.5696436 | 47.3979535 | 527.3 | 10118.5 | 11.017 | 0 | Estimation |
| 33 | 8.5684351 | 47.3960222 | 564.3 | 15465.3 | 8.502 | 1 | Estimation |
| 34 | 8.5661599 | 47.3939720 | 601.2 | 47388.0 | 6.549 | 0 | Estimation |
| 35 | 8.5739628 | 47.3970931 | 487.4 | 179962.0 | 9.497 | 1 | Tracer |
| 36 | 8.5720428 | 47.3963724 | 517.4 | 127672.3 | 8.831 | 1 | Tracer |
| 37 | 8.5710201 | 47.3957909 | 541.6 | 102513.5 | 7.942 | 0 | Estimation |
| 38 | 8.5702065 | 47.3951958 | 562.2 | 90124.8 | 8.064 | 1 | Tracer |
| 39 | 8.5700118 | 47.3950761 | 562.2 | 97854.3 | 7.755 | 1 | Estimation |
| 40 | 8.5690630 | 47.3940425 | 586.0 | 81906.5 | 7.745 | 0 | Estimation |
| 41 | 8.5673174 | 47.3932865 | 602.9 | 4529.0 | 8.450 | 0 | Estimation |
| 42 | 8.5715743 | 47.3996619 | 466.7 | 869227.3 | 10.050 | 1 | EC only |
| 43 | 8.5734816 | 47.3978352 | 481.7 | 897497.8 | 9.773 | 1 | Tracer |
| 45 | 8.5741615 | 47.3971223 | 486.9 | 699600.0 | 9.650 | 1 | EC only |
| 46 | 8.5743186 | 47.3966985 | 492.0 | 651767.0 | 9.405 | 1 | Tracer |
| 47 | 8.5741328 | 47.3966729 | 492.0 | 44662.5 | 12.389 | 1 | Bucket/Estim. |
| 48 | 8.5760739 | 47.3945492 | 521.7 | 308901.5 | 9.430 | 0 | EC only |
| 49 | 8.5765396 | 47.3940279 | 522.8 | 87084.3 | 10.221 | 0 | Tracer |
| 50 | 8.5766260 | 47.3940177 | 522.6 | 10877.0 | 7.859 | 0 | Estimation |
| 51 | 8.5750982 | 47.3941360 | 530.8 | 310236.3 | 9.389 | 0 | Tracer |
| 52 | 8.5747228 | 47.3939371 | 535.5 | 217155.8 | 9.121 | 0 | Estimation |
| 53 | 8.5731566 | 47.3928467 | 559.5 | 171776.0 | 8.700 | 1 | Tracer |
| 54 | 8.5714607 | 47.3921987 | 577.9 | 151799.5 | 8.414 | 1 | Estim./Tracer |
| 55 | 8.5690881 | 47.3918115 | 601.2 | 56110.0 | 7.911 | 0 | Estimation |
| 56 | 8.5672952 | 47.3909742 | 624.0 | 798.3 | 13.303 | 0 | Estimation |
| 57 | 8.5708245 | 47.3912230 | 596.9 | 63775.5 | 8.079 | 0 | Estimation |
| 58 | 8.5694083 | 47.3903332 | 618.7 | 56773.0 | 15.775 | 1 | Estimation |
| 59 | 8.5715816 | 47.3907758 | 596.0 | 17508.8 | 11.178 | 0 | Estimation |
| 60 | 8.5815728 | 47.3924852 | 510.7 | 299184.3 | 9.595 | 1 | Tracer |
| 61 | 8.5812467 | 47.3901497 | 548.9 | 45184.5 | 5.322 | 0 | Tracer |
| 62 | 8.5805114 | 47.3908312 | 548.7 | 22014.3 | 5.775 | 0 | Estimation |
| 63 | 8.5796880 | 47.3913531 | 542.5 | 216130.5 | 9.394 | 0 | Estimation |
| 67 | 8.5791543 | 47.3908220 | 553.6 | 2842.3 | 9.139 | 0 | Tracer |

## A3 Daily discharge maps

Day one (16.11.2022) is missing due to incomplete measurements.

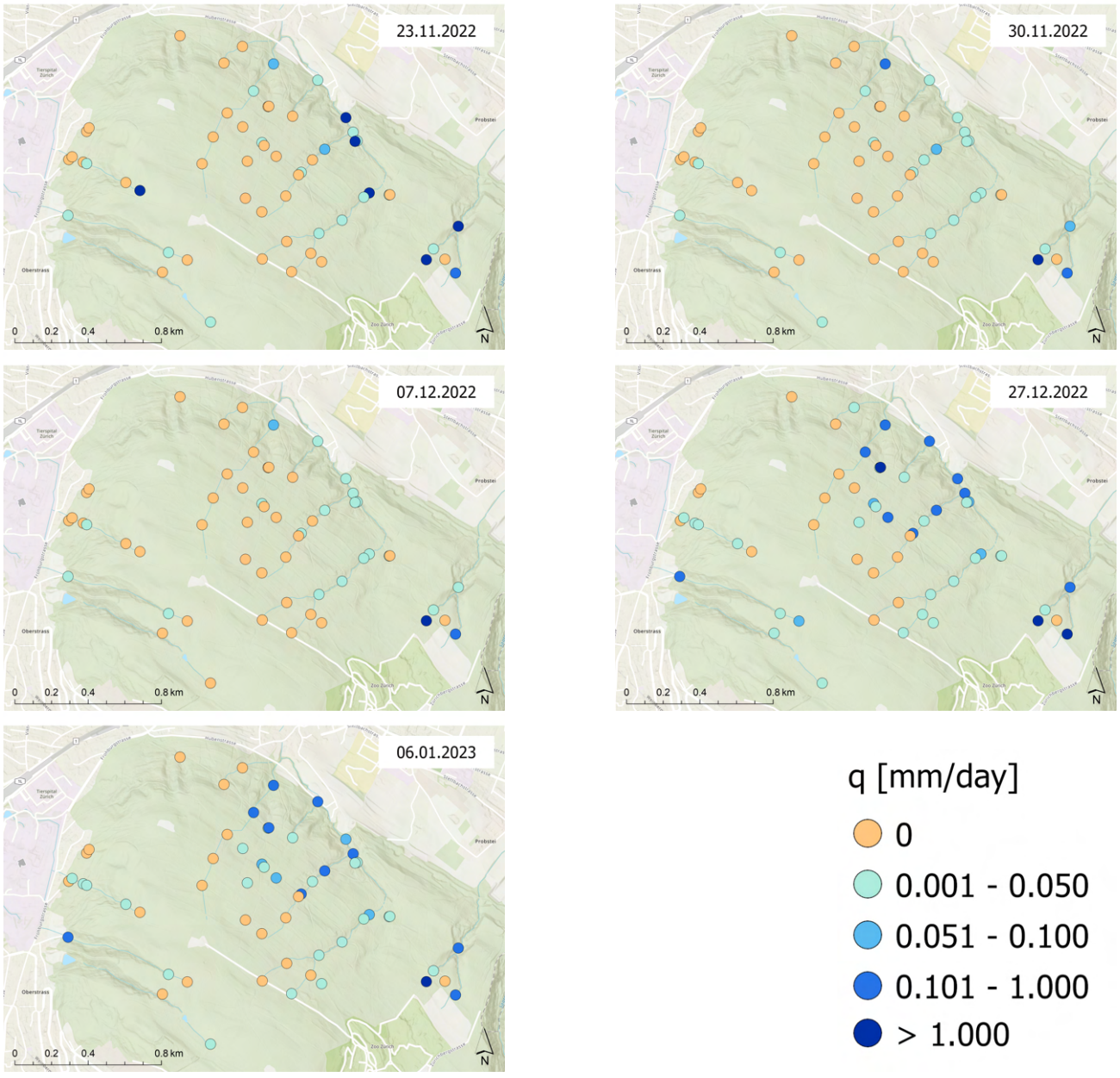


Figure A1: Daily maps of discharge measurements from survey date 2 to 6. Dates are indicated in the maps.

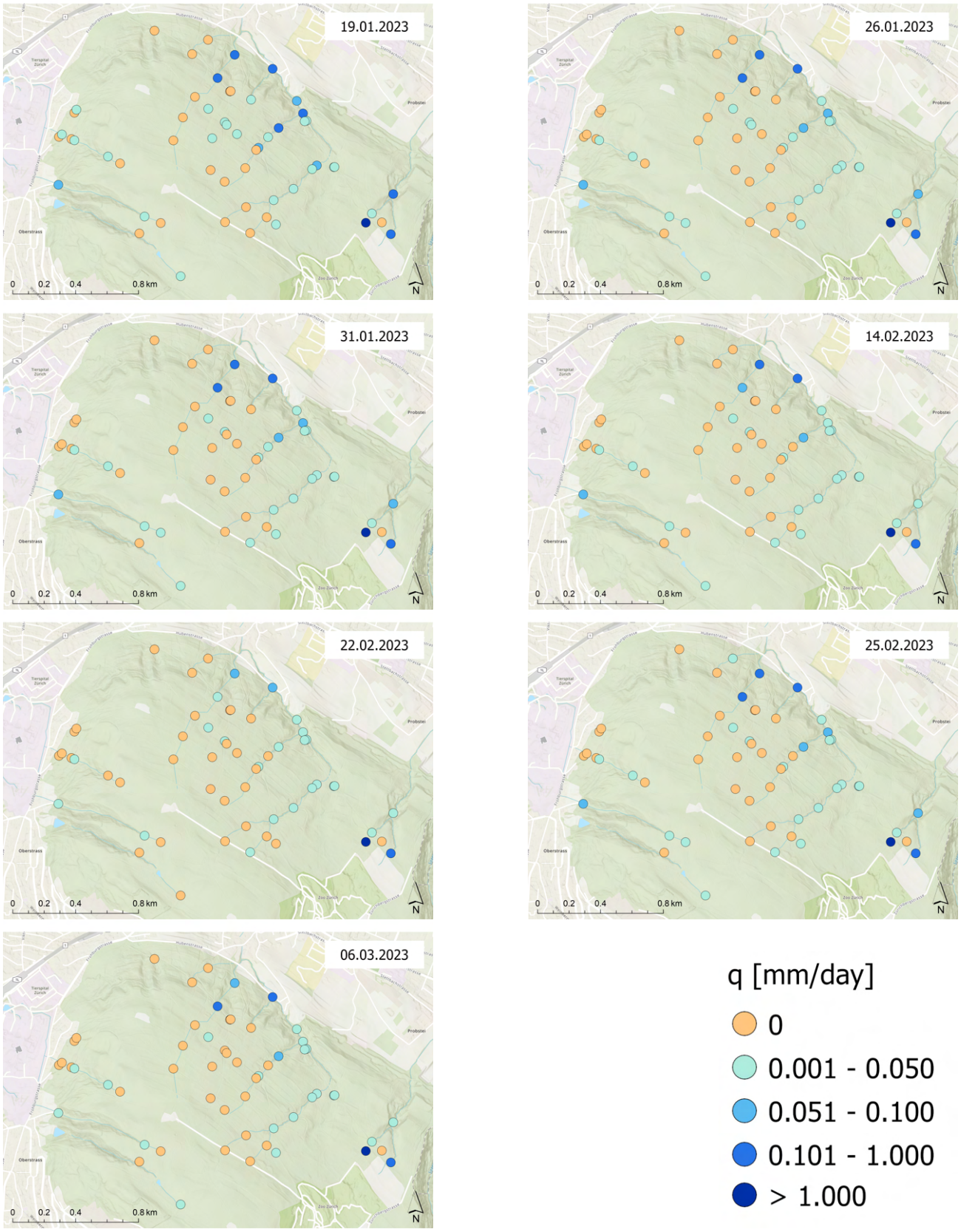


Figure A2: Daily maps of discharge measurements from survey date 7 to 13. Dates are indicated in the maps.

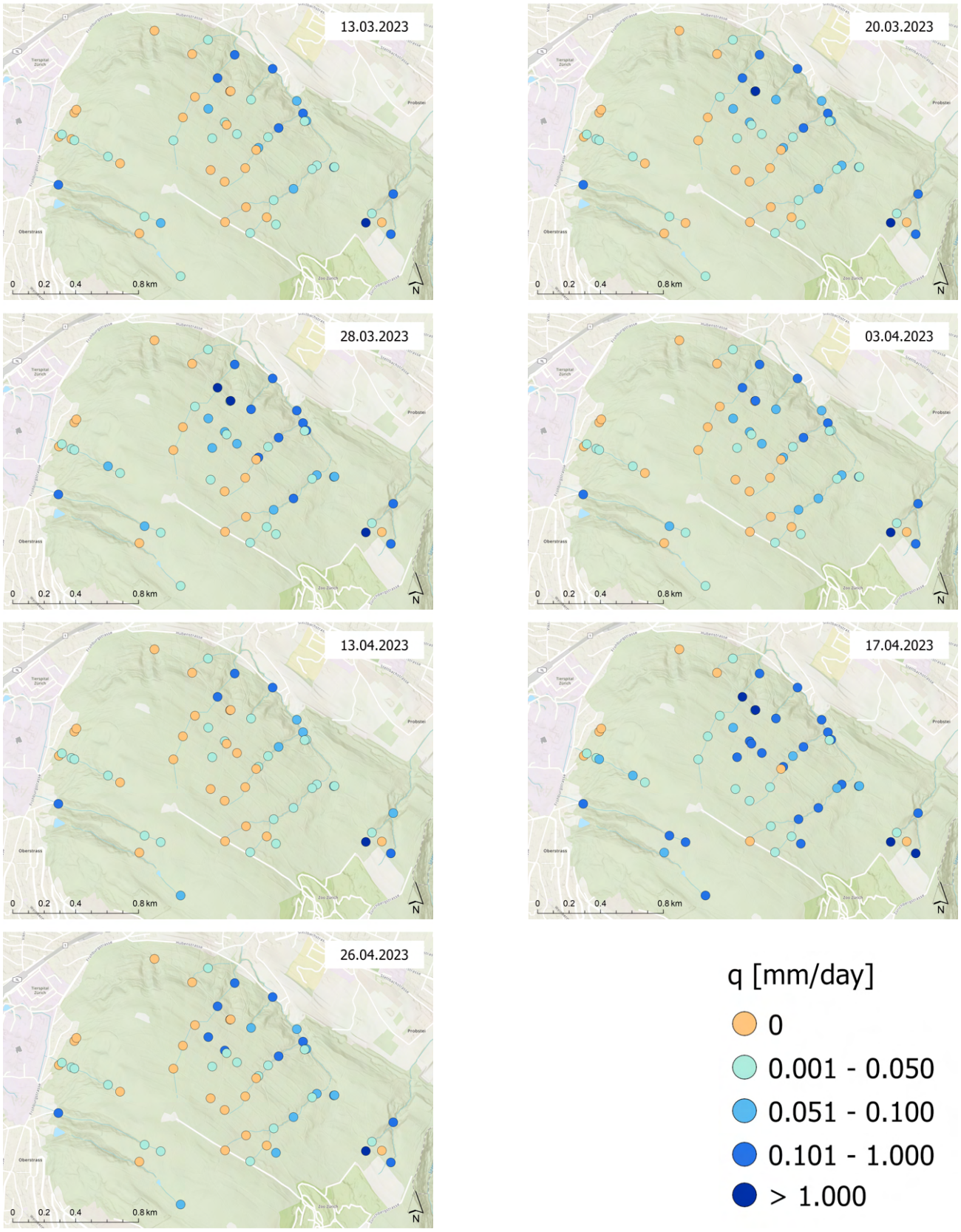


Figure A3: Daily maps of discharge measurements from survey date 14 to 20. Dates are indicated in the maps.

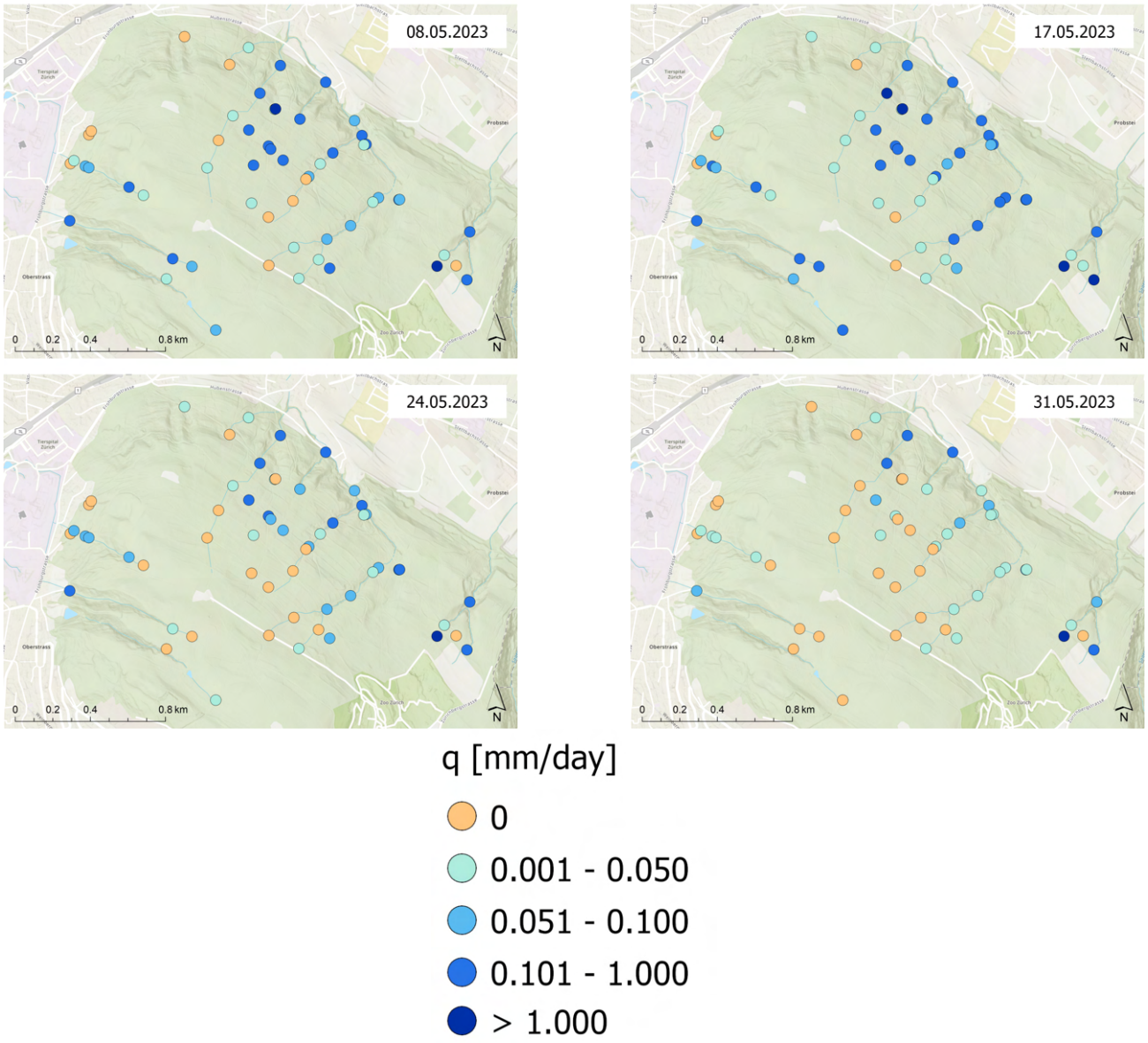


Figure A4: Daily maps of discharge measurements from survey date 21 to 24. Dates are indicated in the maps.

## A4 Daily EC maps

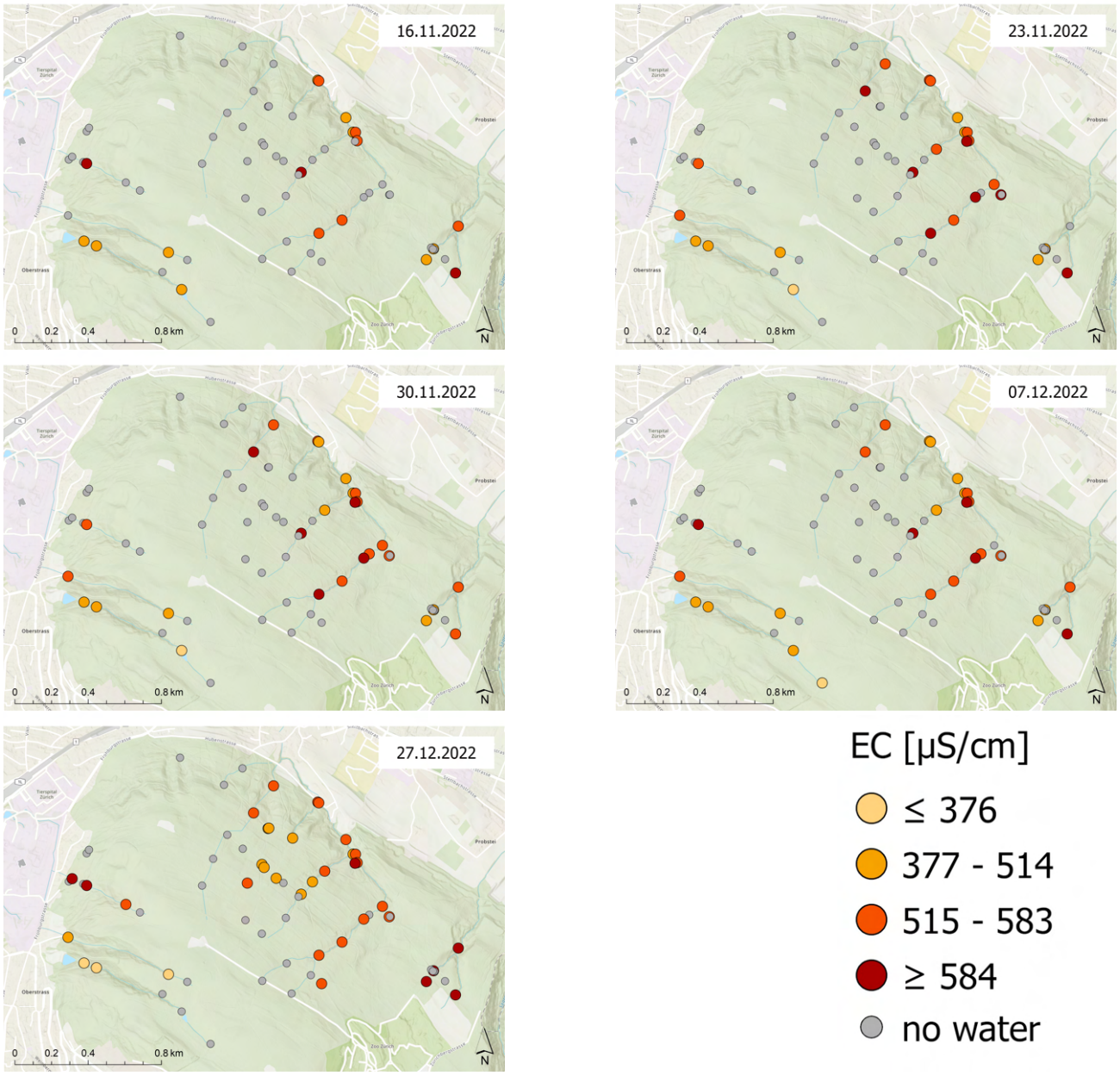


Figure A5: Daily maps of EC measurements from survey date 1 to 5. Dates are indicated in the maps.

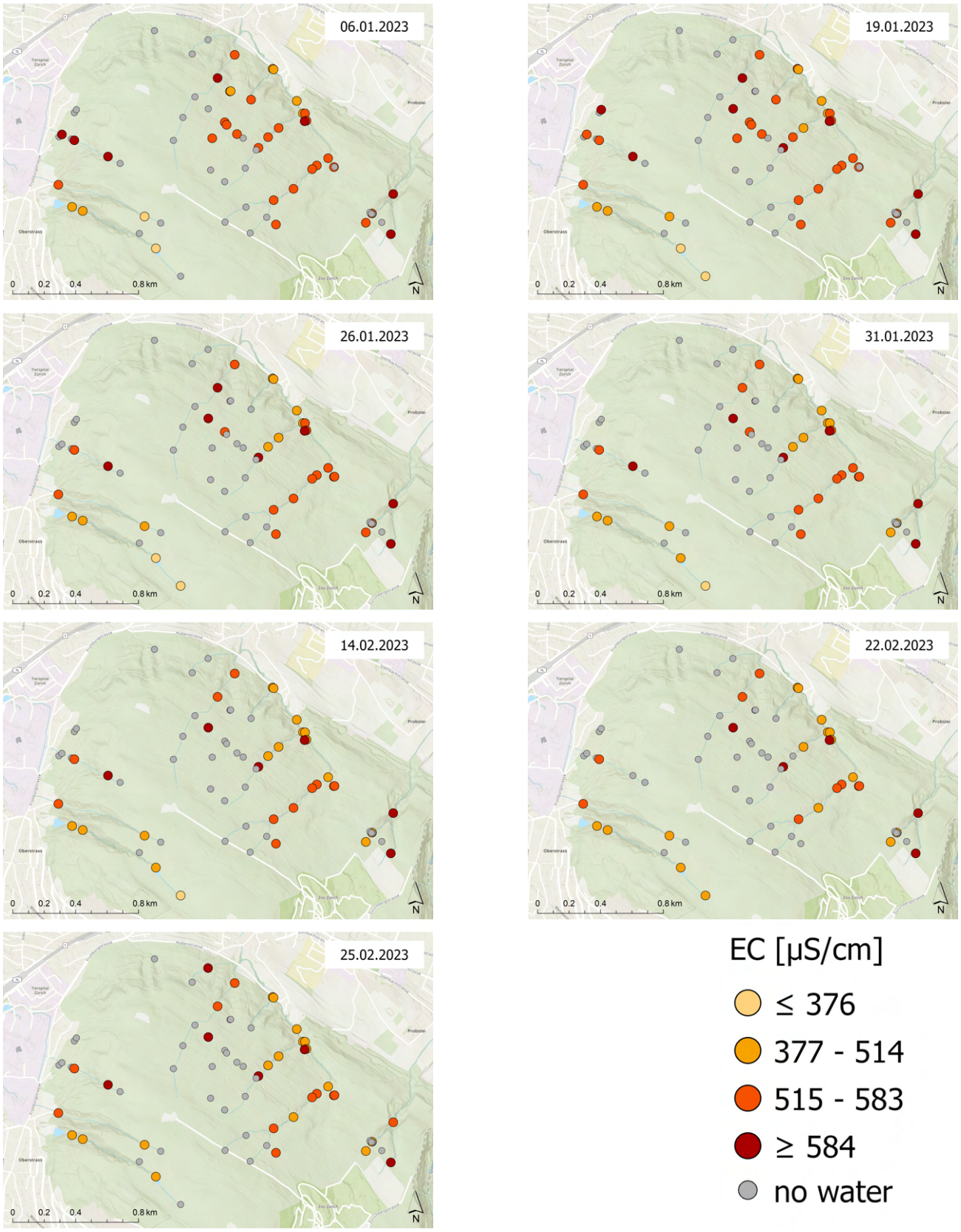


Figure A6: Daily maps of EC measurements from survey date 6 to 12. Dates are indicated in the maps.

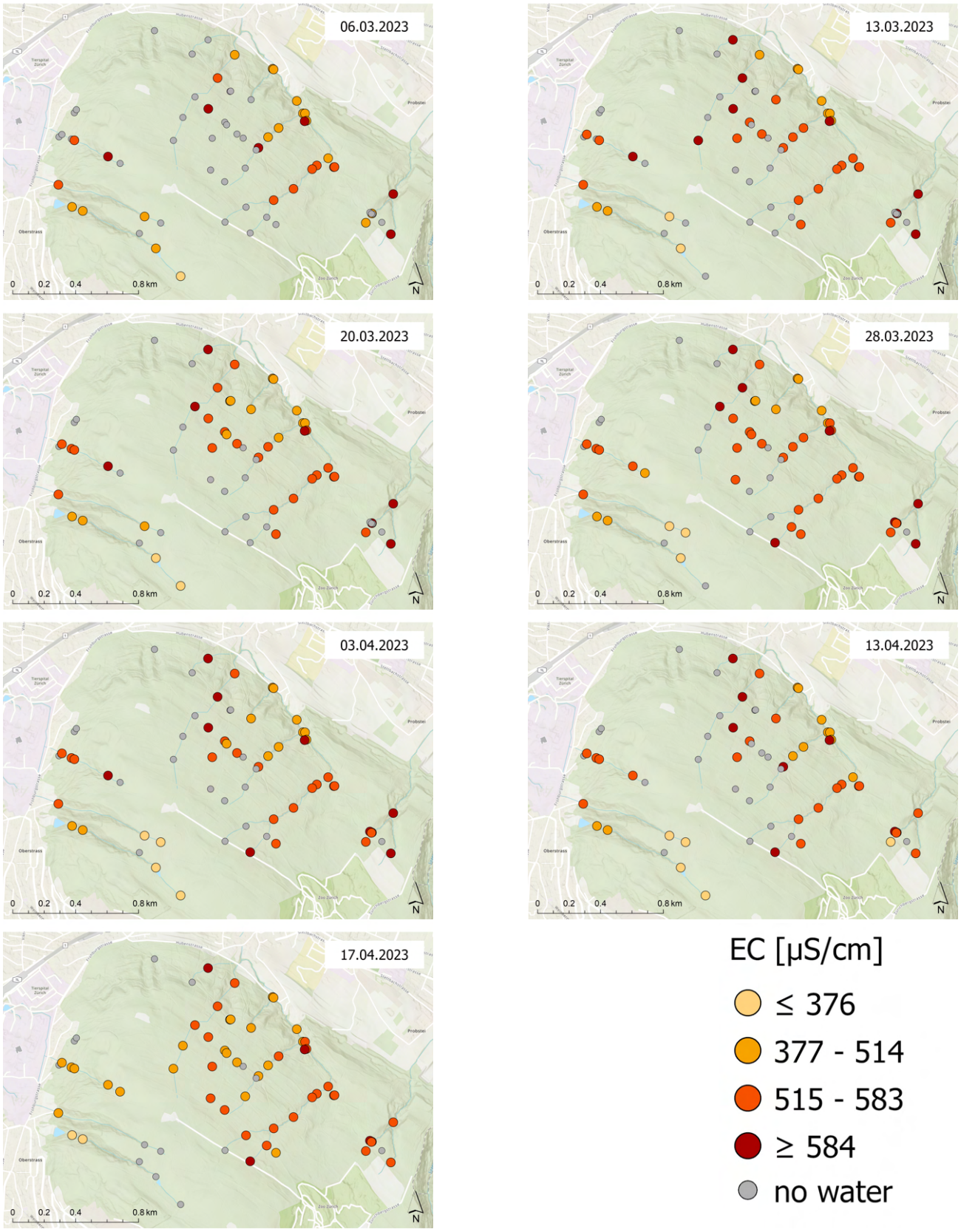


Figure A7: Daily maps of EC measurements from survey date 13 to 19. Dates are indicated in the maps.

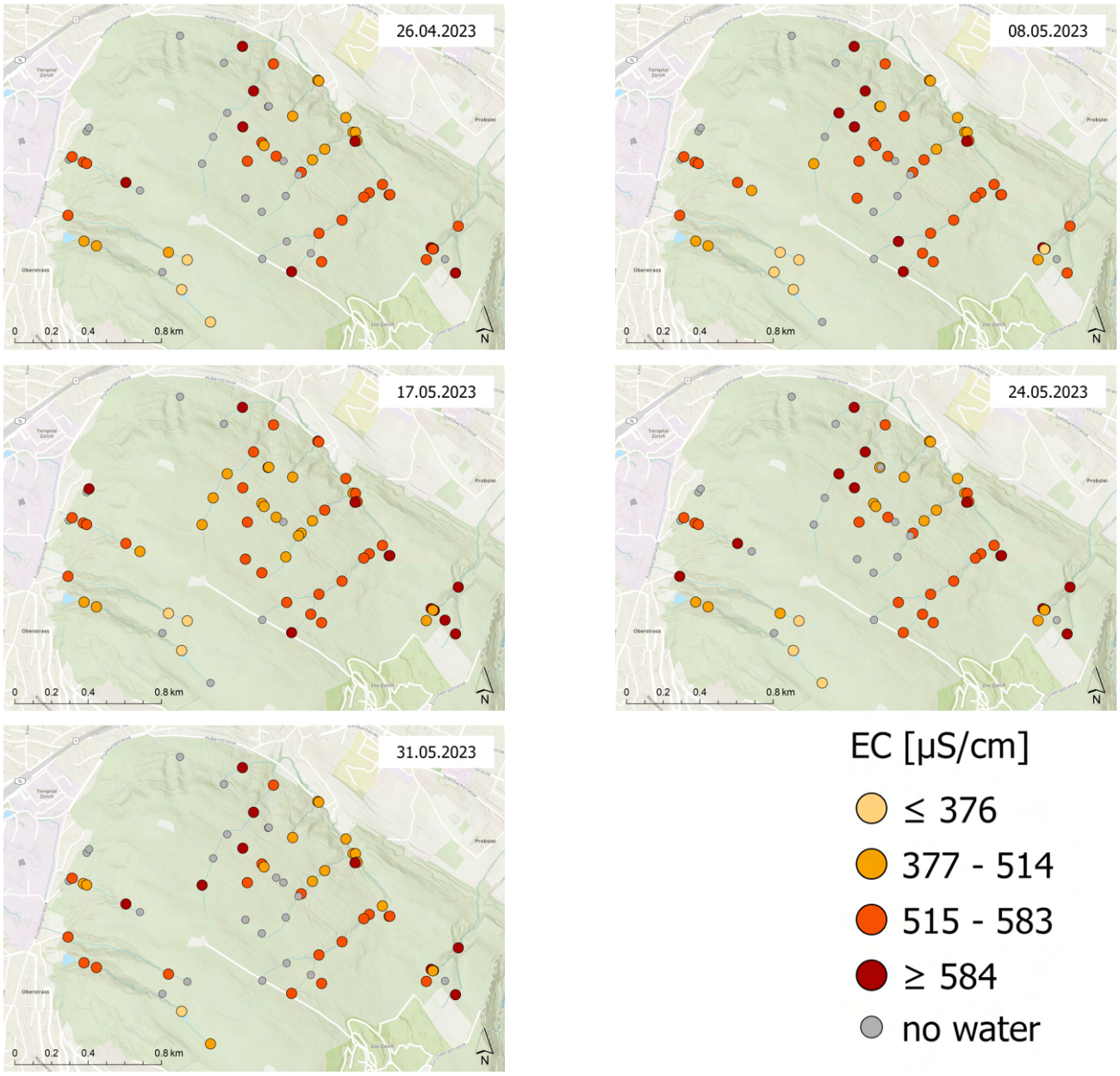


Figure A8: Daily maps of EC measurements from survey date 20 to 24. Dates are indicated in the maps.

## A5 Coefficient of Variation

For ID numbers where values for both the discharge and the EC are missing did not have enough measurements ($\leq$ 5 measurements) to calculate a reliable mean or CV. At locations with IDs where only the values for the discharge are missing, no runoff measurements were taken. These values are therefore missing in Table A2.

Table A2: Coefficient of Variation (CV) and mean discharge and EC per ID number over the full measurement period Nov. 2022 - May 2023

| ID | Mean q (mm/d) | CV q (%) | Mean EC ($\mu$S/cm) | CV EC (%) |
|---|---|---|---|---|
| 1 | | | 460.500 | 10.627 |
| 2 | | | 446.750 | 11.266 |
| 3 | | | | |
| 4 | | | 328.304 | 21.852 |
| 5 | 0.048 | 148.152 | 240.454 | 28.932 |
| 6 | 0.124 | 76.705 | 544.522 | 6.677 |
| 7 | 0.035 | 121.218 | 393.208 | 21.436 |
| 8 | 0.049 | 105.755 | 297.500 | 14.901 |
| 9 | | | | |
| 10 | 0.026 | 93.896 | 559.429 | 4.513 |
| 11 | 0.034 | 89.754 | 523.500 | 4.754 |
| 12 | 0.019 | 136.520 | 552.833 | 5.592 |
| 13 | 0.035 | 120.215 | 588.053 | 5.974 |
| 14 | | | | |
| 15 | | | | |
| 16 | | | | |
| 17 | | | | |
| 18 | 0.001 | 82.094 | 631.583 | 2.753 |
| 19 | | | | |
| 20 | 0.345 | 67.905 | 534.087 | 2.940 |
| 21 | 0.490 | 91.402 | 582.522 | 2.768 |
| 22 | 0.005 | 108.483 | 590.167 | 8.234 |
| 23 | | | | |
| 24 | | | | |
| 25 | 0.016 | 70.305 | 487.250 | 2.506 |
| 26 | 11.026 | 93.603 | 492.429 | 2.439 |
| 27 | 0.064 | 80.925 | 605.944 | 5.404 |
| 28 | 0.069 | 113.467 | 521.938 | 3.167 |

| | | | | |
|---|---|---|---|---|
| 29 | 0.053 | 93.132 | 507.750 | 2.349 |
| 30 | 0.041 | 109.638 | 540.143 | 2.153 |
| 31 | 0.211 | 84.106 | 497.125 | 3.609 |
| 32 | 0.093 | 103.677 | 512.000 | 2.314 |
| 33 | 0.104 | 97.728 | 541.000 | 5.168 |
| 34 | | | | |
| 35 | 0.121 | 70.511 | 476.667 | 2.342 |
| 36 | 0.136 | 65.579 | 507.739 | 2.095 |
| 37 | 0.025 | 89.134 | 509.316 | 3.187 |
| 38 | 0.065 | 104.766 | 574.708 | 5.275 |
| 39 | | | | |
| 40 | | | | |
| 41 | | | | |
| 42 | | | 498.750 | 3.379 |
| 43 | 0.079 | 78.785 | 498.083 | 2.443 |
| 45 | | | 518.083 | 2.898 |
| 46 | 0.057 | 95.616 | 520.292 | 2.688 |
| 47 | 0.016 | 73.672 | 620.304 | 1.939 |
| 48 | | | 523.091 | 2.929 |
| 49 | 0.088 | 120.307 | 551.478 | 3.222 |
| 50 | 0.041 | 104.498 | 565.059 | 3.156 |
| 51 | 0.057 | 105.992 | 536.714 | 2.147 |
| 52 | 0.019 | 141.567 | 547.913 | 4.396 |
| 53 | 0.056 | 107.750 | 532.125 | 2.313 |
| 54 | 0.040 | 114.625 | 567.583 | 1.859 |
| 55 | | | | |
| 56 | | | | |
| 57 | | | | |
| 58 | 0.007 | 98.357 | 586.444 | 1.860 |
| 59 | 0.041 | 97.543 | 551.833 | 4.110 |
| 60 | 0.127 | 75.257 | 603.000 | 8.305 |
| 61 | 0.472 | 69.712 | 644.250 | 13.434 |
| 62 | | | | |
| 63 | 0.010 | 99.468 | 535.708 | 8.341 |
| 67 | 2.595 | 62.372 | 511.625 | 10.760 |

## A6 Percent of streambed states

Table A3: Percent of observations in the flow state of the streambed (dry, wet streambed, standing water, flowing water) per ID over the full survey period.

| ID | Dry (%) | Wet streambed (%) | Flowing (%) |
|---|---|---|---|
| 1 | 0.00 | 0.00 | 100.00 |
| 2 | 0.00 | 0.00 | 100.00 |
| 3 | 50.00 | 33.33 | 16.67 |
| 4 | 0.00 | 0.00 | 100.00 |
| 5 | 0.00 | 12.50 | 87.50 |
| 6 | 0.00 | 0.00 | 100.00 |
| 7 | 0.00 | 8.33 | 91.67 |
| 8 | 37.50 | 12.50 | 50.00 |
| 9 | 100.00 | 0.00 | 0.00 |
| 10 | 41.67 | 0.00 | 58.33 |
| 11 | 50.00 | 0.00 | 50.00 |
| 12 | 0.00 | 8.33 | 91.67 |
| 13 | 8.33 | 12.50 | 79.17 |
| 14 | 79.17 | 4.17 | 16.67 |
| 15 | 95.83 | 4.17 | 0.00 |
| 16 | 87.50 | 4.17 | 8.33 |
| 17 | 75.00 | 16.67 | 8.33 |
| 18 | 8.33 | 37.50 | 54.17 |
| 19 | 91.67 | 8.33 | 0.00 |
| 20 | 0.00 | 0.00 | 100.00 |
| 21 | 0.00 | 0.00 | 100.00 |
| 22 | 75.00 | 0.00 | 25.00 |
| 23 | 87.50 | 4.17 | 8.33 |
| 24 | 54.17 | 29.17 | 16.67 |
| 25 | 58.33 | 8.33 | 33.33 |
| 26 | 58.33 | 12.50 | 29.17 |
| 27 | 20.83 | 0.00 | 79.17 |
| 28 | 0.00 | 4.17 | 95.83 |
| 29 | 33.33 | 16.67 | 50.00 |
| 30 | 25.00 | 16.67 | 58.33 |
| 31 | 0.00 | 0.00 | 100.00 |
| 32 | 41.67 | 0.00 | 58.33 |
| 33 | 50.00 | 0.00 | 50.00 |

| | | | |
|---|---|---|---|
| 34 | 54.17 | 29.17 | 16.67 |
| 35 | 0.00 | 0.00 | 100.00 |
| 36 | 0.00 | 0.00 | 100.00 |
| 37 | 12.50 | 16.67 | 70.83 |
| 38 | 0.00 | 0.00 | 100.00 |
| 39 | 95.83 | 0.00 | 4.17 |
| 40 | 58.33 | 33.33 | 8.33 |
| 41 | 70.83 | 25.00 | 4.17 |
| 43 | 0.00 | 0.00 | 100.00 |
| 46 | 0.00 | 0.00 | 100.00 |
| 47 | 0.00 | 0.00 | 100.00 |
| 48 | 4.17 | 4.17 | 91.67 |
| 49 | 4.17 | 0.00 | 95.83 |
| 50 | 16.67 | 0.00 | 83.33 |
| 51 | 0.00 | 0.00 | 100.00 |
| 52 | 0.00 | 0.00 | 100.00 |
| 53 | 0.00 | 4.17 | 95.83 |
| 54 | 0.00 | 0.00 | 100.00 |
| 55 | 62.50 | 25.00 | 12.50 |
| 56 | 95.83 | 4.17 | 0.00 |
| 57 | 70.83 | 8.33 | 20.83 |
| 58 | 8.33 | 25.00 | 66.67 |
| 59 | 12.50 | 8.33 | 79.17 |
| 60 | 0.00 | 0.00 | 100.00 |
| 61 | 0.00 | 0.00 | 100.00 |
| 62 | 95.83 | 0.00 | 4.17 |
| 63 | 0.00 | 0.00 | 100.00 |
| 67 | 0.00 | 0.00 | 100.00 |

## Personal Declaration

I hereby declare that the submitted thesis is the result of my own, independent work. All external sources are explicitly acknowledged in the thesis.

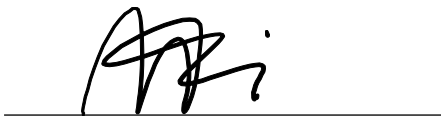

Anja Fischer

Zurich, September 30, 2023